Pediatric Tumor Neuroradiology

62

Sotirios Bisdas and Felice D'Arco

Contents

S. Bisdas (✉)
The National Hospital for Neurology and Neurosurgery, University College London Hospitals NHS Trust, London, UK

Great Ormond Street Hospital for Children, London, UK

Institute of Neurology, University College London, London, UK

Eberhard Karls University, Tübingen, Germany

Lysholm Department of Neuroradiology, London, UK

Department of Brain Repair and Rehabilitation, Queen Square Institute of Neurology, UCL, London, UK

Clinical Lead Neurooncology, Institute of Healthcare Engineering, University College London, London, UK
e-mail: s.bisdas@ucl.ac.uk

Abstract

Tumors of the central nervous system constitute the largest group of solid neoplasms in children. In this chapter, we have assembled a cadre of sections, which cover the whole spectrum of pediatric tumor entities and offer a clinically meaningful insight into the classification, symptoms, and diagnostic criteria in modern clinical neuroradiology with emphasis on the most appropriate imaging techniques selection, the correct interpretation of the imaging findings, and – last but not least – how neuroimaging can integrate optimally into the state-of-the-art management strategies. The tumor entities are broadly grouped into the posterior fossa tumors, the pineal region lesions, the sellar and parasellar tumors, the supratentorial neoplasms, and the spinal entities. Of note, key imaging features derived from advanced imaging techniques,

F. D'Arco
Great Ormond Street Hospital for Children, London, UK

Guy's and St Thomas' NHS foundation Trust, London, UK
e-mail: Felice.D'Arco@gosh.nhs.uk

which are clinically mature and widely disseminated and provide information unattained by other modalities information about the functional status of the lesion, are also highlighted.

Keywords

Brain tumors · Neuro-oncology · Magnetic resonnance imaging · Medulloblastoma · Pediatric brain tumors · Pylocitic astrocytoma · Ependymoma

Abbreviations

ADC	Apparent diffusion coefficient
AT/RT	Atypical teratoid/rhabdoid tumor
CBF	Cerebral blood flow
CBTRUS	Central Brain Tumor Registry of the United States
CBV	Cerebral blood volume
Cho	Choline
CNS	Central nervous system
CP	Craniopharyngioma
CPA	Cerebellar pilocytic astrocytoma
Cr	Creatine
CSF	Cerebrospinal fluid
DDX	Differential diagnosis
DMG	Diffuse midline glioma
DNET	Dysembryoplastic neuroepithelial tumor
DTI	Diffusion tensor images
DWI	Diffusion-weighted images
EPN	Ependymoma
GCT	Germ cell tumors
GRE	Gradient echo sequence
HH	Hypothalamic hamartoma
ICP	Increased intracranial pressure
K27M+	Histone H3-K27M mutations
LCA	Large cell/anaplastic
LCH	Langerhans cell histiocytosis
MBL	Medulloblastoma
MEN	Multiple endocrine neoplasia
MRA	Magnetic resonance angiography
MRS	Magnetic resonance spectroscopy
NAA	*N*-Acetylaspartate
NF1	Neurofibromatosis type 1
NGGCTs	Non-germinomatous germ cell tumors
OPG	Optic pathway glioma

PHS	Pallister-Hall syndrome
PMA	Pilomyxoid astrocytoma
PNET	Primitive neuroectodermal tumor
PPTID	Pineal parenchymal tumors of intermediate differentiation
PTPR	Papillary tumor of the pineal region
PWI	Perfusion-weighted images
PXA	Pleomorphic xanthoastrocytoma
RCC	Rathke cleft cyst
RES	Reticuloendothelial system
SHH	Sonic hedgehog (molecular sub-type medulloblastoma)
SWI/SNF	Chromatin remodeling complex SWItch/sucrose nonfermentable
SWI	Susceptibility-weighted images
WNT	Wingless (molecular subtype medulloblastoma)

General Remarks

Central nervous system (CNS) tumors in the pediatric brain and spinal cord comprise the second most common childhood malignancies, after hematologic malignancies, being the most common pediatric solid organ tumor and are the leading cause of cancer death in children 0 through 14 years. The incidence of childhood CNS tumors varies with age, sex, race, and ethnicity. From the Central Brain Tumor Registry of the United States (CBTRUS) database, the following annual age-adjusted rates of CNS tumors (per 100,000 in 2008–2012) were reported:

- Age <1 year: 6.20 per 100,000
- Age 1 to 4 years: 5.86 per 100,000
- Age 5 to 9 years: 5.06 per 100,000
- Age 10 to 14 years: 5.14 per 100,000
- Age 15 to 19 years: 6.19 per 100,000

Boys seem to suffer at a higher rate compared with girls, whereas the incidence of CNS tumors is greatest in white and Asian/Pacific children.

The clinical symptoms can be broadly summarized into headache, nausea and vomiting, ataxia and gait abnormalities, cranial nerve palsies, impaired vision, seizure, papilledema, macrocephaly, developmental delay, neurocutaneous syndromes, and

endocrinopathies. The acute clinical signs are caused by local invasion, compression of adjacent structures, increased intracranial pressure (ICP), and obstruction of cerebrospinal fluid (CSF) flow, resulting in hydrocephalus. In infants, macrocephaly is the most common presenting symptom as the unfused cranial sutures attempt to accommodate rising ICP. Infants and generally young children may present irritableness as they are unable to articulate symptoms, like headaches. Nausea and vomiting are common presenting symptoms at any age and for many tumors. Older children and adolescents are usually admitted with headaches (supratentorial and centrally located tumors), abnormal gait (brain stem or spinal location), poor coordination (posterior fossa), papilledema, and seizures.

The MRI which is the state-of-the-art modality for investigating the pediatric CNS tumors at the baseline should include:

Pre-contrast Sequences
– 3D T1 MPRAGE 1 mm with reformats in the three planes
– Axial T2 SE-weighted images 4 mm
– Coronal FLAIR images 4 mm
– Axial diffusion-weighted images 4 mm (to probe tumor cellularity, which increases with the malignancy grade)

Post-contrast Sequences
– 3D T1 MPRAGE 1 mm with reformats in the three planes
– Axial T1 SE (increased contrast resolution in case of parenchymal enhancing lesions and useful to exclude artifacts on 3D T1 MPRAGE)

Optional Sequences
• DSC MR perfusion and MR spectroscopy techniques useful to distinguish high- from low-grade gliomas, for "hotspot" imaging prior to biopsy, and to provide hints for differentiating pseudo-progression from tumor relapse
• Diffusion tensor imaging – tractography and fMRI for preoperative planning
• Functional MRI (in preoperative planning)

Spinal Imaging
• Sagittal T1 post-contrast entire spine
• Axial T1 post-contrast on the region of interest

Optional Spinal Sequences
– T2 sagittal entire spine (useful for non-enhancing tumors such as some of the embryonal neoplasms)
– Axial T2 on the region of interest
– Sagittal CISS of the conus and cauda equine roots to visualize small metastatic disease along the cauda equina roots

The imaging surveillance of the pediatric CNS malignancies depends on the therapeutic regimen and on any new clinical symptoms. A robust approach is to follow up the high-grade tumor directly after surgery and perform brain and spine imaging every 3 months for the first 2 years and then every 6 months. For low-grade tumors after complete resection, 6-month interval imaging in the first 2 years and then annually is appropriate.

For more details in the entities' clinical features, epidemiology, state-of-the-art imaging protocol, and follow-up imaging strategy, the readers are referred to the corresponding sections in the chapter embracing the posterior fossa tumors (section "Posterior Fossa Tumors"), the pineal region lesions (section "Pineal Region Masses"), the sellar and parasellar tumors (section "Sellar and Parasellar Tumors"), and the supratentorial neoplasms (section "Non-diffuse Astrocytic Tumors"). The imaging phenotypes of the pediatric spinal tumors are integrated in the adult spinal tumor chapter due to their imaging features and histological origin overlap.

An interpretation checklist is provided for each tumor entity along with a reporting checklist and a sample report after the last section. A schematic diagnostic algorithm at the end of the chapter is proposed to synthesize the current evidence for assessing systematically the posterior fossa lesions, the largest subgroup of intracranial pediatric tumors.

Posterior Fossa Tumors

Medulloblastoma (MBL)

Definition of Entity and Clinical Highlights
MBLs are highly aggressive, hypercellular embryonal brain tumors that most commonly

reside on the midline abutting the roof of the fourth ventricle. They grow rapidly and are usually associated with considerable mass effect resulting in hydrocephalus. In approximately 40% of patients, CSF seeding at the time of diagnosis is present.

Basic Epidemiology/Demographics/Pathophysiology

MBLs are the most common neuropediatric (representing 15–20% of all pediatric brain tumors) and posterior fossa tumors (representing 30–40% of all posterior fossa tumors). Besides the long-established histological variants of MBLs that have clinical utility (e.g., desmoplastic/nodular, medulloblastoma with extensive nodularity, large cell, and anaplastic), it is now widely accepted that there are four genetic (molecular) groups of MBLs: WNT-activated, SHH-activated, and the numerically designated "group 3" and "group 4." The different molecular groups present distinct epidemiological features. Specifically, WNT is seen in children and adults (not seen in infancy) with equal gender predilection; SHH is seen in infants and adults (rare in children) with equal gender predilection; group 3 tumors are diagnosed in infants and children (rare in adults) with higher male predilection; and group 4 tumors are observed in children (being rare in infants) with moderate male predilection with a M:F ratio of 2:1. Taken as a group, 77% of MBLs present before the age of 19 (median age 9 years). MBLs in adults are typically observed in the third and fourth decades, rising in atypical locations but associated with a better prognosis.

Pathological Features

Macroscopically, MBLs are soft, friable tumors, often with necrosis. They are highly cellular tumors with abundant dark staining, round or oval nuclei, and little cytoplasmic differentiation. They may appear with extensive nodularity but with large cell/anaplastic (LCA) features as well. Increased mitoses rate is a histological hallmark, and neuroblastic Homer-Wright rosettes are seen in up to 40% of cases. MBLs express the neuronal markers synaptophysin and nestin, a marker of primitive neuroepithelial cells, in line with their presumed origin from neuronal progenitors in the
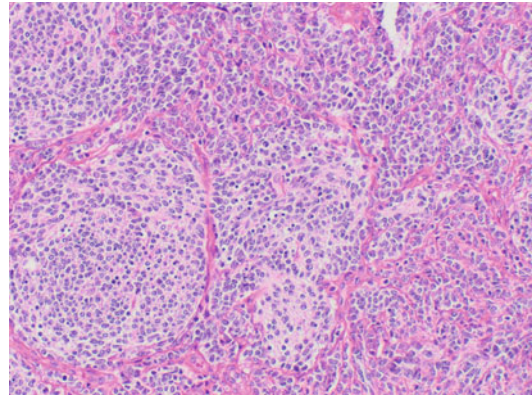
Fig. 1 H&E-stained high-power image of a desmoplastic medulloblastoma with differentiated pale islands that are surrounded by actively proliferating reticulin-rich internodular areas

cerebellum. Nuclear beta-catenin staining is seen in WNT subtypes, and p53 immunostaining can be performed to identify tumors with protein p53 (*TP53*) mutations (Fig. 1).

Clinical Scenario and Indications for Imaging

Rapid clinical onset with symptoms of raised intracranial pressure as a result of obstructive hydrocephalus. In approximately 40% of patients, there is evidence of CSF seeding at the time of diagnosis. Head cross-sectional imaging is indicated for initial assessment. Spinal imaging is indicated to rule out CSF seeding.

Imaging Techniques and Recommended Protocol

Contrast-enhanced CT of the brain. Contrast-enhanced MRI of the brain (axial and coronal T2w/FLAIR, axial DWI/ADC, 3D-T1w pre- and post-contrast, or axial, coronal, and sagittal T1w post-contrast). Sagittal and axial post-contrast T1 of the spine.

Optional sequences: MRS and PWI (DSC) of the brain. Sagittal and axial T2w images of the spine.

Interpretation Checklist

MBLs often arise in the midline with consequent growth in the fourth ventricle. Other possible locations are cerebellar hemispheres (sometimes resembling an extra-axial mass) and in the foramina of Luschka or cerebellopontine angles. Location may be characteristic of different molecular subtypes.

CT Findings

Hyperdense, due to high cellularity, mass in the posterior fossa (often in fourth ventricle) (Fig. 2).

Fig. 2 Axial, unenhanced CT of a 12-year-old boy with medulloblastoma. The mass is hyperdense in comparison to the surrounding cerebellar white matter (white arrows). The fourth ventricle is compressed by the mass (black arrow), and there are some internal areas of calcification (black arrowhead)

Possible presence of calcification/hemorrhages (1/5 of the cases) and small cystic/necrotic areas (up to 50% cases). Often associated with hydrocephalus.

MRI Findings

T2w: Hypointense to white matter (high cellularity) with possible heterogeneity due to hemorrhagic/cystic/calcified components (Fig. 3a).

DWI: Diffusion restriction (low ADC values) related to high cell density (Fig. 3b). Possible pitfall is associated with the less aggressive desmoplastic subtype, which may show minimal or no diffusion restriction.

T1w with contrast: Majority of MBLs enhance strongly (Fig. 3c); however, absence of contrast enhancement does not exclude MBL (Fig. 4). Spinal imaging is mandatory to diagnose CSF dissemination.

MRS: Elevated Cho/Cr and Cho/NAA ratios. As per ADC values, the MRS changes may be less pronounced in the desmoplastic subtype. Tau elevation at 3.3 ppm (short TE MRS). Lactate, glutamine, and glutamate may be elevated. In metastatic MBLs, there is higher total Cho which correlates with the Ki67 index of the tumoral cells (indicating high rate of cellular proliferation).

PWI: Variable permeability and perfusion.
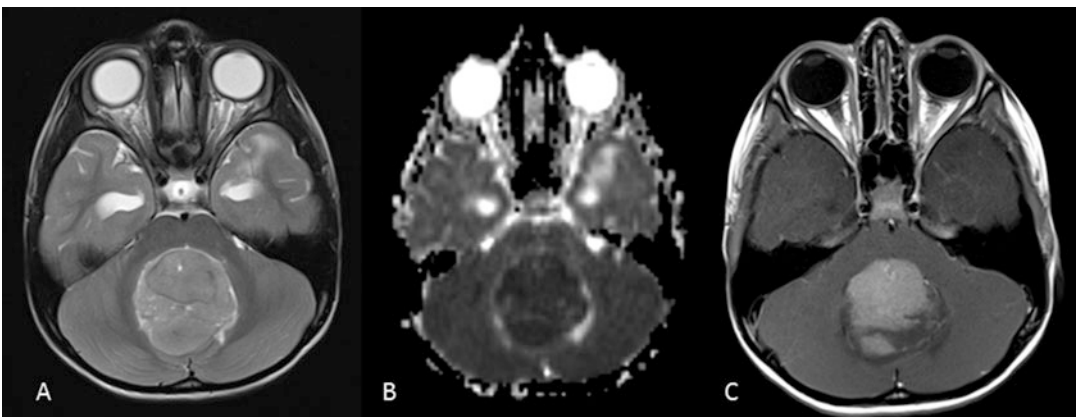
Fig. 3 Medulloblastoma, classic histological type, WHO grade IV (molecular subgroup 3/4): (**a**) axial T2 shows a large midline mass with associated hydrocephalus; (**b**) ADC map shows low ADC values in keeping with marked diffusion restriction (i.e., high cellularity); (**c**) axial post-contrast T1 shows that the mass enhances avidly. There is associated hydrocephalus (dilatation of the temporal horns of the lateral ventricles)

Imaging Pearls

Specific image patterns (together with different epidemiologic features and prognosis) can be associated to different histological and/or molecular MBLs subgroups as follows:

Histologic Subtypes

– Classic: most common histologic subtype accounting for the image findings described above (Fig. 3).


Fig. 4 Small non-enhancing MB noted in the fourth ventricle. Due to the lack of enhancement, the lesion is much better seen in axial T2 WI (arrows in **a**) than in sagittal T1 C+ (arrows in **b**)

– Desmoplastic: all desmoplastic are in the SHH group, although not all SHH are desmoplastic. This is a more hypocellular subtype and thus may have higher ADC values in comparison with the other subtypes and lower Cho/Cr and Cho/NAA ratios. On conventional images, there may be multiple enhancing nodules and presence of cystic components (Fig. 5).
– Extensive nodular: appearances similar to desmoplastic type.
– Anaplastic: very aggressive type. Low ADC values and internal necrotic areas due to high proliferative index. Metastatic deposits may be seen at presentation.

Molecular Subtypes

– WNT (10%): most of them represent the classic histological type. When not in the midline, the cerebellopontine angle, middle cerebellar peduncles, or foramina of Luschka are common locations (Figs. 6, 7, and 8).
– SHH (30%): located in the cerebellar hemispheres (peripheral location) due to their origin from the granular cells of the cerebellum (Fig. 9). They may also be in the midline when originating from the mesial aspect of the cerebellar hemispheres. They have desmoplastic/nodular, anaplastic, or classic features.
– Groups 3 and 4 (non-WNT/non-SHH): classic histological type, typical midline location.
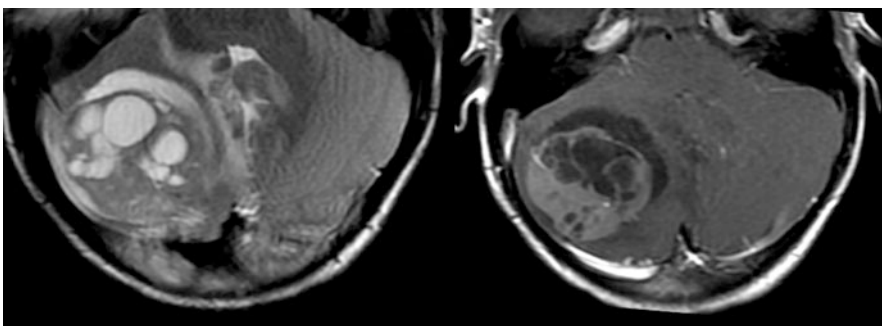

Fig. 5 Axial T2 left and T1 C+ right. Desmoplastic histological subtype. Note the hemispheric location in keeping with SHH molecular group
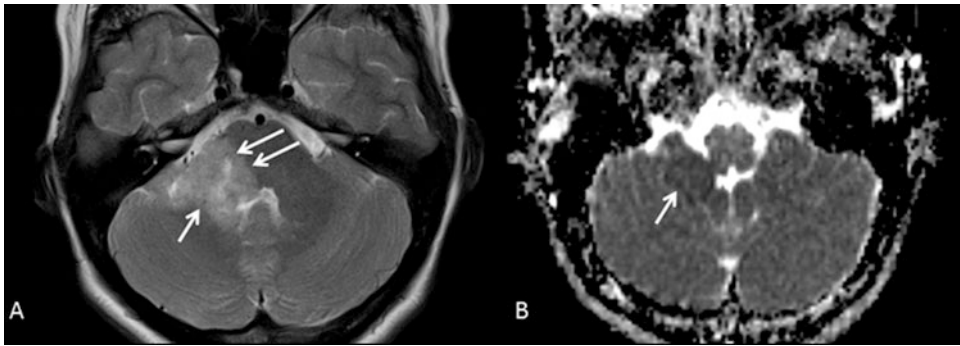
Fig. 6 Axial T2 WI (**a**) and axial ADC map (**b**). Typical location of MB WNT molecular subtype in the right middle cerebellar peduncle (arrows in **a**) with some extension in the pontocerebellar angle (arrow in **b**). Note the low ADC values in keeping with high cellularity (**b**)
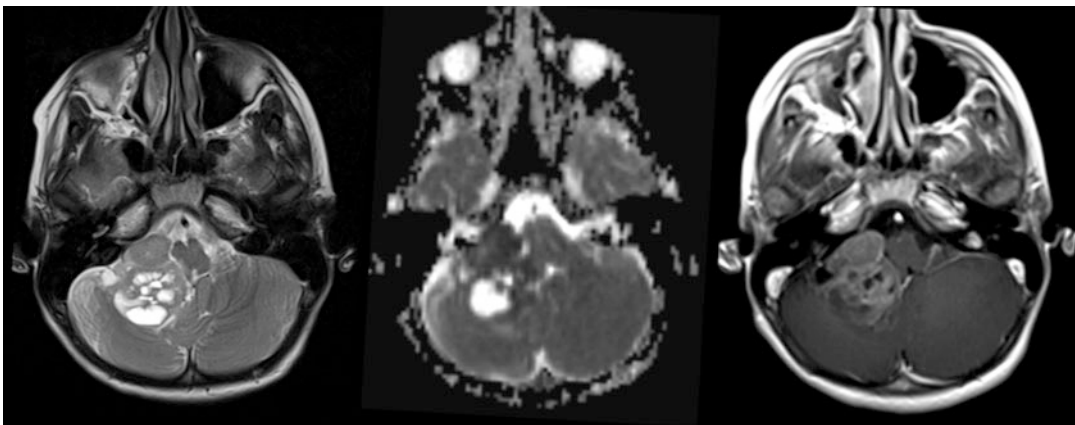
Fig. 7 Axial T2 WI (**a**), ADC map (**b**), and T1 WI C+ (**c**). Typical location of MB WNT in the right pontocerebellar angle. The structure of the mass is heterogeneous with multiple cystic areas. There is compression and distortion of the brain stem
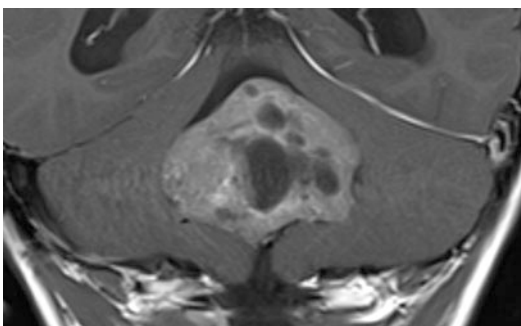
Fig. 8 Coronal T1 WI C+ shows midline location of MB WNT, indistinguishable from group 3 and 4 subtypes

Treatment Monitoring

Main therapeutic option is surgical resection followed by chemotherapy and cranio-spinal irradiation. Follow-up with full brain and spine with and without contrast is necessary to diagnose metastatic disease or local recurrence (Fig. 10). State-of-the-art follow-up schema includes pre- and postoperative images (within 72 h) and first surveillance MRI within 6 weeks after radiotherapy and since then every 12 weeks during chemotherapy, followed every 4 months thereafter.
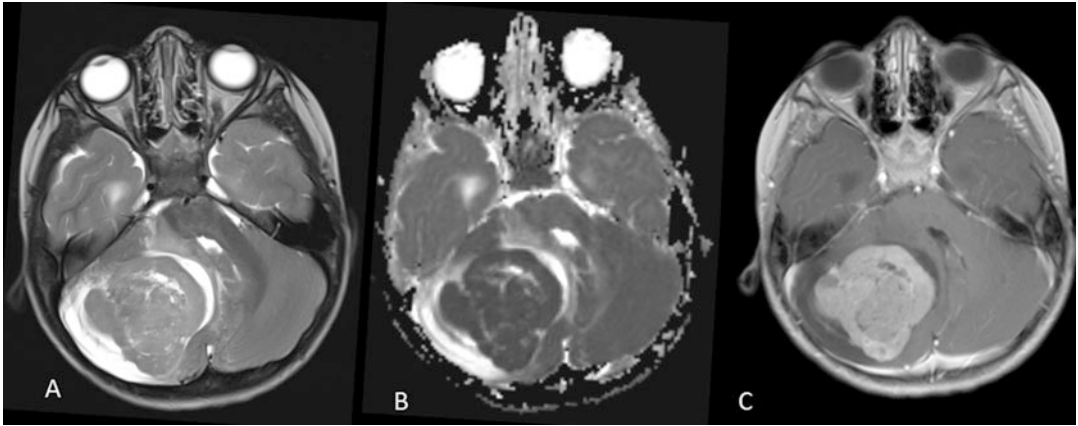
Fig. 9 Axial T2 WI (**a**), ADC map (**b**), and T1 WI C+ (**c**). Typical hemispheric location of MB SHH. Note relatively low T2 signal (**a**), very low ADC values (**b**), and avid post-contrast enhancement (**c**)
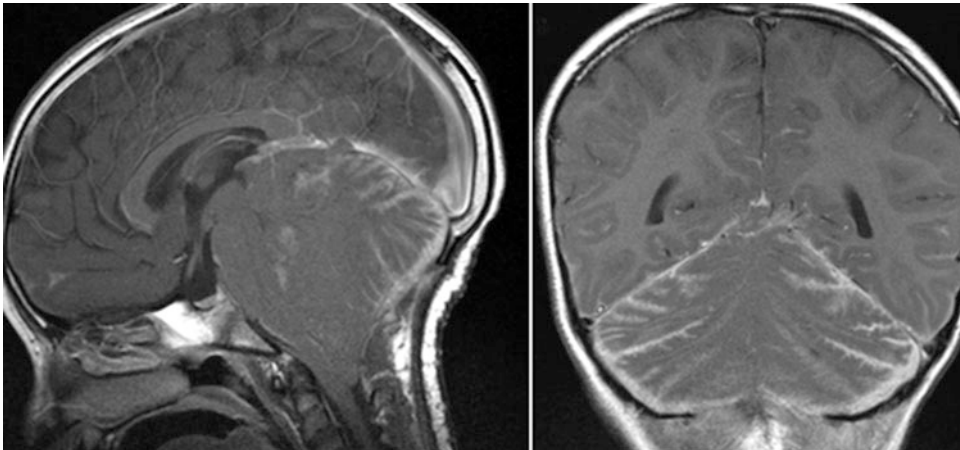
Fig. 10 Sagittal (left) and coronal (right) T1 WI C+ in a patient with high-risk medulloblastoma show diffuse leptomeningeal enhancement involving the infratentorial and, to a lesser extent, supratentorial compartments

Differential Diagnosis

– Atypical teratoid/rhabdoid tumor (AT/RT): not possible to distinguish AT/RT from MBL based on images as both have low ADC values, strong enhancement, and some degree of heterogeneity. As rule of thumb, children with AT/RT are younger than those with MBL.
– Posterior fossa pilocytic astrocytoma (PA): typical cystic and nodular appearance. Higher ADC values compared to MBLs due to lower cellularity. Typical location in the cerebellar hemispheres rather than the fourth ventricle.
– Ependymoma: more heterogeneous appearances (calcifications, hemorrhagic and necrotic areas). "Plastic" extension through the foramina of the fourth ventricle and the foramen magnum. ADC values are intermediate between PA and MBL.

Atypical Teratoid/Rhabdoid Tumors (AT/RTs)

Definition of Entity and Clinical Highlights

AT/RTs are rare highly malignant (WHO grade IV) relatively chemo-resistant tumors, which in the vast majority of cases occur in children younger than 2 years of age, with poorer survival rate than MBLs.

Basic Epidemiology/Demographics/Pathophysiology

Within registries, AT/RTs account for ~40%–50% of all embryonal CNS tumors in the first year of life. The median age of onset in most series is ~18 months. All series report a male predominance, with a 1.3 to 1.5 male to female ratio. AT/RT is the most common malignant CNS tumor in children below 1 year of age. Mutations in genes for components of the chromatin remodeling complex SWItch/sucrose non-fermentable (SWI/SNF) (foremost $SMARCB_1$, rarely $SMARCA_4$) have been recently identified. In the majority of the cases, the tumors were located within the cerebellum or fourth ventricle, followed by the hemispheres including the basal ganglia. Rarely, AT/RTs can be seen in the mesencephalic and pineal regions and in the spine. CSF seeding is common and may be found in 20–30% of cases at diagnosis.

Pathological Features

AT/RT features are similar to that of other small round blue cell tumors characterized by rhabdoid cells and primitive neuroectodermal tumor (PNET) cells (up to 70% of the cases). Necrosis and increased mitotic activity are common. Germ cell markers are negative. Diagnosis of AT/RT requires loss of either INI1 or BRG1 nuclear staining (Fig. 11).

Clinical Scenario and Indications for Imaging

Symptoms suggestive of increased endocranial pressure (headaches, emesis, lethargy and gait ataxia, and macrocephaly and developmental arrest in infants) and cranial nerve deficits consist the common clinical scenario. Hydrocephalus secondary to mass effect has been reported to range from 33% to 52%. Head cross-sectional imaging is indicated for initial assessment. Spinal imaging is indicated to rule out CSF seeding if AT/RT is suspected.

Imaging Technique and Recommended Protocol

Contrast-enhanced CT of the brain. Contrast-enhanced MRI of the brain (axial and coronal T2w/ FLAIR, axial DWI/ADC, 3D-T1w pre-
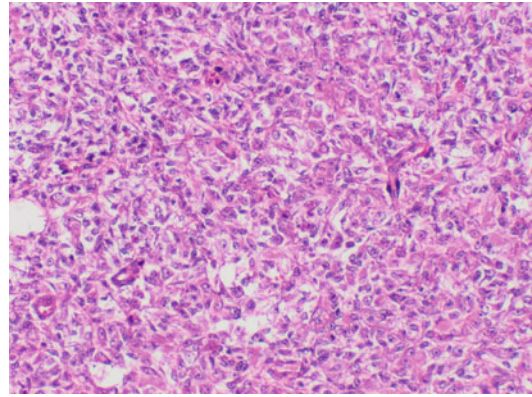
Fig. 11 H&E-stained high-power image of an atypical teratoid/rhabdoid tumor (AT/RT). The cell-dense tumor is composed of pleomorphic rhabdoid tumors cells and carries a typical SMARCB1 mutation

and post-contrast, or axial, coronal, and sagittal T1w post-contrast). Sagittal and axial post-contrast T1 of the spine.

Optional sequences: MRS and PWI (DSC) of the brain. Sagittal and axial T2w images of the spine.

Interpretation Checklist

Heterogeneous tumor with aggressive radiological features. The solid aspect of the tumor shows low ADC, contrast enhancement (90%), and low T2 signal (high cellularity). Very frequent presence of internal cystic-like areas, hemorrhagic foci, and leptomeningeal spread.

Location

Can be in both supra- and infratentorial compartments. In the posterior fossa often located in cerebellar hemispheres or pontocerebellar angle rather than vermis (Fig. 12); in the supratentorial compartment, it can involve the cerebral hemispheres or the midline (i.e., pineal region).

CT Findings

Hyperdense mass in the posterior fossa or supratentorial compartment. The high density in CT reflects the high cellularity (Fig. 13). AT/RT may appear very heterogeneous in comparison to MBL (although there is some overlap) for the presence of blood, cysts, and calcium.
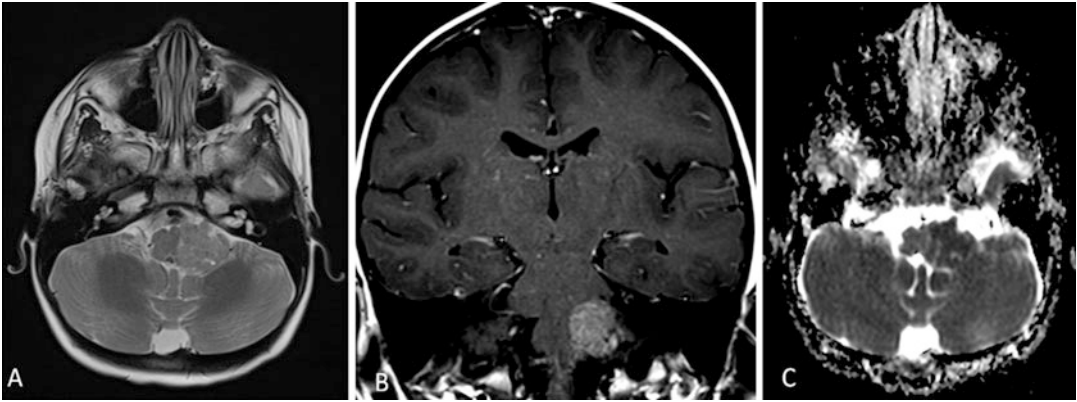
Fig. 12 Axial T2 WI (**a**), coronal T1 WI C+ (**b**), and axial ADC map (**c**) in a 2-year-old male with AT/RT in the left pontocerebellar angle. The tumor is relatively small at the diagnosis and shows relatively low T2 signal (**a**), marked contrast enhancement (**b**), and low ADC values (**c**)

Fig. 13 Axial unenhanced CT shows spontaneous increase of the density in AT/RT (arrow)
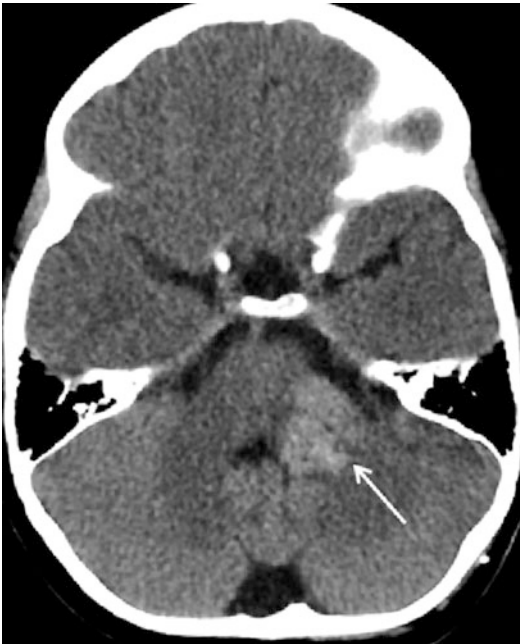
MR Findings

T2w: these tumors are hypointense to white matter (high cellularity) with possible heterogeneity due to hemorrhagic/cystic components (Figs. 12a and 14).

DWI: there is evident diffusion restriction (low ADC values) of the solid components (Fig. 15a, b).

It is important to consider DWI for early diagnosis of metastatic deposits in non-enhancing AT/RTs.

T1w with contrast: the majority of AT/RTs show heterogeneous pattern of enhancement (Figs. 12b and 14 bottom row). Ten percent show no enhancement. Nodular leptomeningeal enhancement in case of metastatic dissemination in the brain and spine.

MRS: increased Cho, markedly reduced NAA, prominent lipid peak (non-specific aggressive MRS features) (Fig. 15b).

Pearls

- Posterior fossa aggressive tumors in children: main differential MBL vs AT/RT. If the patient is younger than 3 years and the mass is heterogeneous, not on the midline, and/or extends in the pontocerebellar angle, consider AT/RT. There is overlap on imaging with off-midline MBL (e.g., WNT), but age group is different (older patients have WNT).
- Possible association with synchronous extra-neural rhabdoid tumors have been described in patient with embryonal tumors and SMARC B1 mutation (AT/RT or pinealoblastoma) (Fig. 16).

Treatment Monitoring

Aggressive surgical resection followed by chemo−/radiotherapy. Follow-up with full brain and spine with and without contrast is indicated to diagnose metastatic disease or local recurrence.
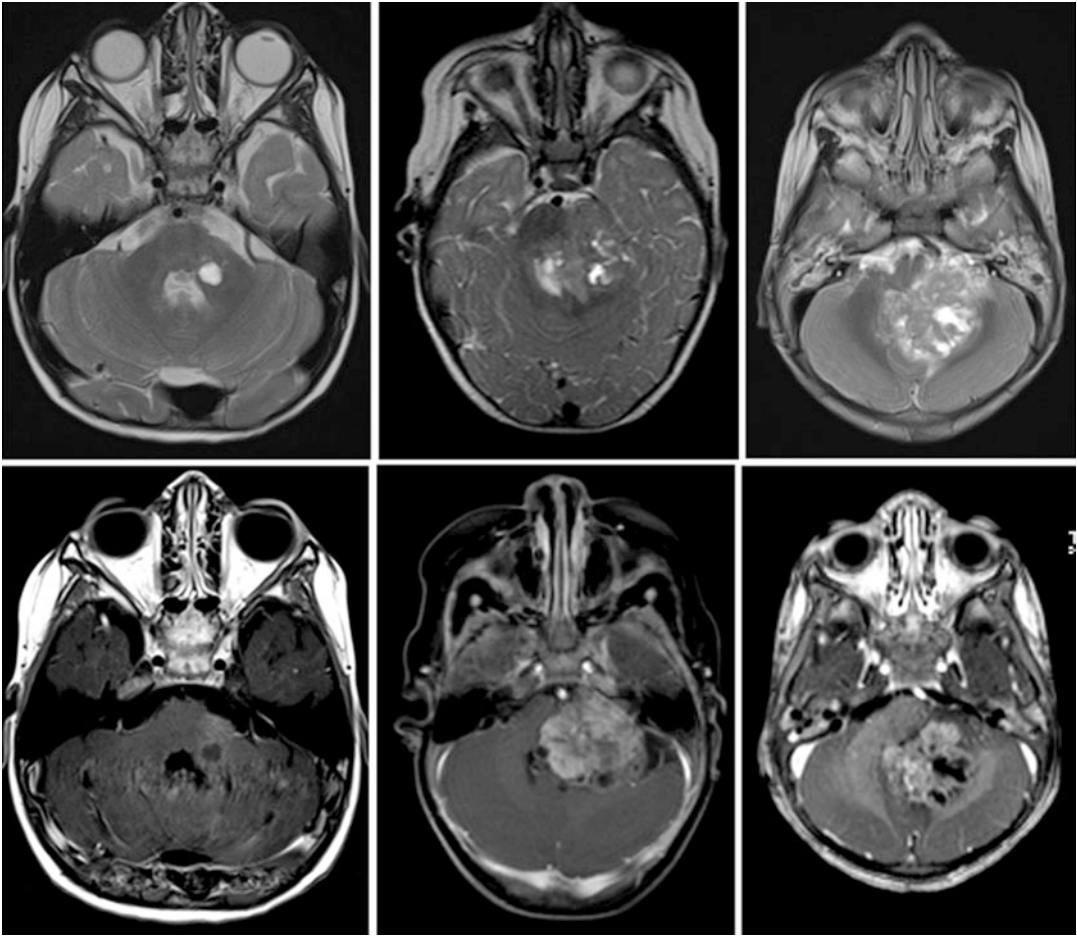
Fig. 14 Heterogeneous appearance of AT/RT. Axial T2 WI (upper row) and axial T1 WI C+ in three different patients with posterior fossa AT/RT show typical heterogeneity of these tumors with multiple cystic areas and enhancement of the solid component. The patient on the left is the same of image 6 one slice above, showing that cysts may be present also in small tumors. Note the typical off-midline location of the posterior fossa AT/RT

Differential Diagnosis

– **Medulloblastoma**: Overlap in radiological findings. Children with MB are often older; the mass is more homogeneous in appearance and frequently on the midline.
– **Teratoma**: Midline supratentorial mass with calcium, hemorrhages, and fatty components.
– **Ependymoma**: "Plastic" extension through the foramina of the fourth ventricle and the foramen magnum. ADC values of solid component are higher than AT/RT.

Cerebellar Pilocytic Astrocytoma (CPA)

Definition of Entity and Clinical Highlights

Low-grade, slow-growing, relatively well-defined astrocytomas that are considered WHO grade I tumors in the current (2016) WHO classification of CNS tumors and correspondingly have a relatively good prognosis. A range of imaging appearances is characteristic of this tumor class, with the majority presenting as a large cystic lesion with a brightly enhancing mural nodule.
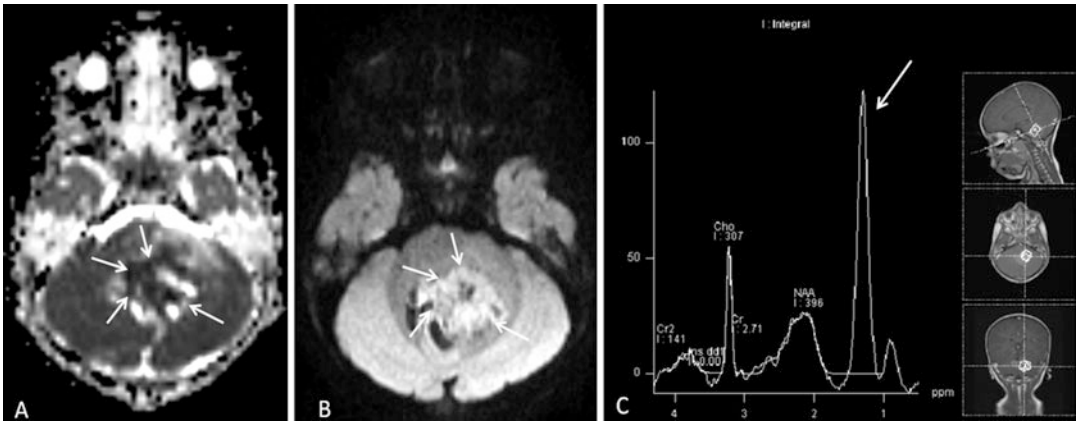
Fig. 15 Axial ADC (**a**) and DWI (**b**) in a 2-year-old male with posterior fossa AT/RT show marked diffusion restriction (arrows in **a** and **b**). MR spectroscopy (single voxel) shows marked lipid peak at 1.3 ppm (arrow in **c**) and reduction of NAA
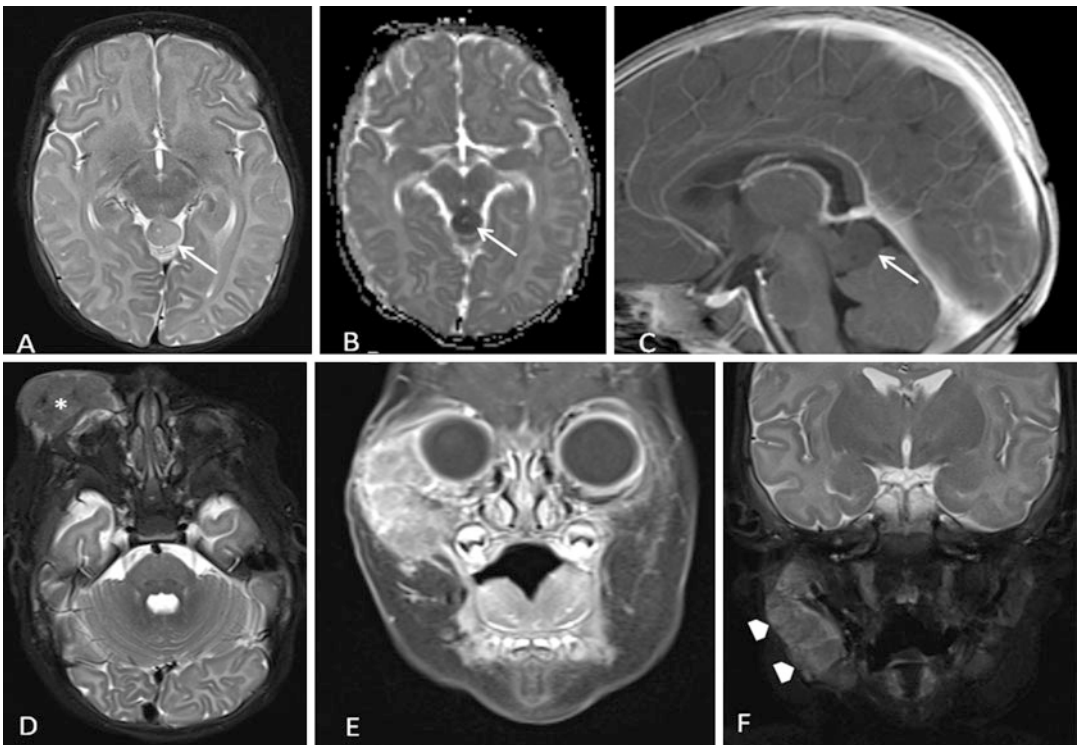
Fig. 16 Axial T2 WI (**a**, **d**), axial ADC (**b**), sagittal T1WI C+ (**c**), coronal T1 WI C+ (**e**), and coronal T2 WI STIR (**f**) in a 10-week-old female with SMARC B1 mutation. There is a supratentorial embryonic tumor in the pineal region (arrow in **a**) that shows diffusion restriction (arrow in **b**) but no enhancement (arrow in **c**). There is the presence of a synchronous lesion in the right periorbital lesion proven to be a rhabdoid tumor (asterisk in **d**) and metastatic nodes in neck (arrowheads in **f**)

Basic Epidemiology/Demographics/Pathophysiology

The most common primary brain tumor of childhood (23.5%) without gender predisposition, accounting for 70–85% of all cerebellar astrocytomas. 75% of PAs occur in the first two decades of life, typically late in the first decade (9–10 years). Pilocytic astrocytomas are slow-growing, and, although many are cured by gross total resection, approximately 20% are located at unresectable sites such as the optic tract and hypothalamus and therefore tend to recur.

Pathological Features

PAs, compared with the fibrillary astrocytomas, feature elongated cells with long processes that form a densely fibrillary background, alternating with regions of loose and microcystic appearances. Rosenthal fibers are frequently observed serving in differentiating these tumors from other astrocytic gliomas. The KIAA1549-BRAF fusion is a useful putative diagnostic marker particularly for PAs, which can show the neuropathologic features of necrosis and microvascular proliferation, which are also seen in high-grade gliomas. Younger patients with infratentorial posterior fossa PAs tend to display a high frequency of the KIAA1549-BRAF fusion. Supratentorial tumors are less frequently fusion positive but have an increased frequency of the oncogenic BRAF V600E mutation. Pilocytic astrocytomas seen in conjunction with neurofibromatosis type 1 lack this fusion gene.

Clinical Scenario and Indications for Imaging

The presenting usually insidiously developing symptoms of these tumors are commonly headache, vomiting, mental change, gait ataxia, tremors, and dysmetria. A low rate of spontaneous though extremely rarely symptomatic hemorrhages in PAs has been reported.

Imaging Technique and Recommended Protocol

Contrast-enhanced MRI of the brain and spine. MRS and PWI can be misleading because PA can mimic high-grade tumors (lipid/lactate peaks and high perfusion values due to pronounced vascularity in PAs). Spine imaging is important to rule out leptomeningeal metastases, which is rare.

Interpretation Checklist and Structured Reporting

Slow-growing tumor in the cerebellar hemisphere. Absence of relevant diffusion restriction, marked enhancement, and presence of cystic component are typical image findings. Absence of cysts does not exclude diagnosis of PA. Usually PAs appear as well-defined mass; however rarely the tumor may be infiltrative with no clearly defined margin, which renders difficult the complete surgical resection.

CT Findings

Solid-cystic mass with hypodensity of the solid component. Marked enhancement of the solid component and of the cyst walls. Associated obstructive hydrocephalus is the most important indirect sign of a mass in the posterior fossa compressing the fourth ventricle.

MR Findings

T2w: solid components are hyperintense to gray matter (low cellularity). Cystic components are isointense to CSF (Fig. 17a). Hemorrhagic foci are possible. The cysts can be slightly hyperintense to CSF in T1 and FLAIR in case of high proteinaceous content (Fig. 17b). Presence of hemorrhagic changes has been described and represents a possible pitfall, mimicking high-grade tumor.

DWI: the solid part of the tumor has low ADC values (absence of diffusion restriction, i.e., low cellularity) (Fig. 17c). Small percentage of PAs (< 10%) can have diffusion restriction due to abundant extracellular matrix.

T1w with contrast: intense enhancement of the solid portion (Fig. 17d). Possible enhancement of the cystic wall. Leptomeningeal dissemination, if present, is evident in post-contrast T1w (Fig. 18).

MRS: increased Cho and lactate/lipid peak (aggressive-like features) (Fig. 19).

PWI: variable, possible high perfusion due to high vascularity of PAs (Fig. 20).
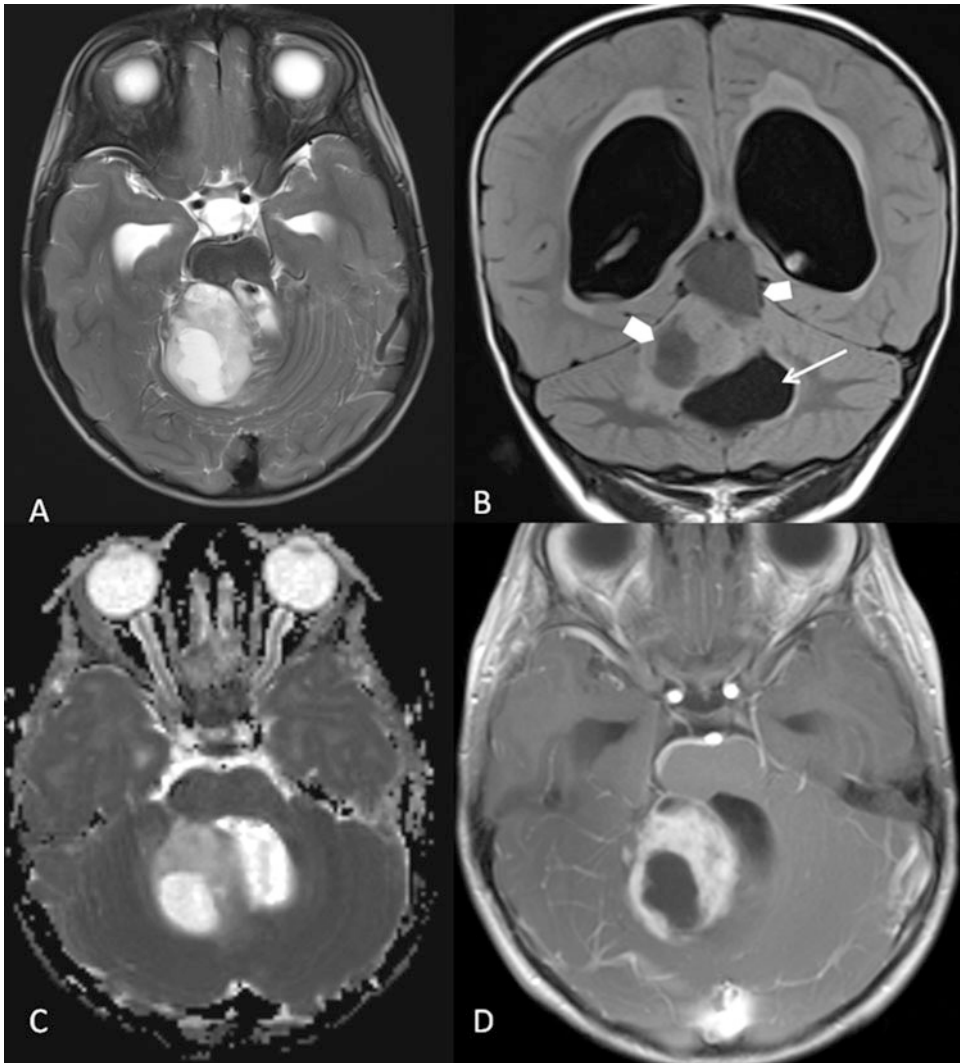
Fig. 17 Axial T2 WI (**a**), coronal FLAIR (**b**), axial ADC (**c**), and axial T1 WI C+ (**d**) in a 2-year-old male with posterior fossa PA. The solid component enhances heterogeneously and shows high ADC values (in keeping with low cellularity). There are two cystic components (arrowheads in **b**) and obstruction of the cerebral aqueduct with consequent dilatation of the IV ventricle (arrow in **b**) and supratentorial hydrocephalus

Pearls

Presence of features resembling high-grade tumors has been described in case of PAs. These include high perfusion, increased Cho and lipids/lactate on MRS, internal bleeding, and, rarely, some degree of diffusion restriction.

Treatment Monitoring

Total surgical resection. Follow-up post-contrast cranio-spinal imaging is necessary. The 5-year survival in PAs is reported as high as 100% when the tumor can be completely resected.

Differential Diagnosis

– **Medulloblastoma**: Typically, hyperdense on CT and with low ADC values (high cellularity). Midline MBLs fill rather than displace the IV ventricle, and internal cysts (when present) are smaller than MBL.

Fig. 18 Sagittal T1 WI C+ of the brain (**a**, **b**) and spine (**c**) in a patient with low-grade astrocytoma of the posterior fossa show pathological leptomeningeal enhancement along the temporo-insular region (arrows in **a** and **b**) and a metastatic nodule abutting the anterior aspect of the conus medullaris (arrow in **c**)

– **Hemangioblastoma**: Strongly enhancing nodule abutting the pia mater with large cystic component. Not infrequently the mural nodule itself has cystic spaces within it. The cyst wall usually does not enhance. The tumor often has prominent serpentine flow voids. Typically, in adult patients with von Hippel-Lindau syndrome.
– **AT/RT**: More aggressive features (similar to MBL) and younger children.
– **Ependymoma**: "Plastic" extension through the foramina of the fourth ventricle and the foramen magnum. ADC values are intermediate between PA (high) and MB and AT/RT (low).

Infratentorial Ependymoma (EPN)

Definition of Entity and Clinical Highlights

EPNs are one of the most common pediatric malignant brain tumors. Prognosis, especially in young children, remains poor due to their inherent chemo- and radioresistance; up to 50% patients may die from the disease. There has not been a significant therapeutic change in the last 20 years.

Basic Epidemiology/Demographics/ Pathophysiology

EPN is the third most common brain tumor in children after astrocytomas and MBLs. They account for up to 33% of pediatric brain tumors occurring less than 3 years of age. It can be located anywhere in the CNS, but is predominantly found in the posterior fossa in children and the spine and supratentorial regions in adults. Myxopapillary ependymomas, presenting with papillary pattern and myxomatous material on light microscopy, occur in the region of the cauda equina.

Pathological Features

Histologically, EPNs resemble the ependymal cells that line the ventricular system. The exact number of molecular subclasses of EPNs is not completely fixed, but there are at least two posterior fossa subtypes. Group A patients are younger, have laterally located tumors with a balanced
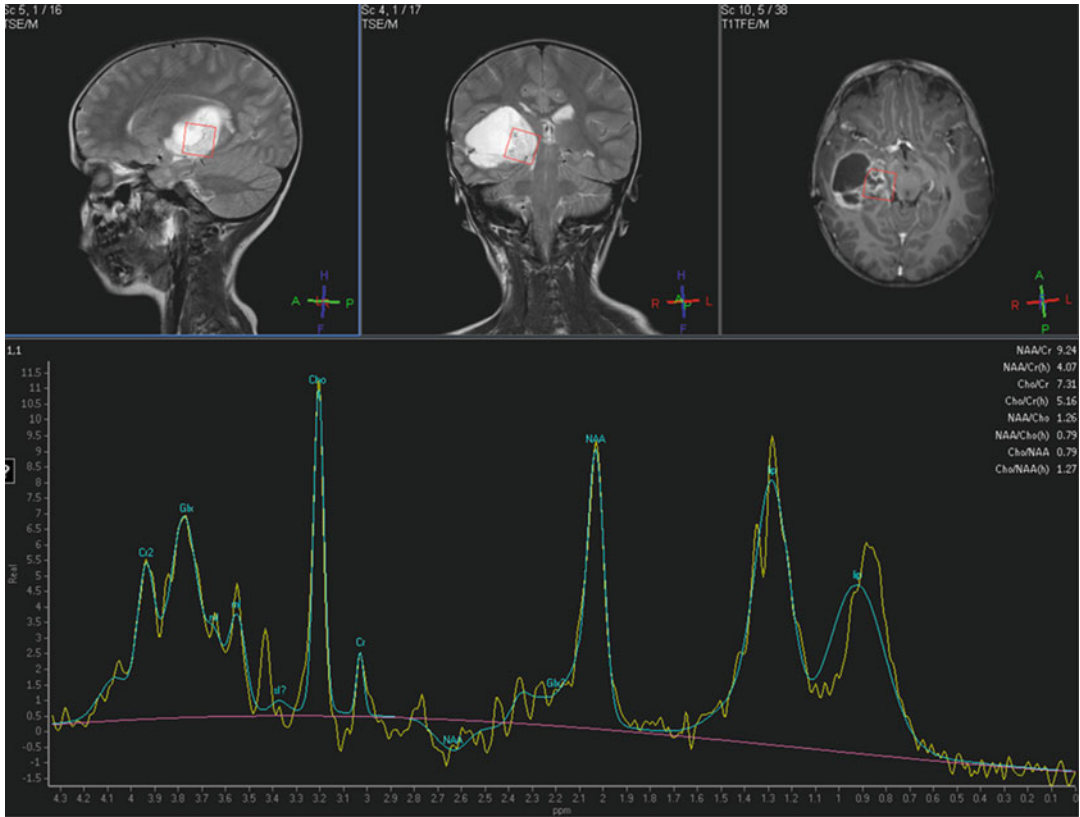
Fig. 19 Confirmed pilocytic astrocytoma (supratentorial) showing typical MRS findings simulating high-grade tumor (i.e., Lac/Lip peaks at 1.3 and 0.9 ppm)
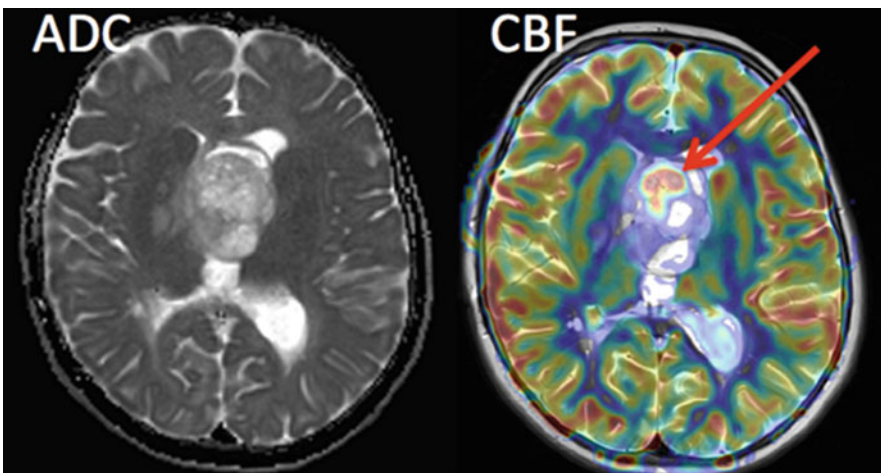
Fig. 20 Axial ADC map (left) and ASL perfusion CBF map (right) in a supratentorial PA. Despite the high ADC values, there is increase CBF of the tumor (red arrow). (Courtesy of Dr. P. Hales, Institute of Child Health – University College of London – UK)
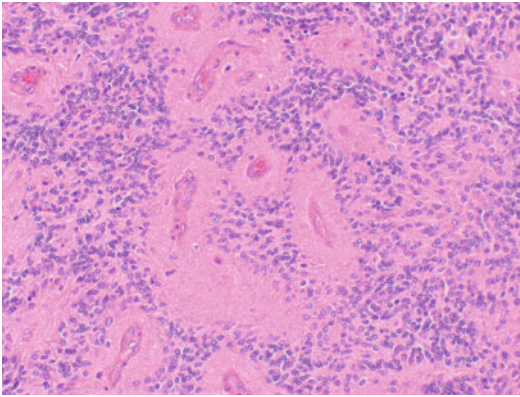
Fig. 21 H&E-stained high-power image of an ependymoma with typical perivascular pseudorosettes

genome, and are much more likely to exhibit recurrence, metastasis at recurrence, and death compared with Group B patients. The most highly differentially expressed genes in Groups A and B revealed candidate marker genes for distinguishing the two groups, the most striking being upregulation of LAMA2 in Group A and NELL2 in Group B. Except for neurofibromatosis type 2, where ependymoma tends to be confined to the spinal cord, no real predisposition syndrome has been linked to ependymoma, and most cases are sporadic (Fig. 21).

Clinical Scenario and Indications for Imaging

Signs and symptoms of raised intracranial pressure are common, particularly with tumors in the fourth ventricle. Other posterior fossa symptoms including ataxia are also reported. Spontaneous hemorrhage is an infrequent clinical manifestation. Head cross-sectional imaging is indicated for initial assessment. Spinal imaging is indicated to rule out CSF seeding if EPN is suspected.

Imaging Technique and Recommended Protocol

CT without contrast may help the diagnosis due to the relatively high frequency of calcifications. Contrast-enhanced MRI of the brain and spine, ideally with high resolution, sagittal T2 to distinguish the origin from the floor of the fourth ventricle. MRS and PWI can help the diagnosis. Spine imaging is mandatory before tumor resection.

Interpretation Checklist and Structured Reporting

Posterior fossa mass with "plastic" extension through the outlet foramina of the fourth ventricle and in the cerebellopontine angle. The mass is typically heterogeneous in appearances with presence of calcium, hemorrhagic components, and cysts. Indistinct separation with the floor of the fourth ventricle is characteristic and may help in differential diagnosis with midline MB. It is not possible to distinguish on imaging between grade II and III ependymomas.

CT Findings

Non-enhanced CT shows calcifications (present in 50% of EPN) (Fig. 22a). Heterogeneous enhancement on CECT. As for the other posterior fossa masses in children, there may be associated hydrocephalus.

MR Findings

T2w: Heterogeneous appearances. The solid part is, as a general rule, more hyperintense in comparison with MB and AT/RT; however this is not always the case especially in anaplastic subtype (Fig. 22b). Cystic high signal areas + low signal foci due to Ca^{++} or blood (Figs. 22, 23, and 24).

T1w: Heterogeneous appearances. Cystic areas may be hyperintense to the CSF (high proteinaceous content). Foci of hyperintense signal are related to calcium or blood (Fig. 24b).

DWI: ADC values are intermediate between PA and MBL or AT/RT. Although areas of restriction are more suggestive of grade III (anaplastic) EPN, there is an overlap between ADC values of grades II and III. Furthermore, some degree of overlap is described also with MBL. Presence of blood or calcium within the EPN can complicate the appearance on DWI (Fig. 24c, d).

T2*GRE/SWI: "Blooming" artifact due to Ca^{++} or blood.

T1w with contrast: Heterogeneous enhancement of variable degree (mild to moderate) (Fig. 22).

MRS: On short TE there is typical high myo-inositol (mI). Reduction of the NAA/Cho ratio has also been described, but this is higher than described MBL and non-specific for ependymoma.
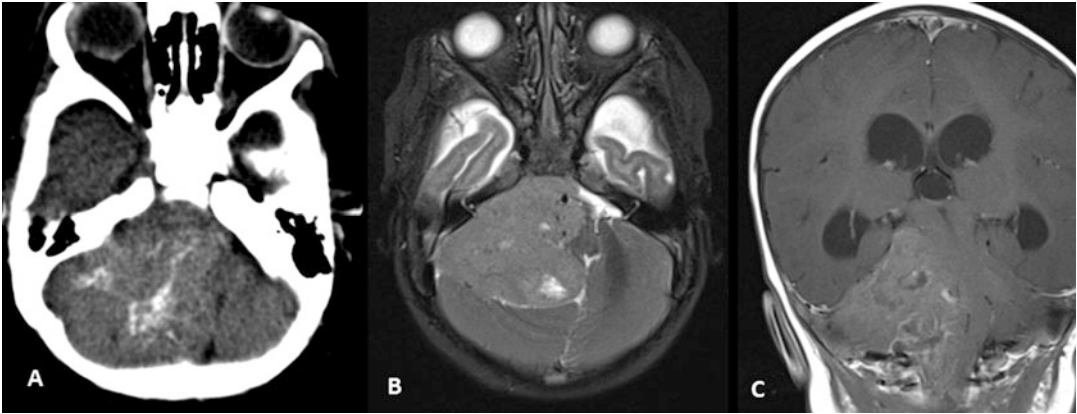
Fig. 22 Axial NECT (**a**), axial T2 WI (**b**), and coronal T1 C+ (**c**) in a 1-year-old boy with ependymoma show internal calcification clearly evident in CT and mild contrast enhancement (**c**). Note atypical low signal in T2

Fig. 23 Post-contrast sagittal T1 shows (**a**) inhomogeneous contrast enhancement. Axial T2 (**b**) shows extension through the right foramen of Luschka (red arrows) and some small foci of hemorrhage (blue arrow)

PWI: Marked elevation of the rCBV with incomplete recovery of the time signal intensity curve to the baseline.
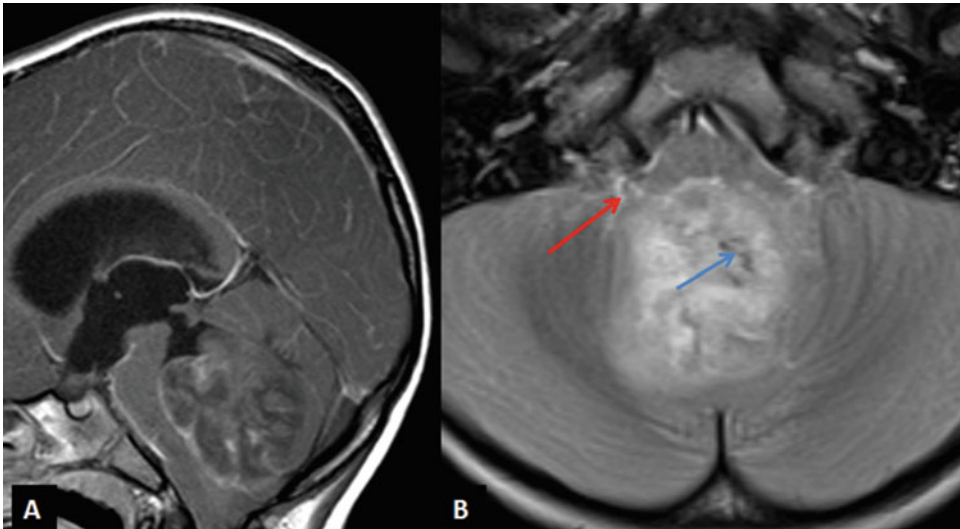
Pearls

Heterogeneous, plastic mass with no clear border with the floor of the fourth ventricle (Fig. 25). The presence of CSF spread is rare in EPN (~10%) and may help in differential from MBL.

Treatment Monitoring

Complete surgical resection may be challenging due to infiltration of the surrounding structures by the tumor; however it is critical to improve survival removing any small residual areas. RT follows resection. The median time of the first recurrence is around 1 year (range 3–65 months). Increasing age (adults vs children), spinal location, and complete resection are associated with improved survival. Suggested surveillance
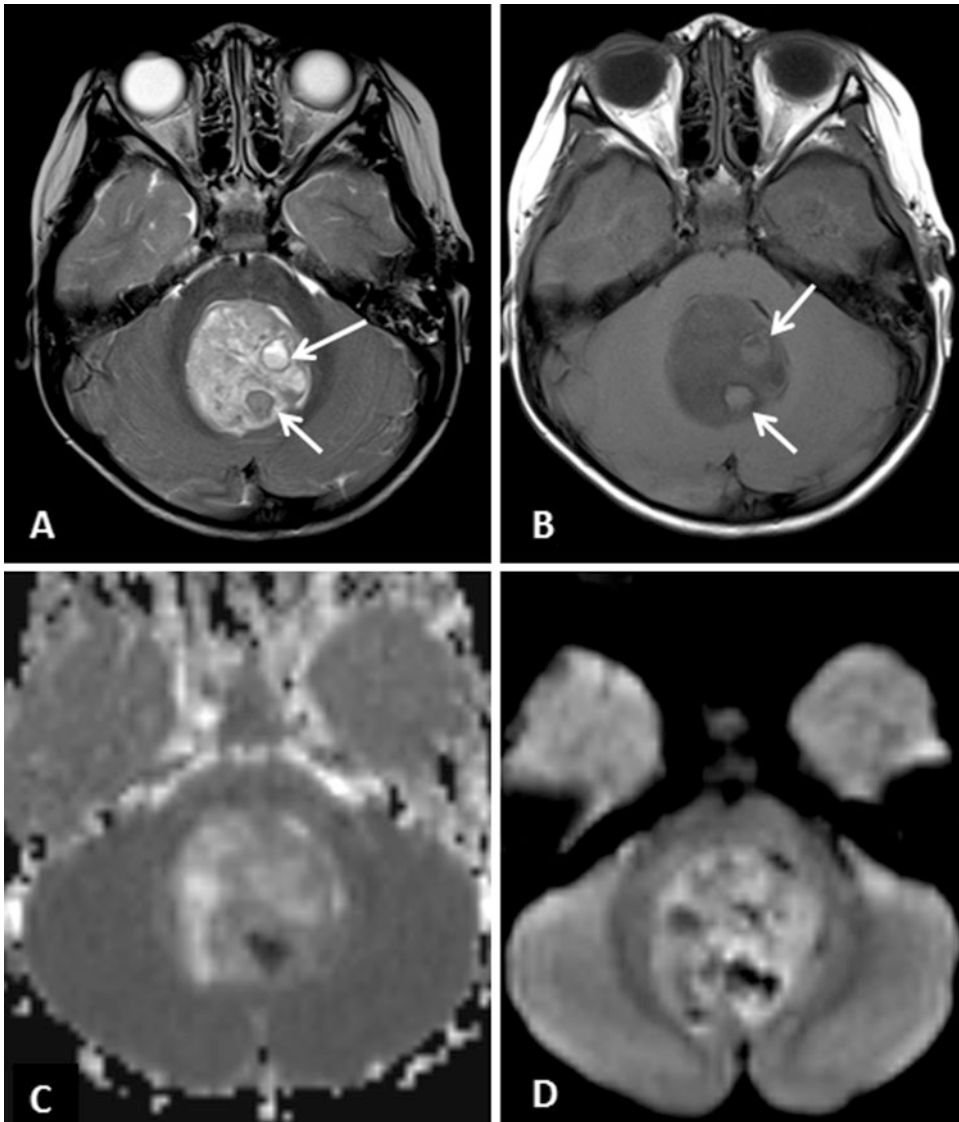
Fig. 24 A 3-year-old female with anaplastic ependymoma. Axial T2 WI (**a**), axial T1 WI (**b**), axial ADC (**c**), and DWI (**d**). The mass shows typical heterogeneous appearance with internal, partially hemorrhagic cysts (arrows in **a** and **b**) and no diffusion restriction of the solid component

protocol is 24–48 h after surgery, then 3–6 months for the first year, and every 6 months afterward.

Differential Diagnosis
– **Medulloblastoma (MBL)**: hyperdense on CT and with low ADC values (high cellularity). Midline MBLs originating from the roof of the fourth ventricle (rather than the floor). More homogeneous mass.

– **Pilocytic astrocytoma (PA)**: the solid portion is more homogeneous. Typical appearance of nodule and cyst helps the diagnosis. Rare internal calcifications and hemorrhages.
– **AT/RT**: can be very heterogeneous but shows aggressive radiological features in the solid portion (i.e., low ADC values).
– **Choroid plexus papilloma**: posterior fossa CPP is more common in adults and in lateral
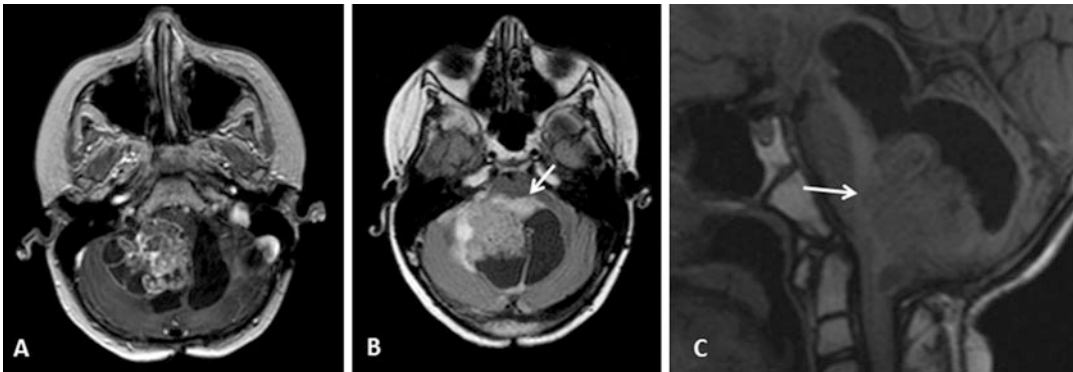
Fig. 25 Axial T1 WI C+ (**a**) and axial FLAIR WI (**b**) show marked heterogeneous appearance of the tumor and the enhancement of the solid part. On sagittal FLAIR (**c**) it is evident the infiltration of the floor of the brain stem which helps in the differential with MB

ventricles in the pediatric population. Strongly enhancing "cauliflower-like" mass with speckled calcifications in some cases. Hydrocephalus is common.

– **Brain stem glioma**: location is critical; they are within the brain stem and may protrude posteriorly in the fourth ventricle either flattening of the floor of the fourth ventricle ("flat floor of fourth ventricle sign") or exophytically outward into the basal cisterns and fourth ventricle. Usually homogeneous tumor (prior to any treatment) with possible necrotic foci.

Brain Stem Gliomas

Diffuse Midline Gliomas (DMGs): Formerly Diffuse Intrinsic Pontine Gliomas DIPGs

Definition of Entity and Clinical Highlights

According to the 2016 update to the WHO classification of CNS tumors that utilizes integrated diagnosis incorporating both morphologic and molecular features, these tumors are classified under diffuse midline glioma, H3-K27 M-mutant. DMGs are the main cause of brain tumor-related death in children with a median survival of approximately 10 months and <10% 2-year survival. In the majority of cases diagnosis is based on clinical and MRI findings.

Basic Epidemiology/Demographics/Pathophysiology

DMGs typically manifest in childhood (3–10 years of age) and account for 20–30% of pediatric posterior fossa tumors. They are the most common type of brain stem glioma, accounting for 60–80% of these tumors. There is an association with neurofibromatosis type I, which however carries a better prognosis with a more indolent course.

Pathological Features

DMGs are usually high-grade astrocytomas, although up to 25% share histological features with low-grade counterparts. Remarkably, histopathologic grade does not correlate with prognosis and behave aggressively with poor prognosis.

Mutually exclusive mutations in either H3F3A, one of two genes encoding the histone H3.3 variant, or HIST3BHI, one of several genes encoding histone H3.1, have been identified in nearly 80% of DMGs. Genomic analysis of DMGs with histone H3-K27 M mutations (K27 M+) has revealed that these tumors often also carry TP53 (present in 40–77% of cases) and ATRX mutations but do not have IDH1/2 mutations. A subset of K27 M+ DMGs were found to also harbor missense mutations in the ACVR1 (recurrent somatic mutations in activin A receptor gene, type 1), whereas other occasional alterations include PIK3CA mutation, PDGFRA (platelet-derived growth factor receptor) mutation or amplification, PPM1D mutation, and
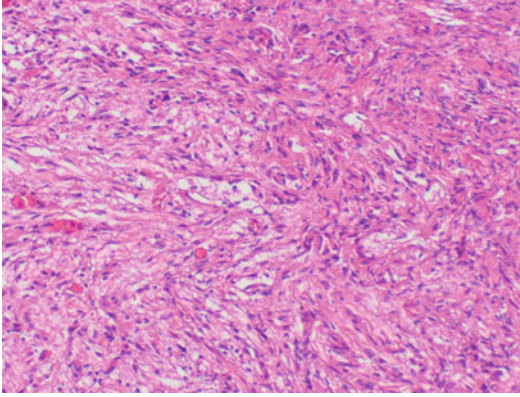
Fig. 26 H&E-stained high-power image of a diffuse midline glioma with a H3.3-K27 M mutation. Note the astrocytic differentiation and pleomorphism of the tumor cells

amplification of cell cycle genes including CCND1, CDK4, and CDK6. H3-K27 M+ DMGs arise also in the thalamus, pons, and spinal cord of children and young adults and are associated with poor prognosis. They are by definition WHO grade IV even when they have the histologic/radiological appearance of a low-grade glioma (Fig. 26).

Clinical Scenario and Indications for Imaging

The diffusely infiltrative tumor pattern results in multiple cranial nerve palsies, and its intrinsic and possibly exophytic growth may raise the intracranial pressure. Cerebellar signs including ataxia, dysarthria, nystagmus, and sleep apnea are frequently reported.

Imaging Technique and Recommended Protocol

MRI of the brain and spine with contrast is the state-of-the-art modality; PWI, DTI, and MRS may increase diagnostic sensitivity. Special attention should be paid to obtain sagittal T2-weighted images.

Interpretation Checklist and Structured Reporting

Tumor is centered within the pons, which is expanded with consequent effacement of the surrounding CSF spaces. There is often typical encasement of the basilar arteries (Fig. 27a, b). Usually pontine DMGs do not enhance (Fig. 27d, e); however localized areas of enhancement (correlated with lower T2 signal and lower ADC values) have been described as areas of focal anaplasia and consist a possible target of biopsy, if needed.

CT Findings

Expansive mass in the brain stem with reduced density, effacement of the surrounding cisterns. Often the hydrocephalus is not present at diagnosis (DDX with other posterior fossa masses in children) (Fig. 27a).

MR Findings

T1w: brain stem expansion. The mass is centered in the pons and shows moderate hypointense signal (Fig. 28).

T2w: hyperintense mass. Some areas of relative hypointensity may represent areas of higher cellularity but need to be differentiated from spared white matter tract. The encasement of the basilar artery (when present) is well seen on axial T2 (Fig. 27b, c).

DWI: as a general rule, pontine DMGs do not show restriction; however some areas of restriction are associated with areas of anaplasia (together with relatively low T2 signal and/or contrast enhancement) (Fig. 29a, c).

T2∗ GRE/SWI: possible foci of "blooming" in case of internal hemorrhages.

T1w with contrast: they usually do not enhance. There may be focal areas of enhancement associated with high grade (Fig. 29b). Metastatic dissemination is possible in the infra- and supratentorial compartments and in the spine.

PWI: related to the tumor grade, generally low perfusion (Fig. 27f). Areas of higher perfusion may indicate more aggressive behavior and can be used as target for biopsy.

MRS: decrease of NAA/Cho ratio associated with worse prognosis and/or disease progression. Reduction of citrate levels can be related to therapy (i.e., RT, steroids) or indicate malignant transformation. Presence of lactate indicates necrosis (Fig. 29d).
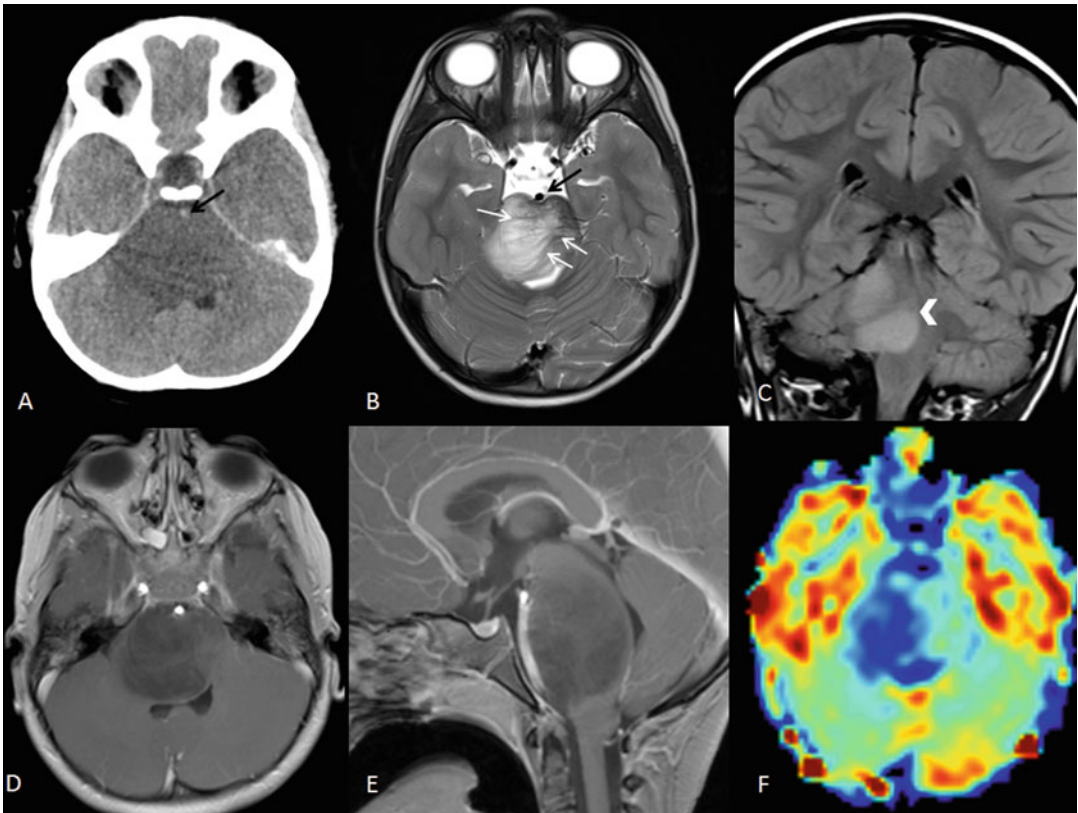
Fig. 27 Axial unenhanced CT (**a**), axial T2 (**b**), coronal FLAIR (**c**), axial and sagittal T1 C+ (**d** and **e**), and axial ASL perfusion rCBF map (**f**). Characteristic infiltrative nature of the tumor is evident with encasement of the basilar artery (black arrow in **a** and **b**). Note the presence of spared white matter tracts (white arrows in **b**) and absence of enhancement or areas of pathological increase of perfusion (**d**–**f**). There is mass effect on the midline (arrowhead in C). The area of slight increase of the perfusion noted in the left side of the pons (**f**) corresponds to spared white matter fibers and not to an area of high cellularity

Pearls

– Invasion of the middle cerebellar peduncles/cerebellar white matter, midbrain, or medulla oblongata is associated with more aggressive behavior (Fig. 30).
– Changes in the pattern of enhancement are possible during treatment and of uncertain significance.
– Areas of enhancement/increased perfusion/low T2 signal (not related to spared white matter fibers)/diffusion restriction should guide biopsy.
– DMGs are identified on the basis of the presence of H3-K27 M mutation irrespective of their location (supra- or infratentorial). It is important than to consider DMGs in the differential of supratentorial gliomas in children (Fig. 31).
– Spinal seeding is rare but can be observed in the end stages of the disease.

Treatment Monitoring

DTI, perfusion imaging, and MRS should be used as they have demonstrated promising prognostic significance. T2 hypointense areas and/or areas of reduced ADC and/or areas of increase perfusion have been reported as the most significant to assess the tumor response.

Differential Diagnosis

Main differential includes low-grade gliomas (non-DMG) of the brain stem often located in
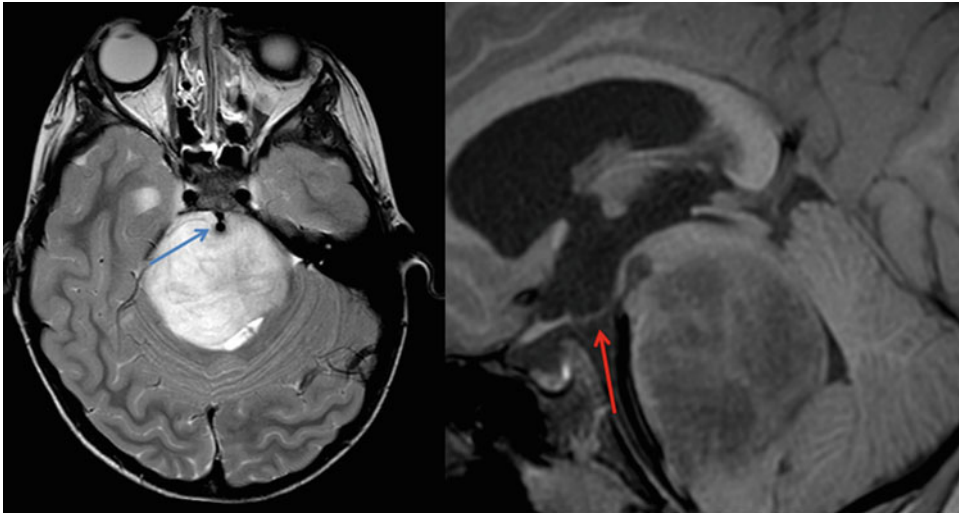
Fig. 28 Axial T2 (left) and sagittal T1 (right). Diffuse midline glioma located in the pons with typical expansion of the pons, encasement of the basilar artery (blue arrow), obstruction of the fourth ventricle, and associated hydrocephalus (red arrow: inferior bulging of the floor of third ventricle)

the medulla (usually pilocytic astrocytomas) or in the tectum (Fig. 32). Pilocytic astrocytomas show enhancement; tectal low-grade gliomas often do not enhance and may be associated with hydrocephalus. White matter tract disruption in DTI suggests DMG rather than the relatively uncommon focal brain stem glioma, which demonstrates a sharply demarcated mass with relatively frequent enhancement.

Pineal Region Masses

Germ Cell Tumors

Entity (with alternative names and abbreviations): Germinoma, also known as dysgerminomas or extra-gonadal seminomas.

Definition of Entity and Clinical Highlights

In general, the primary pineal tumors can be divided into three groups: (1) tumors of germ cell origin, (2) tumors of pineal parenchymal origin (e.g., pineocytoma, pineoblastoma), and (3) tumors of tissues supporting or adjacent to the pineal gland (e.g., meningioma, glioma). Germinoma is a type of germ cell tumor predominantly seen in pediatric populations with the

highest survival rate (>79% at 5 years) representing the most curable intracranial malignancy.

Basic Epidemiology/Demographics/Pathophysiology

The exact incidence of pineal germ cell tumors is largely unknown. Estimates on the proportion of pineal tumors vary from 3% to 5% of intracranial tumors in children. The majority (73–86%) of these pineal region tumors are of germ cell origin. The databases show a male predominance for pineal germ cell tumors (>90%), and >72% of patients were Caucasian. The peak number of cases occurs in the 10–19-year age group and declined significantly thereafter. Germ cells' normal destination (via the dorsal mesentery of the hindgut) is the ovaries or testes, but it is believed that some germ cells migrate to other locations within the developing embryo. The cause of this migration remains unknown, but the cells are found mainly in midline sites, including the mediastinum, sacrococcygeal region, and the third ventricle with the pineal gland (80–90% of the germinomas arise here) being in the vicinity. Germinomas may be also found suprasellar and on the paraventricular parts of the basal ganglia and thalamus.
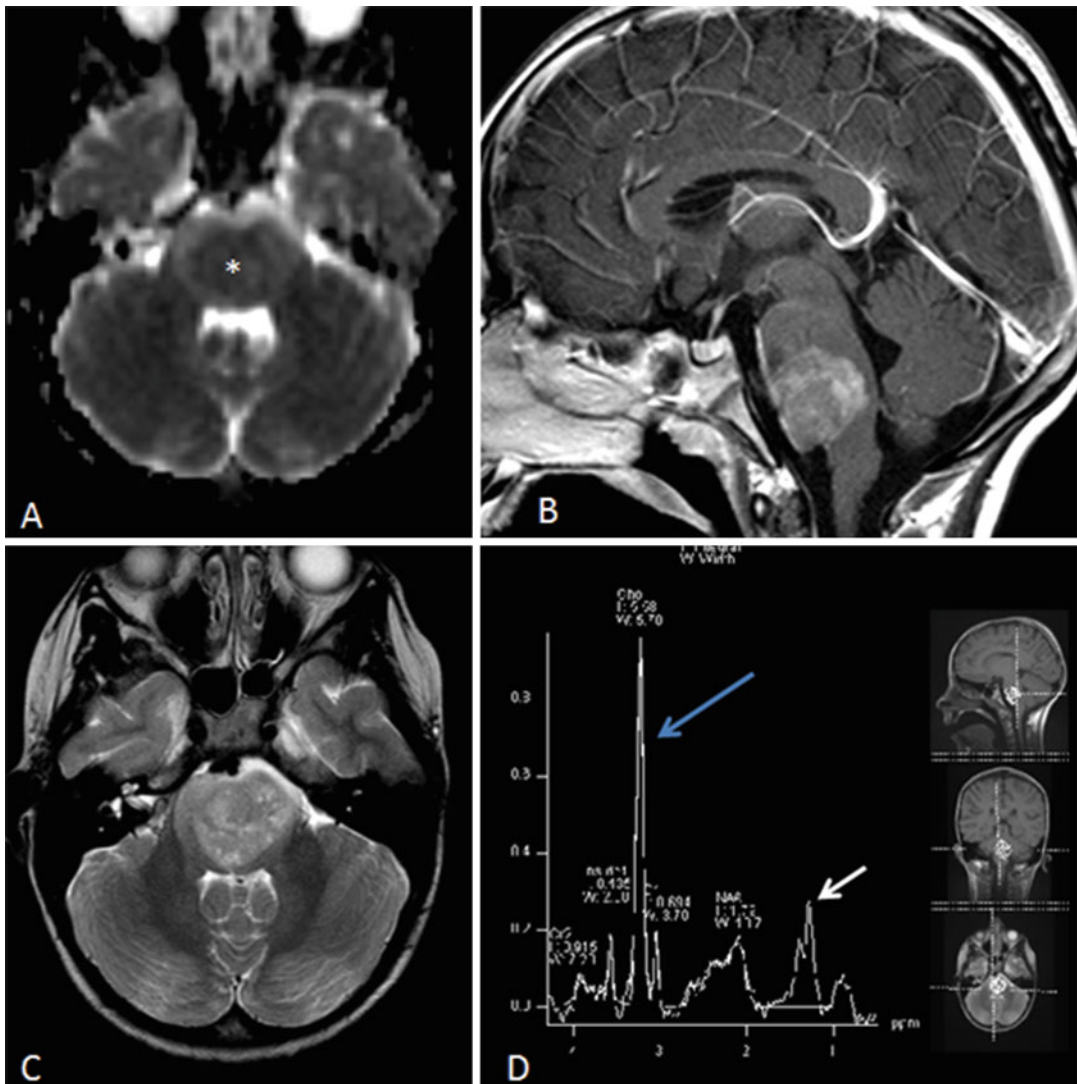
Fig. 29 Axial ADC maps (**a**), sagittal T1 C+ (**b**), axial T2 (**c**), and SV MRS (**d**). Biopsy proved high-grade DMG shows central area of low ADC values (asterisk in **a**), marked heterogeneous contrast enhancement and areas of low T2 signal (**b** and **c**), decreased NAA/Cho ratio (blue arrow in **d**), and lactate peak (white arrow in **d**)

Pathological Features

Well-circumscribed lesions with a two-cell pattern of lymphocytes and large polygonal primitive germ cells as cardinal features. Germinomas can be divided into two subtypes: pure germinoma and germinoma with syncytiotrophoblastic cells. Those containing syncytiotrophoblastic giant cells are associated with higher recurrence rate, hence decreased long-term survival. Also, they demonstrate elevated CSF levels of hCG (Fig. 33).

Clinical Scenario and Indications for Imaging

Presentation depends on location, with compression of the tectal plate leading to obstructive hydrocephalus with headache, nausea and vomiting, and Parinaud syndrome. Involvement on the pituitary infundibulum leads mainly to diabetes insipidus, followed by hypopituitarism and compromise of the neighboring optic chiasm.
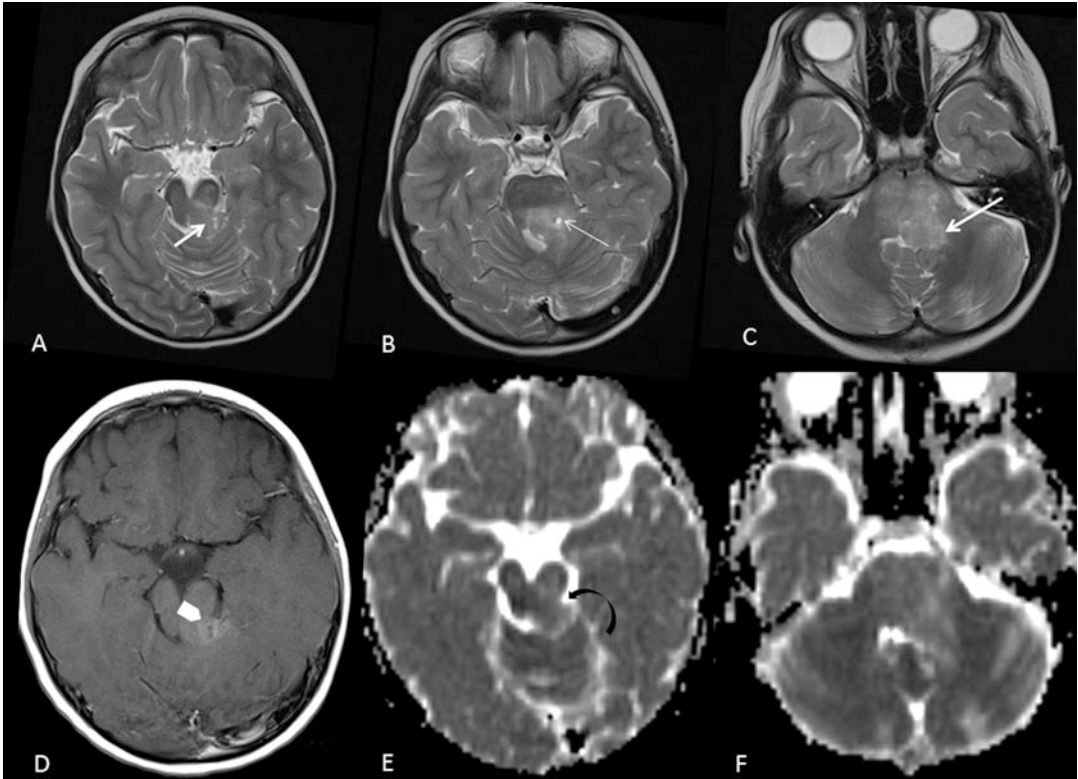
Fig. 30 Axial T2 (**a**–**c**), axial T1 C+ (**d**), and axial ADC maps (**e** and **f**). Invasion of the middle cerebellar peduncles/cerebellar white matter indicative of more aggressive behavior (white arrow in **a** and **c**). Note the presence of cystic components (thin arrow in **b**), mild enhancement (arrowhead in **d**) and some reduction of the ADC values in the superior aspect of the tumor **e** (curved arrow) compared to **f**. The combination of findings is in keeping with an anaplastic area invading the brain stem (confirmed on biopsy)

Imaging Technique and Recommended Protocol (For All Pineal Region Tumors)

T1w, T2w, and FLAIR in three planes, axial DWI. Sagittal planes are optimal for midline lesions such as lesions of the pineal region; best option is 3D T1w images (pre- and post-contrast) with reformats in different planes. High-resolution sagittal 3D T2 is optimal to depict anatomy. PWI and MRS are used to assess the tumor grade. T2 ∗ GRE or SWI may be useful to assess the presence and pattern of calcifications. Preoperative images of the spine are mandatory.

Interpretation Checklist and Structured Reporting

Midline, calcified, typically enhancing mass involving the pineal or pituitary region in a young (often male) patient, it can involve both locations in

20% of the cases (*synchronous germinoma* in 6–13% of the cases). Being non-encapsulated tumors, they can invade surrounding brain structures or present with CSF seeding.

CT Findings

The mass is hyperdense (due to abundance of lymphocytes) with central "engulfed" calcification (useful element for differential diagnosis with pineal parenchymal tumors). Pituitary germinomas may thicken the stalk. The involvement of basal ganglia is characterized by negative CT scan in the early stages or presence of calcified foci (Figs. 34a and 35a).

MR Findings

T1w: In case of pituitary gland involvement, absent spontaneous T1 hyperintense "bright" spot in the
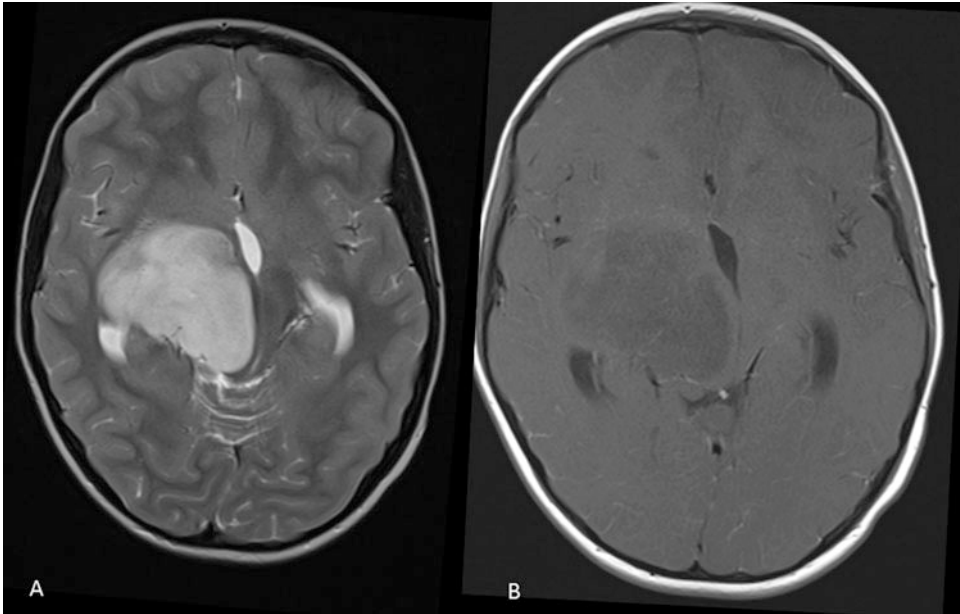
Fig. 31 Axial T2 (**a**) and T1 C+ (**b**). Biopsy proved supratentorial DMG
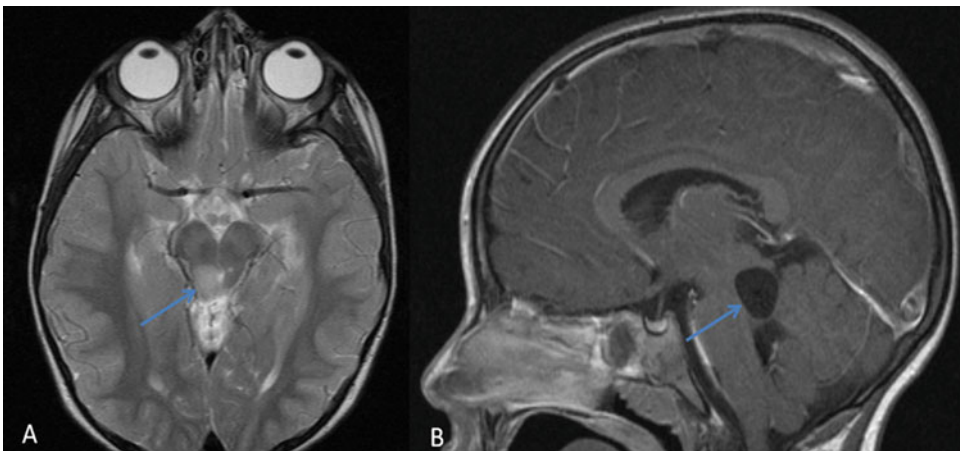
Fig. 32 Axial T2 (**a**) and sagittal T1 C+ (**b**). Low-grade glioma of the tectum (blue arrows). Note the exophytic nature of the tumor and the presence of cystic component with mass effect on the inferior aspect of the cerebral aqueduct

posterior pituitary gland (corresponding to the neurohypophysis) (Fig. 36). Mass isointense to gray matter in the pineal region.

T2w: Often hypointense to the gray matter (indicating high nucleus/cytoplasm ratio) (Fig. 34b). Small cysts may be seen.

DWI: Restriction due to high cellularity and high nucleus/cytoplasm ratio (abundance of lymphocytes) (Fig. 34c).

T2∗ GRE/SWI: presence of "blooming" artifacts due to calcifications and hemorrhages.

T1w with contrast: Moderate to strong homogeneous enhancement (Figs. 34d and 35b). Post-contrast T1w is useful to diagnose CSF spreading. Notably, germinomas in the basal ganglia region exhibit faint enhancement.

MRS: Non-specific increase of the Cho and decrease of NAA. Higher lipids and taurine but

not pathognomonic to distinguish pineoblastomas from germinomas.

PWI: Scarce data reports rCBV and rCBF increase in germinomas probably in relation to the absent blood-brain barrier.

Pearls

– If pineal germinoma is suspected, check for CSF spread and/or simultaneous involvement of the sellar region (thickening of the stalk/mass in the suprasellar region and diabetes insipidus) (Fig. 37).
– Involvement of basal ganglia is rare but important: typically the lesion has no mass effect, and there is associated ipsilateral hemiatrophy; however large lesions with mass effect are also possible (Fig. 38).
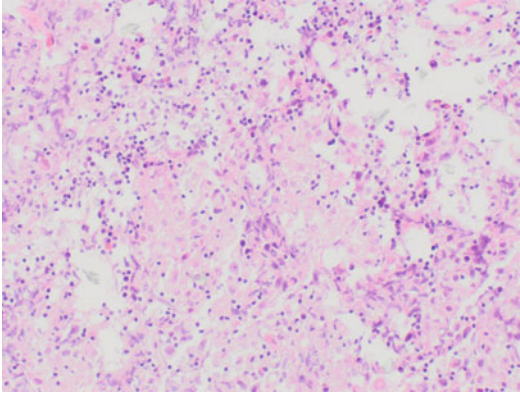
Fig. 33 H&E-stained high-power image of a germinoma with large physaliformic tumor cells and intermingled lymphocytes

– ADC values initially thought to be useful in differentiation between germinomas and pinealoblastomas (suggesting lower ADC in pinealoblastomas) have been debated.

Treatment Monitoring

Radiotherapy offers in ~85% of the cases long-term cure. Leptomeningeal seeding or spillage during surgery is associated with poorer prognosis. Increasing ADC values related to therapy response together with reduction in size.

Differential Diagnosis

– **Non-germinomatous germ cell tumors (nGGCTs) incl. teratomas, yolk sac tumors, embryonal carcinoma, choriocarcinoma, and mixed germ cell tumors**: These tumors tend to be more heterogeneous (i.e., cysts, hemorrhagic changes). In case of teratomas, mixed calcium, fat, and solid components are observed.
– **Pinealoblastoma/pineocytoma**: They are often larger and more heterogeneous at diagnosis (frequently with associated hydrocephalus) than germinomas. They tend to have peripheral calcifications (vs central calcifications in germinomas). Pinealoblastoma, similarly to germinoma, shows diffusion ADC restriction and may not enhance.
– **Astrocytoma**: Tumor with T2 hyperintensity compared to gray matter, with or without enhancement. ADC values are generally lower.
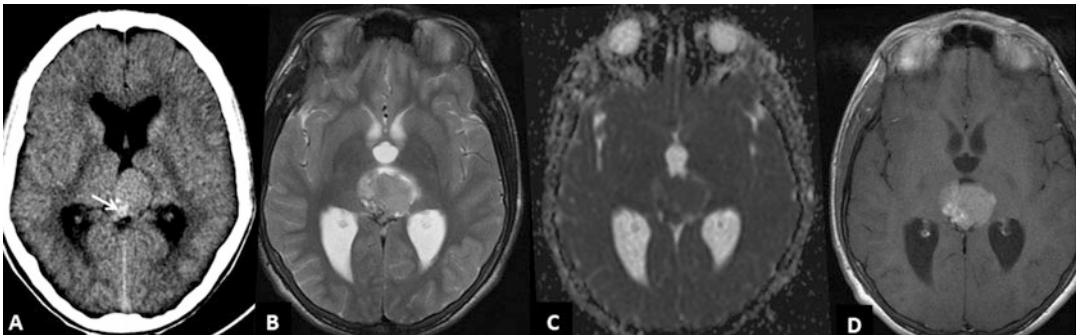
Fig. 34 Pineal region germinoma. Axial non-enhanced CT (**a**) demonstrates foci of calcification in the posterolateral aspect of the mass (white arrow). Axial T2 WI (**b**) and ADC maps (**c**) show relatively low T2 signal and ADC values in keeping with high cellularity. The neoplasm has moderate and homogeneous enhancement (**c**)

Fig. 35 Axial non-enhanced CT (**a**) and axial T1 post-contrast MRI (**b**): typical centrally calcified pineal germinoma with moderate enhancement and associated hydrocephalus
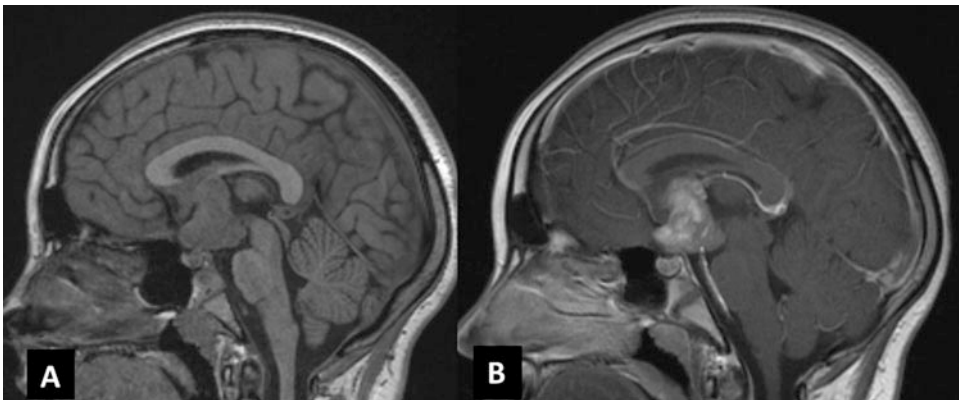
Fig. 36 Isolated suprasellar germinoma in patient with diabetes insipidus. Sagittal T1 WI (**a**) and sagittal T1 + C (**b**). Note the absence of normal posterior pituitary "bright spot" in pre-contrast T1 WI (**a**)

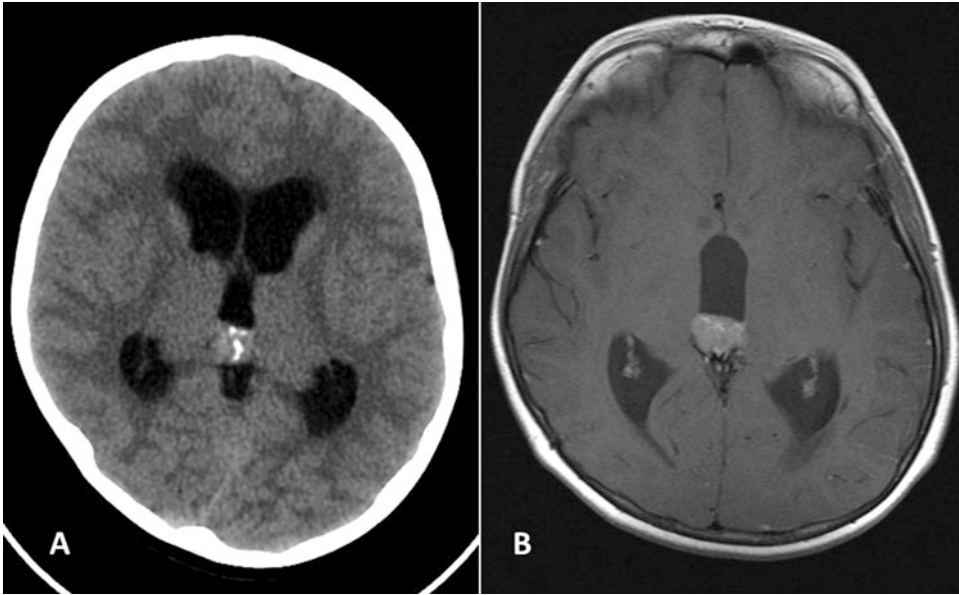## Non-germinomatous Germ Cell Tumors

Entity (with alternative names and abbreviations): Non-germinomatous germ cell tumors (nGGCTs) include teratomas, yolk sac tumors, embryonal carcinoma, choriocarcinoma, and mixed germ cell tumors (GCTs).

Definition of Entity and Clinical Highlights
nGGCTs are located in the body midline and rarely occur in the CNS. They consist of histologically varying tumors and tend to have a more heterogeneous appearance than germinomas caused by coexistent hemorrhage and necrosis. The prognosis is variable according to the entity.

Basic Epidemiology/Demographics/Pathophysiology

The overall peak in incidence for pineal gland tumors occurs between 10 and 19 years of age with slightly earlier peak for non-germinomatous germ cell tumors. The non-germinomatous tumors carry much worse prognosis with survival rates ranging between 40% and 70% than the germinomas. Intracranial embryonal carcinoma is a relatively rare neoplasm (composed of cells with an embryonic and anaplastic epithelial appearance) with punctate foci of hemorrhage or necrosis and propensity to metastasize systemically. A yolk sac tumor demonstrates a reticular pattern

characterized by a loose meshwork of communicating spaces lined by primitive tumor cells. This tumor is also known to be an α-fetoprotein-producing tumor. Choriocarcinomas are composed solely of cytotrophoblastic and syncytiotrophoblastic cells that produce β-human chorionic gonadotropin. Intratumoral hemorrhage and necrosis are quite common. Teratomas are uncommon neoplasms (accounting for 26–50% of fetal brain tumors) that contain elements derived from the three germ cell layers: endoderm, mesoderm, and ectoderm. These tumors usually contain sebaceous fat, which is a characteristic of this tumor and is identifiable radiologically. Their prognosis depends on the degree of differentiation (mature vs immature) and further on any malignant transformation in the tumors with mature differentiation. Mature teratomas are indolent, whereas immature teratoma's survival rates range between 50% and 70%. Prognoses for mixed GCTs depend on the element with the worst prognosis; that is, if a small amount of choriocarcinoma is included, the prognosis depends on the choriocarcinoma.

Pathological Features

Mature teratomas are lobulated with a complex mixture of adult-type tissues from all three embryonic germ layers (skin elements due to the ectodermal component; cartilage, bone, fat, and smooth and skeletal muscle due to mesoderm; respiratory or enteric epithelium from the endodermal component). Immature teratomas contain

Fig. 37 Sagittal T2 WI on the midline. Pineal germinoma with associated small synchronous, suprasellar lesion abutting the floor of the third ventricle (black arrow)
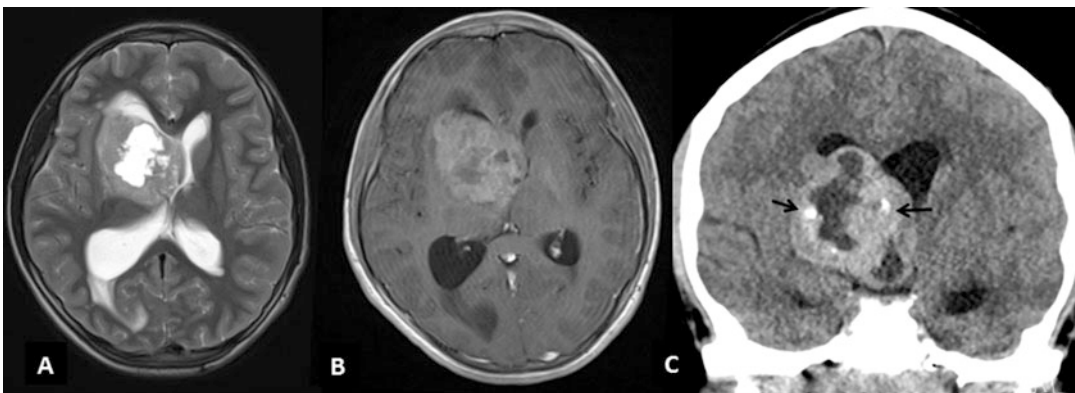
Fig. 38 Large basal ganglia germinoma. Axial T2 WI (**a**), axial T1 WI C+ (**b**), and coronal unenhanced CT (**c**) demonstrate large mass in the right basal ganglia with cystic components and internal calcifications (black arrows in **c**)

incompletely differentiated tissue elements that resemble fetal tissue.

Clinical Scenario and Indications for Imaging
These tumors, like the germinomas, can easily cause hydrocephalus by both direct invasion and leptomeningeal seeding. If present in the suprasellar region, precocious pseudopuberty and diabetes insipidus, with or without adenohypophyseal

dysfunctions, are frequent. Rarely, when intracranial dermoid cysts are ruptured, they cause headache and seizures.

Interpretation Checklist and Structured Reporting
Teratomas are characterized by the presence of fat, cystic, and solid areas and calcifications (Fig. 39). Other nGGCTs are not distinguishable
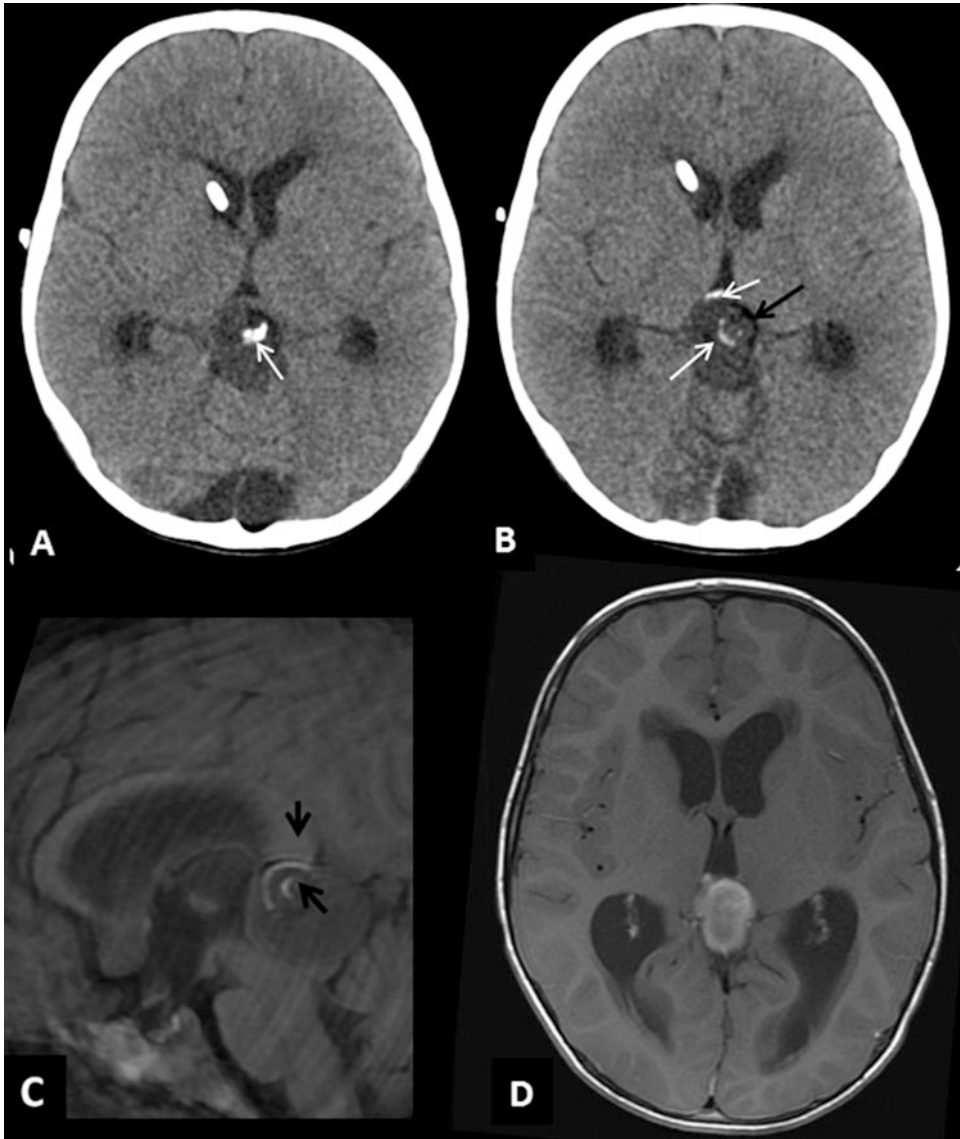
Fig. 39 Typical CT and MRI appearances of pineal teratoma. Unenhanced axial CT (**a** and **b**): evident areas of hyperdensity in keeping with calcifications (white arrows) and hypodensity compatible with fat (black arrow in **b**).

Sagittal pre-contrast T1 WI confirms presence of calcium as hyperintense linear areas (black arrows in **c**). The mass has strong and homogeneous enhancement in T1 WI + C (**d**)

from each other and from germinoma based on imaging criteria.

Pearls
Oncologic markers may better differentiate different nGGCTs.

- B-hCG (beta-human chorionic gonadotropin): Increased in choriocarcinomas, mixed GCTs, and syncytiotrophoblastic germinoma
- AFP (alfa-fetoprotein): Significantly increased in yolk sac tumors, mixed GCTs, and immature teratoma
- PLAP (placental alkaline phosphatase): Profoundly increased in embryonal carcinomas, mixed GCTs, yolk sac tumors, choriocarcinomas, and syncytiotrophoblastic germinoma

Pineal Parenchymal Tumors

Pineoblastoma
Definition of Entity and Clinical Highlights
They represent the most aggressive and highest-grade (WHO grade IV) entity among pineal parenchymal tumors. They demonstrate poorly defined borders to the adjacent brain parenchyma, frequently CSF seeding, and historically poor prognosis (median survival time approx. 2 years) depending however to the extent of resection, early detection, and treatment based on chemotherapy (preferably a high-dose regime with stem cell rescue).

Basic Epidemiology/Demographics/ Pathophysiology
Pineoblastomas are rare, representing less than 0.1% of all primary brain tumors. Pineoblastomas usually occur in children, whereas adult account for less than 10% of the cases in published series. Pineoblastomas account also for a substantial proportion of pineal parenchymal tumors (24–50%). In contrast to pineal germinomas, pineoblastomas demonstrate a slight female predilection (M:F 0.7:1; similar to other pineal parenchymal tumors). Pineoblastomas are grossly invasive with poorly defined borders and frequent leptomeningeal spread. They are very similar to medulloblastoma and primitive neuroectodermal tumors. They are characterized by high cellularity with aggregated small poorly differentiated cells. Mitoses are found along the Homer-Wright rosettes (which are also found in medulloblastomas and are widely thought to represent abortive attempts at neuroblastic differentiation), Flexner-Wintersteiner rosettes, and necrotic areas.

Pathological Features
Highly cellular embryonal neoplasms with features reminiscent to primitive neuroectodermal neoplasms. Hemorrhage and/or necrosis may be present. Tumor cells have scant cytoplasm and are arranged in diffuse sheets. Homer-Wright rosettes (neuroblastic differentiation) or Flexner-Wintersteiner rosettes (retinoblastic differentiation) are evident.

Clinical Scenario and Indications for Imaging
Parinaud syndrome resulting from compression of the tectal plate and obstructive hydrocephalus are the clinical sign hallmarks in pineoblastomas, which have often considerable size at the time of diagnosis. They are prone to CSF tumor cell dissemination (present in 15% of patients at the baseline diagnosis).

Interpretation Checklist and Structured Reporting
Young child with large, heterogeneous pineal mass with associated hydrocephalus and radiological aggressive features. Typically, pinealoblastomas have peripheral calcifications. It is possible to have internal hemorrhages and cystic components (Fig. 40). The mass often involves surrounding structures, and there is relatively high rate of CSF dissemination (Fig. 41). Heterogeneous and variable enhancement (sometimes absent).

CT Findings
The solid aspect of the tumor is moderately hyperdense with typical presence of peripheral calcifications ("exploded" calcification). Hydrocephalus is almost always present (Fig. 41).
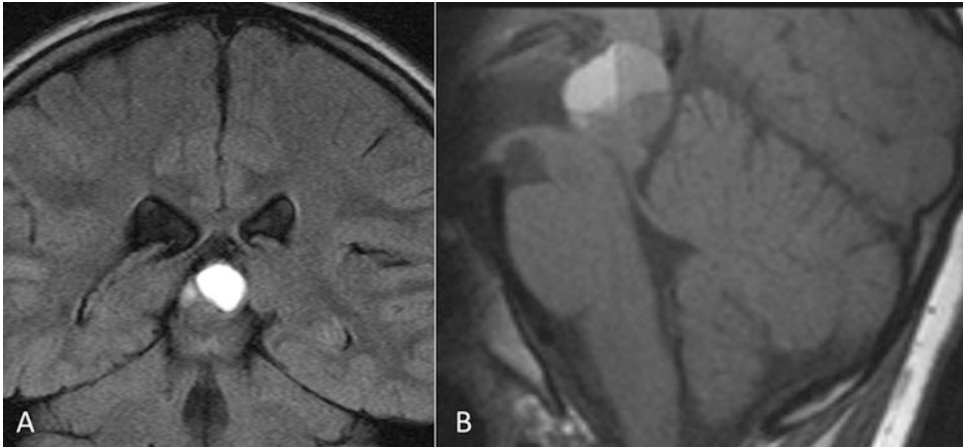
Fig. 40 Coronal FLAIR (**a**) and sagittal T1 WI (**b**). Midline complex solid-cystic mass showing internal hemorrhagic changes as areas of hyperintense signal in both FLAIR and pre-contrast T1 WI
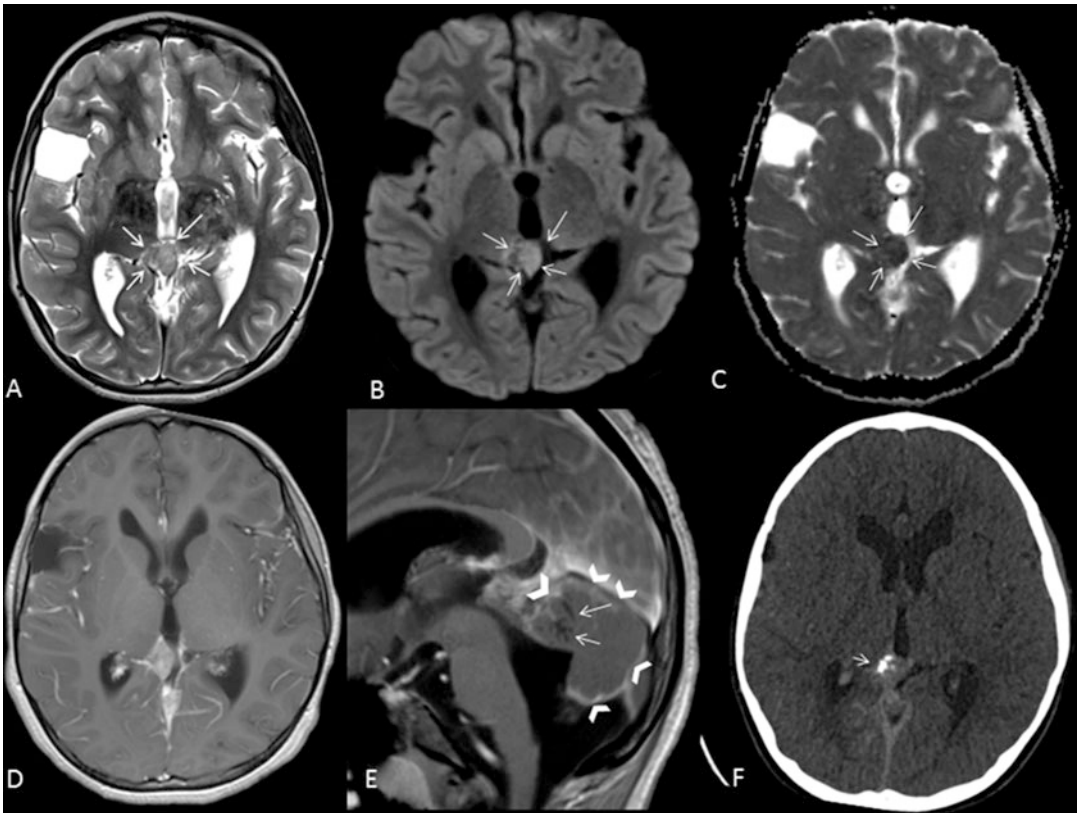
Fig. 41 Disseminated pinealoblastoma in a 6-year-old female. Axial T2 WI (**a**), axial DWI (**b**), axial ADC maps (**c**), axial T1 WI C+ (**d**), sagittal T1 C+ (**e**), and axial unenhanced CT (**f**). A small mass is demonstrated in the pineal region showing relatively low T2 signal (arrows in **a**), diffusion restriction (arrows in **b** and **c**), and enhancement (**d**). Note the presence of diffuse leptomeningeal spread in the posterior fossa (arrowheads in **e**) and consequent entrapment of the cerebellar subarachnoid spaces (thin arrows in **e**). Typical peripheral calcifications are noted in CT (arrow in **f**)

MR Findings

Being very heterogeneous mass, the following descriptions refer to the solid aspect of the tumor.

T1w: Isointense/hypointense to the adjacent brain.

T2w: Variable. As a general rule, the low T2 signal of the solid portion is more frequent (high cellularity) (Fig. 41). Peritumoral edema can be present.

DWI: Restriction (high cellularity and high nucleus/cytoplasm ratio) (Fig. 41).

T2∗ SWI: Useful to diagnose calcifications and hemorrhages.

T1w with contrast: Heterogeneous enhancement which may vary from strong to mild (Fig. 41). Sometimes no enhancement.

MRS: Non-specific increase of the Cho and decrease of NAA. Higher lipids and taurine (similar to germinomas). Increased myoinositol peak is also possible.

PWI: There are limited data regarding perfusion in pinealoblastomas. Increased rCBV has been reported.

Pearls

Pineoblastomas can occur in association with retinoblastoma (trilateral retinoblastoma) so it is important to look for eyes' involvement.

Treatment Monitoring

Similar to medulloblastomas and other embryological tumors: Imaging of the brain every 3 months for the first 3 years and then every 6 months for the ensuing 5 years. MRI of the spine every 3 months for the first 2 years and then every 6 months for 5 years.

Differential Diagnosis

– Germ cell tumors (GCTs): (i) Germinoma shows engulfed calcifications and is more homogeneous. (ii) Teratoma has cystic, calcium, and fatty components. (iii) Other GCTs are very difficult to differentiate from other aggressive pineal tumors; tumor markers may help.
– Pineocytoma: more common in adults. They are WHO grade I and thus have no aggressive radiological features (i.e., no diffusion restriction or increased perfusion). They are well-defined without invasion of the surrounding tissues.
– Astrocytoma: T2 hyperintense to gray matter, with or without enhancement. ADC values are generally lower.

Pineal Parenchymal Tumors of Intermediate Differentiation (PPTID)

Definition of Entity and Clinical Highlights

The pineal parenchymal tumors of intermediate differentiation (PPTID) and biological behavior are considered WHO grade II–III tumors, and hence, they fall between the well-differentiated WHO grade I (i.e., pineocytoma) and the poorly differentiated WHO grade IV (i.e., pineoblastoma) entities.

Basic Epidemiology/Demographics/ Pathophysiology

No age predilection. They are often encountered in middle-aged adults (20–70 years of age) (F>M).

Pathological Features

PPTID is grossly similar in appearance to pineocytoma. Non-necrotic, diffuse sheets of uniform cells and the formation of small rosettes, with features intermediate between those of pineocytoma and those of pineoblastoma are encountered. Low to moderate mitotic activity and nuclear atypia are seen.

Clinical Scenario and Indications for Imaging

Reminiscent to the other pineal parenchymal tumors.

Interpretation Checklist and Structured Reporting

Their radiographic appearance is also intermediate but not rarely may show aggressive-like features that do not correlate with the grading. The size of the mass is variable from small to >5 cm, and invasion of surrounding structures is possible. Imaging characteristics are similar to those of pinealoblastoma. It is important to distinguish grade II from III; this differentiation is histological although ADC and perfusion characteristics may

be helpful. Rare but described CSF spread; therefore imaging of the entire cranio-spinal axis is therefore required. MIB-1 (proliferative marker) has been described as useful to distinguish between the two groups.

MR Findings
Relatively rapid growth and/or low ADC values in a well-circumscribed pineal tumor with appearance akin to a pineocytoma may suggest PPTID.

Treatment Monitoring
The optimal management for PPTIDs remains to be determined, and patients may be with surgery alone, whereas postoperative treatment in a manner similar to that for pineoblastomas is recommended for seeding tumors. The available studies on the treatment of PPTID regarding radiation therapy and chemotherapy are limited. Although PPTID may be aggressive, PPTID patients may survive long term, even after recurrence suggesting an optimization of the irradiation field and usage of chemotherapy after surgery.

Pineocytoma

Definition of Entity and Clinical Highlights
Pineocytomas are principally slow-growing, grade I tumors with a relatively good prognosis.

Basic Epidemiology/Demographics/Pathophysiology
Pineocytoma accounts for 14–60% of pineal parenchymal neoplasms. It occurs throughout life (predominantly middle-aged adults without gender predilection). The 5-year survival is 86–100%, and there are no reported relapses after gross total resection. Cerebrospinal fluid (CSF) dissemination rarely occurs.

Pathological Features
Relatively small, uniform, mature cells that resemble pineocytes is the cardinal finding. Lobular architecture and pineocytomatous rosettes are also common.

Clinical Scenario and Indications for Imaging
Signs and symptoms of the pineal region mass are most often related to mass effect on the adjacent structures. Pineocytoma is often an incidental finding.

Interpretation Checklist and Structured Reporting
The radiological characteristics reflect the low grade of the tumor. Thus, the mass is generally homogeneous, well-defined, T2 hyperintense/isointense to the gray matter (low cellularity in keeping with low grade) and with lower intrinsic perfusion and no diffusion restriction (Fig. 42).
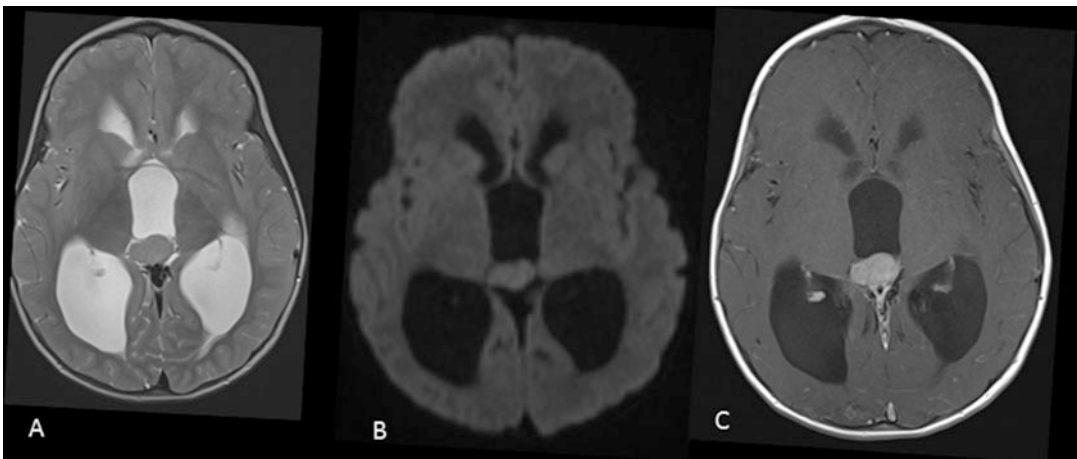
Fig. 42 Rare, biopsy-confirmed pinealocytoma (grade I) in a 3-year-old female, showing isointense signal on T2 WI (**a**), absence of diffusion restriction (**b**), and homogeneous enhancement (**c**). Note associated hydrocephalus
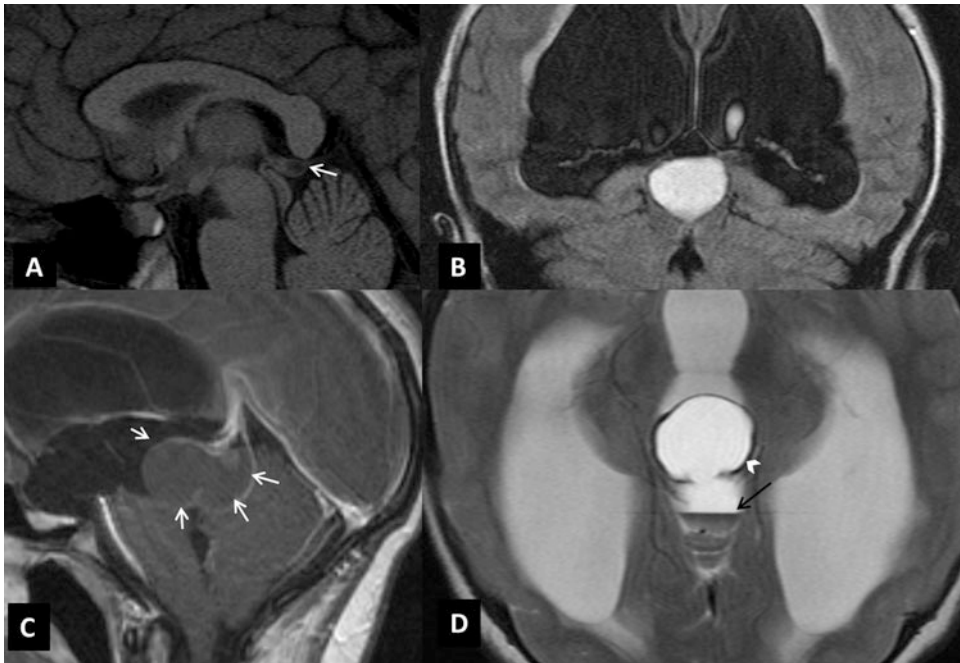
Fig. 43 Normal cystic pineal gland on sagittal T1 WI without contrast (**a**). Note small internal cyst without atypical features (arrow). Coronal FLAIR (**b**), sagittal T1 C+ (**c**), and axial T2 WI in another patient with a hemorrhagic pineal cyst. There are hyperintense FLAIR internal signal (**b**), linear peripheral enhancement without internal enhancement (arrows in **c**), and linear hemosiderin deposit (arrowhead in **d**) with fluid-fluid level in the posterior aspect of the cyst (black arrow in **d**) evident in T2

Furthermore, peripheral calcifications and homogeneous enhancement are usually present. Internal cystic or hemorrhagic areas can be sometimes demonstrated (Fig. 40). CSF spread is extremely rare. Pineocytoma may be completely cystic and mimic a pineal cyst (Fig. 43).

Treatment Monitoring
Pineocytomas are treated surgically with excellent prognosis after complete resection. A 5-year survival of 86% has been reported with very rare recurrent lesions or CSF seeding. Long-term follow-up is generally recommended if incomplete resection is achieved.

Papillary Tumor of the Pineal Region

Definition of Entity and Clinical Highlights
The papillary tumor of the pineal region (PTPR) is recognized in the WHO 2007 classification and is thought to arise from ependymocytes localized in the subcommissural organ, which is located in the pineal region. PTPRs are well-circumscribed lesions that can measure up to 5 cm and may have a cystic component.

Basic Epidemiology/Demographics/Pathophysiology
Rare neuroepithelial neoplasm that occurs in both children and adults (5–66 years; mean age, 31.5 years).

Pathological Features
PTPRs demonstrate an epithelial-like growth pattern, papillary features, rosettes, and perivascular pseudorosettes. Owing to their rarity, the histologic grading criterion has yet to be defined, ranging between WHO grades II and III.

Clinical Scenario and Indications for Imaging
Signs and symptoms similar to other pineal region masses.

Interpretation Checklist and Structured Reporting

MR Findings

T1w: variable signal intensity. Hyperintensity has been described due to the presence of glycopeptides.

T2w: high signal intensity.

T1w with contrast: enhancement.

Treatment Monitoring

CSF dissemination has been reported in 7%. The 5-year survival and progression-free survival have been reported 73% and 27%, respectively. Local recurrence may be present even after compete resection and radiation therapy. Watchful monitoring may be warranted.

Pineal Cyst

Definition of Entity and Clinical Highlights

Common, usually asymptomatic, and typically incidental lesions. The uncertainty in differentiating them from cystic pineal tumors, especially when large or when atypical features are present, is the main reason for prolonged MRI follow-up.

Basic Epidemiology/Demographics/ Pathophysiology

Typically found in young adults (20–30 years, 3:1 F/M). It has been postulated that hormonal changes play a part in their formation, hence the higher frequency in females. As these women get older, the cyst initially enlarges and then shrinks. In males, the cyst is rather stable over time.

Pathological Features

Three concentric layers comprise the lesion. The inner layer contains hemosiderin and fibrillary glial tissue; the middle layer is the pineal parenchyma with or without calcification; and the outer layer is composed of thin fibrous connective tissue.

Clinical Scenario and Indications for Imaging

The pineal cysts are predominantly asymptomatic. When larger, mass effect on the tectal plate (resulting in Parinaud syndrome) or cerebral aqueduct compression (leading to obstructive hydrocephalus) may be encountered. Rarely, hemorrhage can cause rapid expansion and so-called pineal apoplexy.

Interpretation Checklist and Structured Reporting

Fluid-filled, thin-walled, <1 cm mass in the pineal region. Possible variations in the appearances: (1) multicystic; (2) associated mass effect and occasionally hydrocephalus; and (3) may be larger than 1 cm (up to 4 cm reported). As is the case with the rest of the pineal gland, the walls of pineal cysts do not have a well-formed blood-brain barrier, and as such, smooth enhancement of the wall is common. 20–25% of the pineal cysts have calcifications of the wall.

Intracystic hemorrhage is possible but very rare and can cause diagnostic challenge. FLAIR hyperintense signal can be present (the cyst typically contains proteinaceous fluid). In other MR sequences, the signal is similar to CSF.

Pearls

Pineal cyst is a normal finding that is found in ~5% of brain MRIs and 20–40% of autopsy series. Typical appearing pineal cyst does not need follow-up; however when cysts are above 10–12 mm in diameter, follow-up should be considered as pineocytoma may be indistinguishable on imaging when cystic.

Treatment Monitoring

Clinical management is controversial as the natural history is not completely understood and other studies have demonstrated stability at follow-up (0.5–9.1 years), whereas those that changed in size were not associated with clinical findings. Some authors advocate only clinical follow-up for asymptomatic pineal cysts, with the caveat that pineal neoplasms may rarely mimic pineal cysts. Larger pineal cysts (≥10 mm) are followed up with imaging studies to document stability. Occasionally, surgical intervention may be sensible to establish the diagnosis.

Sellar and Parasellar Tumors

Sellar Tumors

Craniopharyngioma
Definition of Entity and Clinical Highlights
Craniopharyngiomas (CPs) are relatively benign (WHO grade I) lesions comprising ~1–5% of the primary brain tumors. Two subtypes of CP have been described: a) adamantinomatous subtype arises from the Rathke pouch remnant, and it is typical in children and older adults (>65 years old), and b) squamous papillary subtype occurs in middle-aged adults, and it is thought to derive from the adenohypophysis (part tuberalis). Whether or not they represent distinct entities or a spectrum of morphology remains a little controversial. In approx. 15% of the cases, mixed pathological types are found.

Basic Epidemiology/Demographics/Pathophysiology
Bimodal distribution, with the first peak between the ages of 10 and 14 years (almost exclusively adamantinomatous type) and a second smaller peak in adults >50 years old (mostly of papillary subtype) in an equal incidence in both males and females.

Pathological Features
CPs derive from Rathke cleft. The adamantinomatous type is peripherally palisading and consists of reticular epithelial cells akin to the enamel pulp of developing teeth. It is usually calcified, and the single or multiple cysts are filled with proteinaceous, oily fluid high in blood products and/or cholesterol (so-called machinery oil). "Wet keratin nodules" are also present. Irregular, infiltrative borders are common. BRAF V600E mutation is observed in 95% of cases.

The papillary subtype (papillary configuration with cauliflower-like morphology) is seen almost exclusively in adults and is formed of solid sheets of well-differentiated nonkeratinizing squamous epithelium. "Wet keratin" and calcification are absent and the tumor is more solid (Fig. 44).
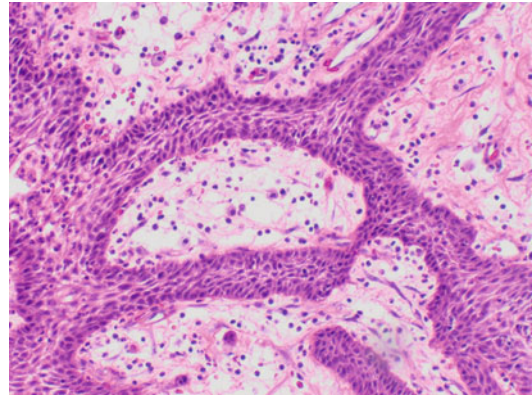
Fig. 44 H&E-stained high-power image of a papillary craniopharyngioma with epithelial tumor cells surrounding a loose reticular matrix

Clinical Scenario and Indications for Imaging
Clinical presentation is variable on account of the variable location and size of the lesion. The commonly presenting symptoms include visual disturbances (mostly in adults), obstructive hydrocephalus, mental/personality changes (due to frontal or temporal lobe extension), hyperprolactinemia ("pituitary stalk effect"), diabetes insipidus, amenorrhea, and other hormonal imbalances.

Imaging Technique and Recommended Protocol
This protocol is the same for all the sellar and parasellar lesions. High-resolution T1w and T2w sequences in coronal and sagittal planes centered on the sellar region. Post-contrast T1w coronal (with the option of a dynamic study to rule out microadenoma) and sagittal post-contrast on the sellar region. Axial FLAIR/T2w, DWI, and 3D T1w post-contrast on the brain are also recommended. CT or T2∗/SWI sequences may help demonstrate calcifications (90% of CPs).

Interpretation Checklist and Structured Reporting
Lobulated, mixed solid/cystic suprasellar mass in child with calcifications and enhancement of the solid portions. The mass can occur anywhere along the infundibulum (from the floor of the third ventricle to the pituitary gland) and often invades multiple cranial fossae and compresses the
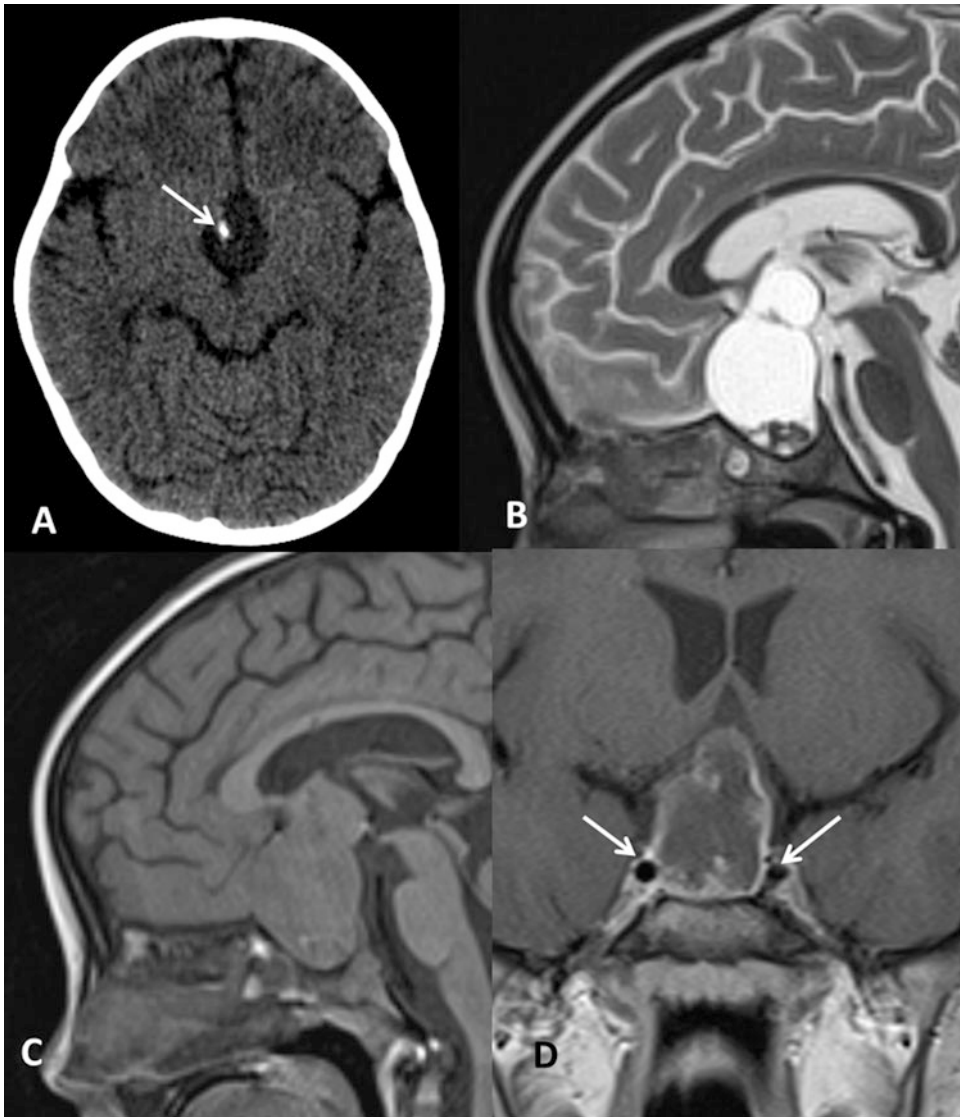
Fig. 45 Axial unenhanced CT (**a**), sagittal T2 WI (**b**), sagittal T1 WI (**c**), and coronal T1 WI C+ (**d**). Typical appearances of adamantinomatous CP: a small focus of calcification is noted in CT (arrow in **a**); mixed solid/cystic structure is seen in MR with isointense T1 signal in keeping with high-density cystic fluid (**c**) and enhancement of the cystic wall (**d**). Note the close relationship with both carotid arteries (arrows in **d**)

optic chiasm. It is important to describe the relationship with the chiasm, vessels of the circle of Willis, hypothalamus, and third ventricle (Figs. 45 and 46).

Note that there are some differences between the two subtypes of CP (adamantinomatous and squamous papillary, see "Pearls" for details).

CT Findings

Remember "the rule of 90" (applies to adamantinomatous-type CP): 90% of CPs have internal calcifications, 90% enhance in the solid parts, and 90% are mixed solid/cystic (Figs. 45a and 46a).
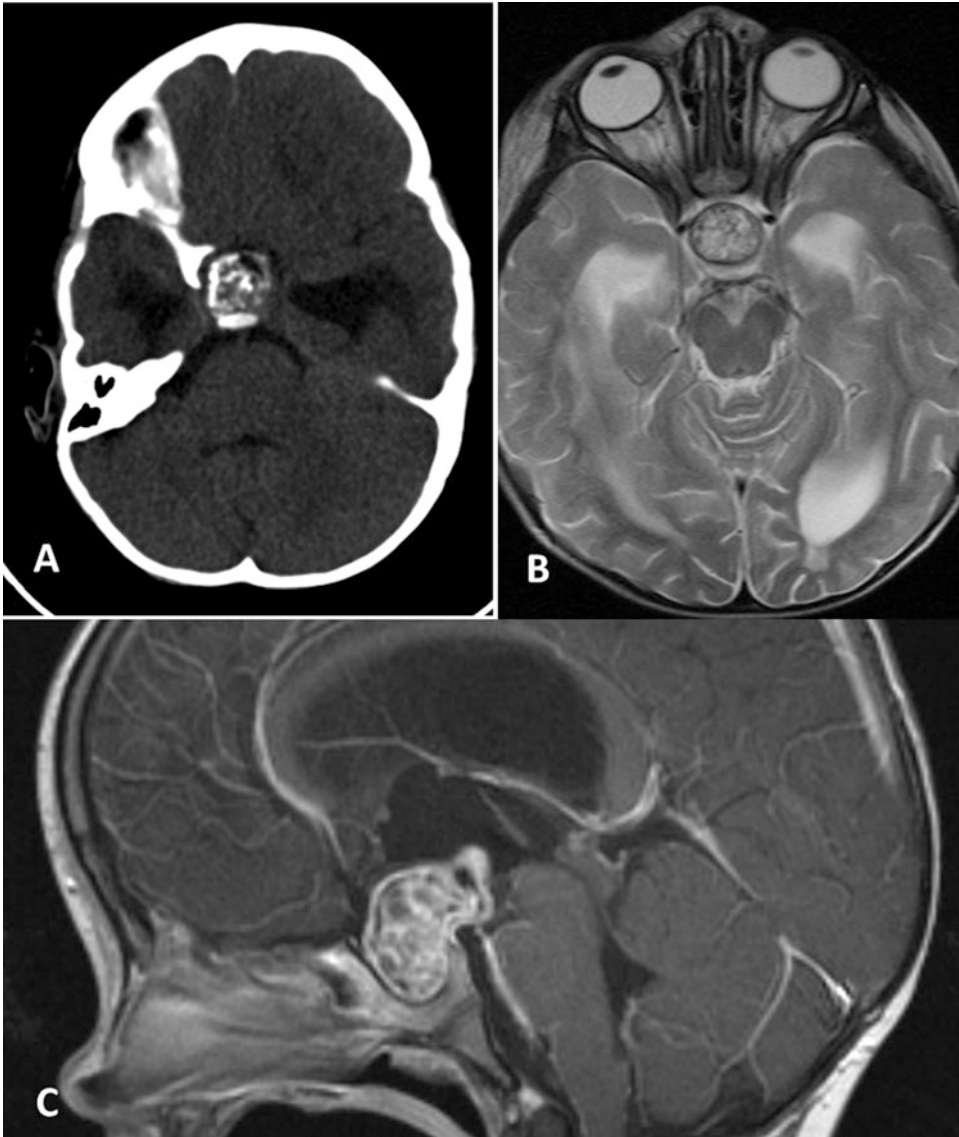
Fig. 46 Adamantinomatous CP: axial unenhanced CT (**a**), axial T2 WI (**b**), and sagittal T1 WI C+ (**c**). The mass is mostly calcified and enhances strongly post-contrast. There is associated hydrocephalus and extension within the third ventricle

MR Findings

T2w: Mixed signal due to multiple solid and cystic components (Fig. 45b). The cysts may be hyperintense in FLAIR. Look for abnormal T2 signal in the surrounding structures which may indicate invasion, edema, or inflammation due to spillage of cystic fluid.

T1w: Variable signal. One of the most useful signs is the presence of spontaneous hyperintense T1 signal within some of the cysts (about 33% of cases) because of proteinaceous content or methemoglobin (Fig. 45c) (described mostly in the adamantinomatous type). In the squamous papillary subtype, the cystic components (when present) are isointense to CSF.

DWI: Variable and heterogeneous signal, mostly related to the density of the fluid in the cystic aspect of the tumor.

T2∗/ SWI: It may show blood and calcium though CT is more reliable to demonstrate presence of calcium, which helps in the differential diagnosis with other sellar lesions.

T1w with contrast: Strong and homogeneous enhancement of the solid portions and of the cystic walls (Fig. 45d).

MRS: Broad lipid peak corresponding to high cholesterol content in the cysts.

Pearls

Adamantinomatous-type CPs have image characteristics described above. The squamous papillary subtype of CP has been described as more rounded, mostly solid, and with cysts that do not have the high proteinaceous content (i.e., signal similar to CSF). Note that it is not always possible to distinguish these two entities on the basis of radiological appearances.

Treatment Monitoring

Concerning the presurgical planning, different groups depending on the relationship with optic chiasm have been identified: a) sellar type (CP with sellar and suprasellar extension but no mass effect on the chiasm), b) prechiasmatic type (CP located anterior to the chiasm which is displaced posterosuperiorly), and c) retrochiasmatic type (located posteriorly to the chiasm which is displaced anteriorly) (Fig. 46). Overall size and clinical sings are the main criteria for the follow-up of the CPs. The recurrence rate is more for CPs larger than 5 cm at diagnosis.

Differential Diagnosis

– Rathke cleft cyst (RCC): benign cyst arising from the Rathke cleft that can also show spontaneous hyperintense T1w signal. RCCs lie between anterior and posterior pituitary glands and are very small although they can expand overtime. Lack of solid enhancing components is helpful for differential diagnosis from CPs together with location and size.

– Pituitary adenoma: it is not frequent before puberty. When hemorrhagic component can mimic a CP, however the low T2w signal related to deoxy- or methemoglobin in adenomas helps in the differential diagnosis. Furthermore, the normal pituitary gland is often clearly distinguishable in CPs.

– Hypothalamic and chiasmatic optic pathway gliomas: common in NF1 patients. They have variable enhancement which is, as a general rule, milder than in CP. Often they do not have cystic component or cysts are smaller than CPs. These neoplasms are in continuity with optic pathways rather than compressing the chiasm.
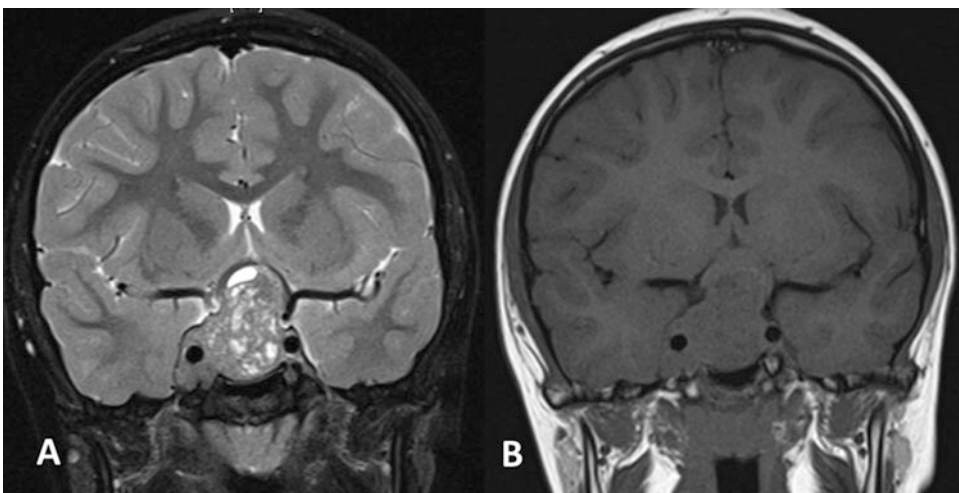
Fig. 47 Petrous bone involvement of LCH. Extensive bone destruction is demonstrated on CT (left) in the left petrous bone; corresponding enhancing soft tissue is visible on coronal T1 WI C+ (right)

– Germ cell tumors: they appear as thickened infundibulum with CSF spread and possible involvement of the pineal region.
– Pituitary hyperplasia: non-neoplastic increase in size of the pituitary gland. It is physiological in the puberty, pregnancy, or lactation. When pathological, it is associated with endocrinological disorders such as primary hypogonadism or thyroid insufficiency. The gland is diffusely enlarged without asymmetry or areas of heterogeneity noted. Normal pituitary height is 3–6 mm, but it can reach 12 mm during puberty, pregnancy, or lactation.

Pituitary Adenoma
Definition of Entity and Clinical Highlights
By definition, pituitary microadenomas are less than 10 mm in diameter and are located in the pituitary gland. Macroadenomas are adenomas over 10 mm in size that first expand the sella turcica and then grow upward.

Basic Epidemiology/Demographics/ Pathophysiology
Adenomas are the most frequent lesions of the pituitary region in children and adolescents. Pituitary adenomas constitute less than 3% of supratentorial tumors in children and 2.3–6% of all pituitary tumors treated surgically. There is no known gender or racial difference in prevalence (which increases with age) and greater frequency of prolactinomas in young women. Pituitary macroadenomas are approximately twice as common as microadenomas. In a small fraction of patients, adenomas are associated with multiple endocrine neoplasia type I (MEN I), multiple endocrine neoplasia type IV (MEN4), Carney complex, McCune-Albright syndrome, and familial isolated pituitary adenoma. Pituitary carcinomas are rare in adults and extremely rare in children.

Pathological Features
Pituitary adenomas share characteristics with other adenomas of endocrine glands: granular cytoplasm, round nuclei with finely dispersed chromatin, and multiple distinct nucleoli; they generally also express both markers of neurosecretory granules (synaptophysin, chromogranin) and epithelial differentiation (cytokeratins).

### Clinical Scenario and Indications for Imaging
Prolactinoma is the most frequent adenoma histotype in children, followed by the corticotrophinoma and the somatotropinoma. Nonfunctioning pituitary, TSH-secreting, and gonadotrophin-secreting adenomas are very rare in children accounting for only 3–6% of all pituitary tumors. ACTH-secreting adenomas have an earlier onset and predominate in the prepubertal period, while GH-secreting adenomas are very rare before puberty. Similar to adults, presenting symptoms are generally related to the endocrine dysfunction, such as growth delay and primary amenorrhea, rather than to mass effects (headache, visual disturbance, invasion into the cavernous sinus, hydrocephalus by compressing the midbrain or distorting the third ventricle).

By Definition, Pituitary Microadenomas
Image findings are identical of those in adult population. Microadenomas often show delayed enhancement and are identified on contrast enhancement sequence as an area of reduced contrast in comparison to the remaining gland (dynamic contrast imaging are particularly useful in diagnosis of microadenomas). Macroadenomas often extend in the suprasellar region with typical "snow man" appearance due to the narrowing at the level of the sellar dural diaphragm. Extension laterally in the cavernous sinuses is also expected (Fig. 48). The signal in macroadenomas is more heterogeneous, and hemorrhagic component can mimic a CP.

Treatment and Monitoring
Indications for therapy are (1) to reduce tumor size and (2) to control prolactine excess. In the absence of complications needing immediate surgery, pharmacotherapy with dopamine agonists (e.g., bromocriptine, quinagolide, or cabergoline) should be considered the first treatment approach. Transsphenoidal adenomectomy is the treatment of choice for ACTH-, TSH-, and GH-secreting adenomas in childhood and adolescence. Surgical
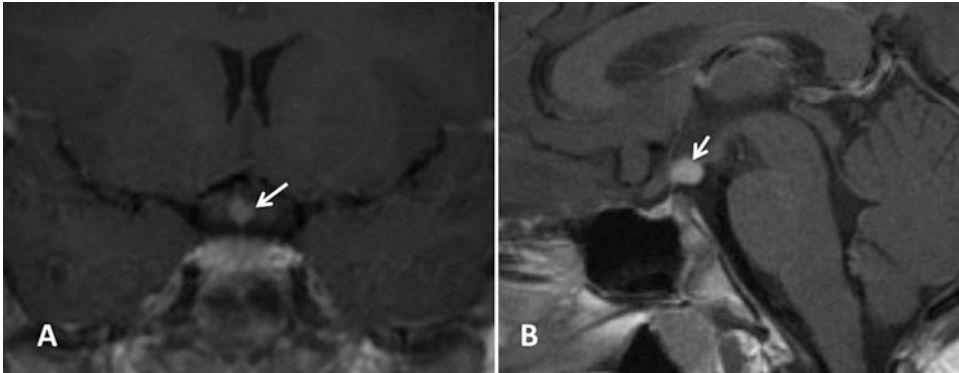
Fig. 48 Pituitary macroadenoma in a 10-year-old child. Coronal T2 WI (**a**) and T1 WI (**b**) show a sellar/suprasellar mass with the typical "snowman" appearance and lateral extension within the cavernous sinuses. The lesion has heterogeneous appearance due to the presence of internal cysts

excision is successful in the majority of children, with initial remission rates of 70–98% and long-term cure of 50–98% in most studies. Treatment with somatostatin analogs is very effective in patients with GH excess. Radiation therapy is rarely applied to pediatric patients, as radiation-induced damage of the surrounding normal pituitary tissue results in hypogonadism, hypoadrenalism, or hypothyroidism in most patients within 10 years. Long-term follow-up with dedicated unenhanced T1w and T2w sequences is recommended along with hormone status exams.

Infundibular Lesions

Langerhans Cell Histiocytosis (LCH)
Definition of Entity and Clinical Highlights
Langerhans cell histiocytosis, formerly known as histiocytosis X, is a disease entity composed of three rare proliferative disorders of bone marrow-derived antigen-presenting cells of the dendritic cell line, also known as Langerhans cells. The disorder involves the skin, bones, orbit, lungs, and central nervous system (CNS) (being present in only 6% of cases at the time of diagnosis). Granulomas are formed from a proliferation of histiocytes. There is debate to whether or not LCH should be categorized as a tumor or as an inflammatory process. These granulomas can be found in the hypothalamus and infundibulum.

Diabetes insipidus is reported to occur in 5–50% of patients with LCH.

Basic Epidemiology/Demographics/Pathophysiology
LCH is more common in children but generally is a rare disease, with a reported incidence of 0.2–2.0 cases per 100,000 children under 15 years old. LCH is composed of three distinct clinical syndromes that show indistinguishable histology (eosinophilic granuloma, Hand-Schüller-Christian disease, Letterer-Siwe disease). Eosinophilic granuloma is limited to bone in patients usually 5–15 years old. Hand-Schüller-Christian disease is characterized by multifocal bone lesions and extraskeletal involvement of the reticuloendothelial system (RES) and pituitary gland, usually seen in children 1–5 years old. In Letterer-Siwe disease, there is disseminated involvement of the RES with a fulminant clinical course in children less than 2 years old.

Pathological Features
Cells with abundant eosinophilic cytoplasm and reniform (kidney−/coffee bean-shaped) nuclei with grooves are typical. Furthermore, variable collagen, gliosis, and infiltrating T cells with partial infiltration of surrounding CNS parenchyma or circumscribed granulomas are evident. These lesions stain positively with histochemical stains, S-100 and CD1a.

Clinical Scenario and Indications for Imaging

LCH is usually a self-limited disease, with a varied clinical and radiologic presentation. The most common CNS locations involved are the hypothalamic-pituitary axis and cerebellum. The infundibular manifestations include diabetes insipidus, hormone deficiencies (GH deficiency is the most common followed by gonadotropin, ACTH, and TSH deficiencies), and possibly obstructive hydrocephalous. Neurodegeneration characterized by psychomotor deterioration and ataxia is the second most frequent pattern, although still considered rare, affecting about 1–3% of LCH patients.

Imaging Technique and Recommended Protocol

In clinical suspect of LCH, include the spine and full brain for other locations. CT may better depict LCH lesions in the skull or in the petrous bones.

**Interpretation Checklist and Structured Reporting**

In LCH, infundibulum is involved in about 20% of the cases (Fig. 49). Marked thickening and avid enhancement of the infundibulum/pituitary stalk is the main image finding (normal values: 2 mm proximal stalk; 3 mm distal stalk). Invasion of the pituitary gland is rare (10%). There is significant overlap in sellar appearances between LCH, germinomas, and lymphocytic hypophysitis.

CT Findings

Not useful for LCH location in the sellar region. Look for lytic lesions in the skull with sharp margins and more prominent involvement of the inner table. In the mastoids there can be extensive erosive process, uni- or bilateral. In the spine there may be typical diffuse loss of vertebral height (vertebra plana) (Figs. 47, 50, and 51).
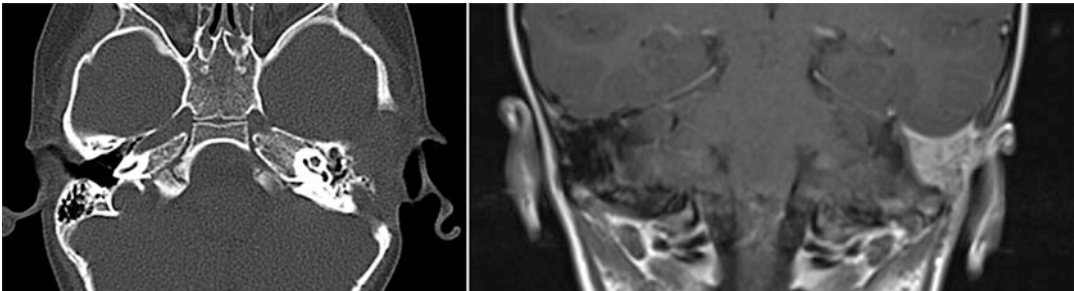
Fig. 49 Coronal (**a**) and sagittal (**b**) T1 C+ on the sellar region show enhancing soft tissue mass in a patient with LCH (arrows)
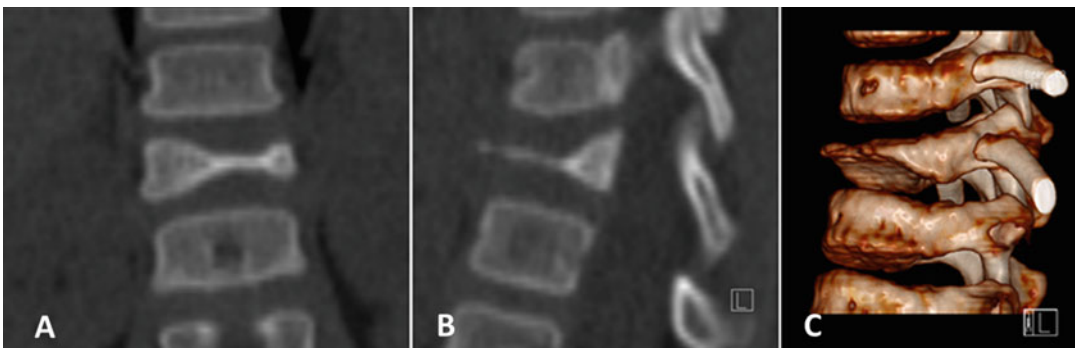
Fig. 50 Typical diffuse loss of vertebral height ("vertebra plana") in patient with LCH demonstrated on coronal (**a**), sagittal (**b**) reformats and 3D volume rendering (**c**) CT images
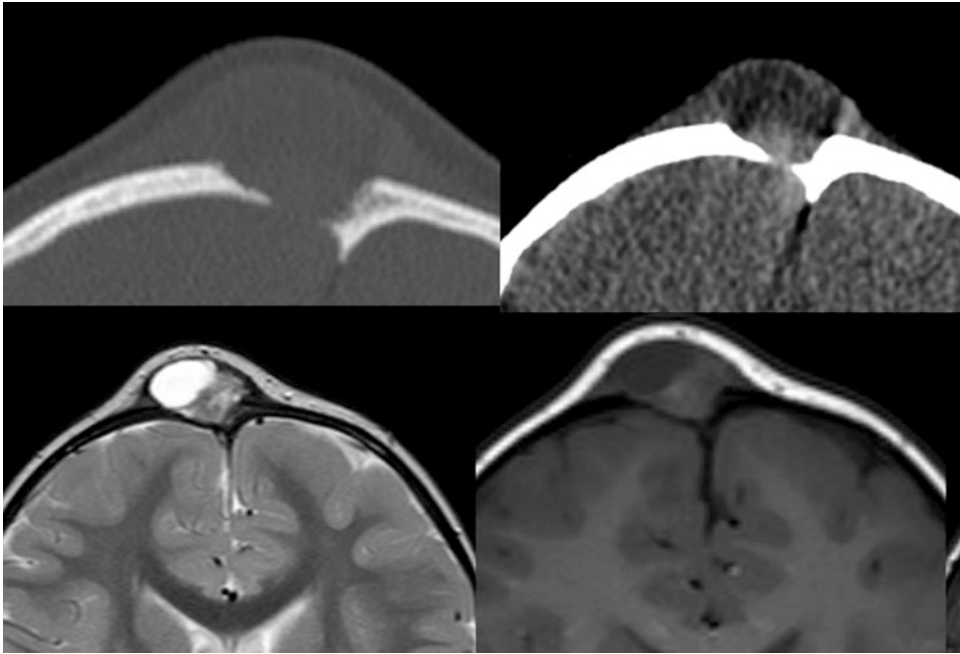
Fig. 51 CT and MRI appearances of LCH lytic lesions in the skull. CT bone window (upper row left) and soft tissue window (upper row right); MR T2 WI (upper row left) and T1 WI (lower low right)

MR Findings

T1w: absent posterior pituitary spontaneous T1 signal (pituitary "bright spot"), thickening of the stalk. Sometimes there is frank soft tissue mass visible (Fig. 52).

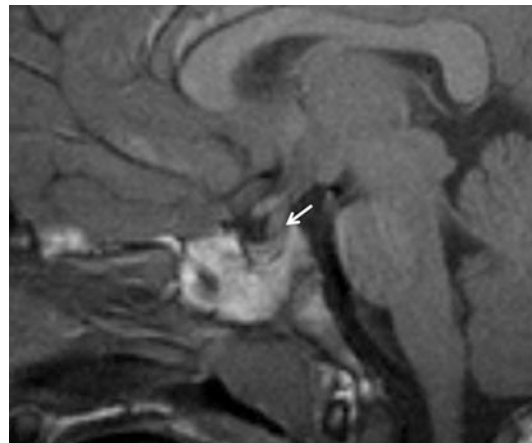T2w: stalk thickening and hyperintensity. Look for enlarged perivascular spaces and bilateral symmetric lesions in the cerebellum and basal ganglia of variable signal intensity, depending on site and stage of the lesion (Fig. 53).

T1w with contrast: enhancement of the pituitary stalk and of the associated soft tissue mass (Fig. 49). Enhancing masses may be seen in the skull or mastoids. Areas of abnormal enhancement have been reported in the leptomeninges, choroid plexus, basal ganglia, and vertebrae.

Fig. 52 Sagittal T1 WI without contrast. Thickening of the pituitary stalk (arrow) and absent posterior pituitary "bright spot"

Pearls

– Isolated CNS involvement is rare; thus, patients tend to present with other manifestations of LCH. In order to make the diagnosis of LCH, one must search for extracranial manifestations of LCH with a radiographic skeletal survey, skull series, chest radiograph, and bone scan so that these lesions can be biopsied.
– Diabetes insipidus, stalk thickening, and loss of pituitary "bright spot" are suggestive of LCH, germinoma, or lymphocytic hypophysitis.
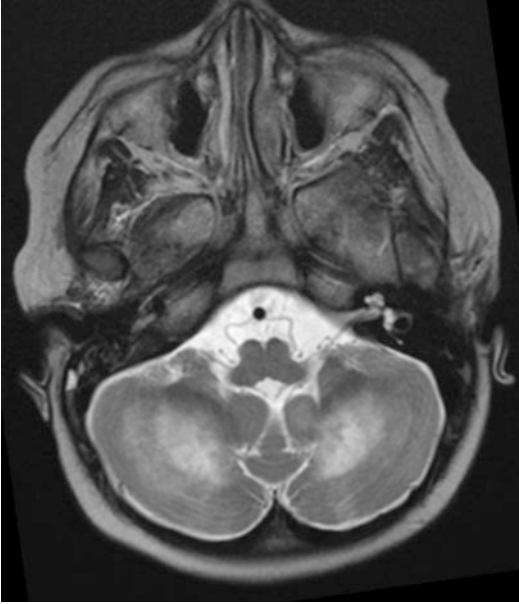
Fig. 53 Axial T2 WI. Immunomediated abnormalities in the cerebellar white matter in a patient with LCH

Treatment and Lesion Monitoring

Treatment involves prednisolone and chemotherapy, including desmopressin for diabetes insipidus. There is no established and effective treatment of neurodegeneration in LCH. MRI every 6 months for 2 years. and then after 1 year. for patients with diabetes insipidus with or without pituitary stalk thickening. Enlargement of the pituitary stalk (> 6.5–7 mm) is an indication for biopsy.

Differential Diagnosis

– Germinoma: may be very difficult to distinguish from LCH in absence of other locations. Look for CSF spread and pineal region involvement in germinoma.
– Neurosarcoidosis: associated meningeal thickening and nodular enhancement. Other associated findings are vasculitis, parenchymal masses, and perineural spread.
– Lymphocytic hypophysitis: inflammatory, immune-mediated disease affecting pituitary gland in woman immediately pre- or postpartum. Can involve the entire pituitary gland, only the adenohypophysis or infundibulum and neurohypophysis. It is rare in children.

Image findings include absence of the pituitary "bright spot," thickening of the stalk, and enhancing soft tissue centered in the adenohypophysis without stalk deviation and with cranial extension. May have dural tail and inflammation of the sphenoidal mucosa.

Suprasellar Tumors

Hypothalamic and Chiasmatic Optic Pathway Glioma (OPG)
Definition of Entity and Clinical Highlights
OPGs in children are often low-grade, indolent gliomas which involve the anterior visual pathway of the optic nerve (25–35%) or the posterior visual pathways (chiasmal and postchiasmal) and hypothalamus. OPGs are the most common central nervous system tumors associated with NF1 (approx. 15% of NF1 patients).

Basic Epidemiology/Demographics/Pathophysiology
OPGs account for approximately 2% of cerebral gliomas. They are typically slow-growing neoplasms that occur mainly in children, with 75% diagnosed before the age of 10. NF1 tumors more commonly involve the anterior visual pathway, while tumors in NF1-negative children are more frequent in the posterior visual pathway. OPGs have also been described in patients with NF2. Spontaneous regression can occur, especially in patients with NF1.

Pathological Features
OPGs consist mostly of WHO grade I tumors represented by pilocytic astrocytomas (PA), the rest being pilomyxoid astrocytomas (PMA) – WHO grade II tumors. The tumors may appear smooth, fusiform, eccentric, or lobulated. BRAF duplications have been identified in approximately 70% of cases. OPGs in NF1 exhibit a characteristic loss of neurofibromin (which functions as a negative growth regulator for astrocytes) and increased RAS activation.

Clinical Scenario and Indications for Imaging
Although infrequently resulting in death, OPGs cause significant visual morbidity, including

proptosis and a progressive loss of vision, as well as symptoms of raised intracranial pressure. Endocrinopathies and hypothalamic dysfunction such as the diencephalic syndrome have been observed in a minority of cases. In many cases, the tumors are clinically indolent.

Imaging Technique and Recommended Protocol

Full brain tumor protocol needs to be added to the specific sequences on the sellar region in patients with NF1. In such patients, consider optional use of MRA to diagnose cerebrovascular disease.

Interpretation Checklist and Structured Reporting

Fusiform enlargement of the chiasm and/or hypothalamus with T2w/FLAIR hyperintensity, variable enhancement, and no diffusion restriction. Large OPGs can have cystic degeneration and extend inferiorly (Fig. 54). Cystic components are much more frequent in patients without NF1.

CT Findings

Enlargement of the chiasm and/or hypothalamus. Cystic hypodense areas may be present in large lesions.

MR Findings

T1w: Isointense or mildly hypointense to the brain parenchyma. If areas of spontaneous hyperintense signal in keeping with hemorrhagic changes are present, think of pilomyxoid astrocytoma.

T2w/FLAIR: OPGs are often hyperintense to the brain tissue (Fig. 54a, b).

DWI: No diffusion restriction (low cellularity).

T1w with contrast: Variable enhancement particularly in NF1 cases. In sporadic cases, the enhancement has been described as moderate to intense (Fig. 54c). No enhancement of the optic glioma is frequent in NF1. The enhancement pattern is often variable over time, without any clinical consequences.

PWI: Areas of possible high perfusion due to the intrinsic tumor vascularity are not indicative of anaplasia. However, increased baseline permeability is suggestive of aggressive entities.

MRS: Increased choline/NAA ratio. Aggressive lesions demonstrate significantly lower baseline myoinositol peak than the stable tumors.

Pearls

– Pilomyxoid astrocytoma (PXA) is a more aggressive variant of the pilocytic astrocytoma (PA) that may be centered in the hypothalamic/chiasmatic region and has higher rate of recurrence and CSF dissemination. Presence of intratumoral hemorrhage, invasion of surrounding structures (e.g., temporal lobes and basal ganglia), strong enhancement, and young age favor PXA over PA (Fig. 55).
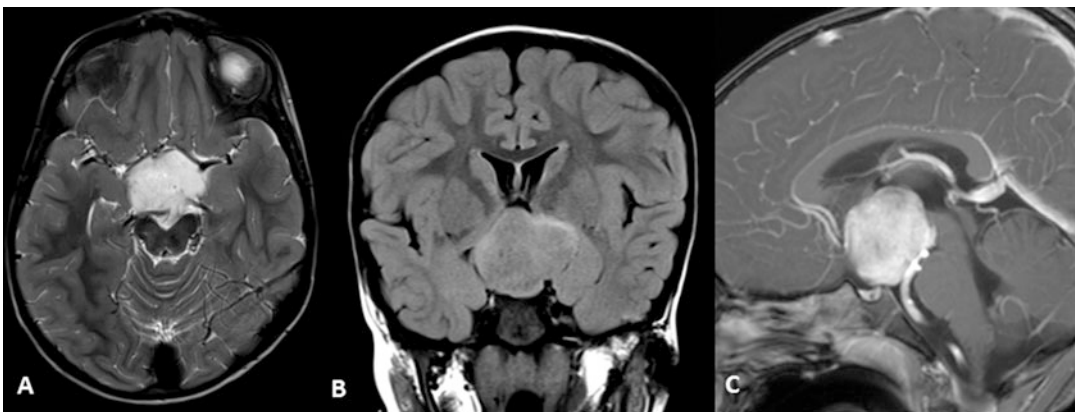
Fig. 54 Axial T2 WI (**a**), coronal FLAIR (**b**), and sagittal T1 WI C+. Typical suprasellar OPG. There are mass effect on the surrounding structures, sparing of the pituitary gland, and strong enhancement
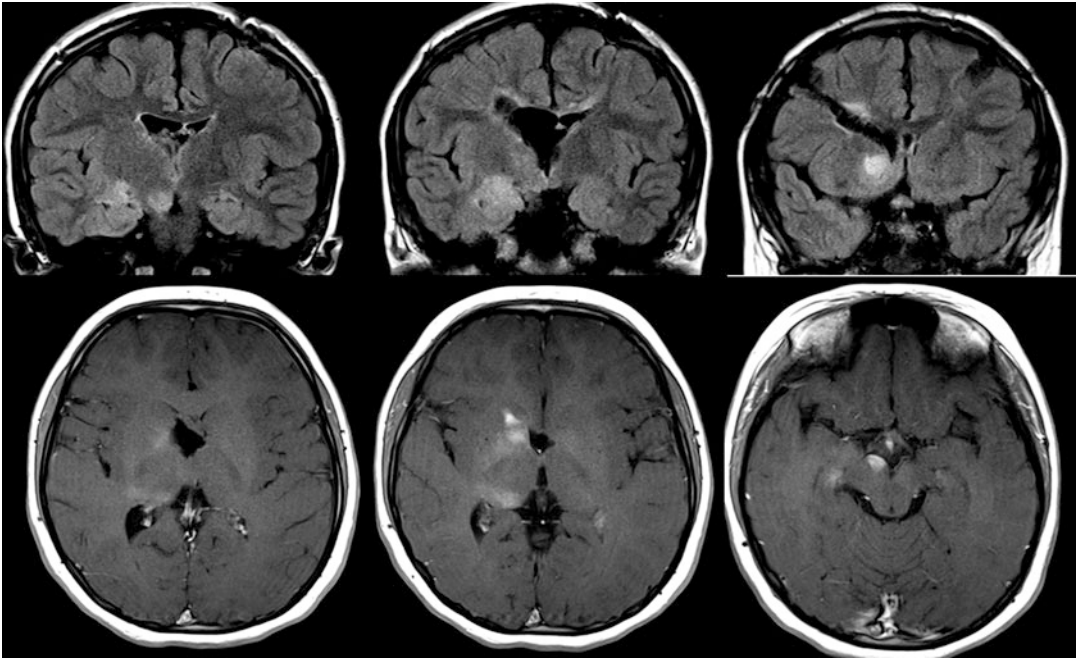
Fig. 55 Infiltrative appearances of biopsy-confirmed pilomyxoid astrocytoma. Coronal FLAIR (upper row) and axial T1 WI C+. Note the surgical tracts from previous tumor debulking in the frontal lobes

– Involvement of the intraorbital optic nerve results in its enlargement and tortuosity. The affected nerve may be diffusely infiltrated and appears T1w hypointense and T2w hyperintense, with quite homogeneous enhancement. If an infiltration of the subarachnoid spaces, sparing the optic nerve itself, is present, T2w hyperintensity and a rim of enhancement around the unaffected nerve are seen. Compare this to the enlargement of the subarachnoid spaces with no enhancement, which is frequently observed in patients with NF1 this is like (Fig. 57) an hamartoma hypothalamicus.
– Look for other radiological findings in NF1 patients: (a) focal, ill-defined areas of T2/FLAIR hyperintense signal mostly located in the basal ganglia, cerebellum, hippocampi, and cerebellar white matter, (b) sphenoid wing hyperplasia, (c) vascular dysplasia, and (d) plexiform neurofibromas this is an hamartoma.
– The most widely used classification is the Dodge classification based on anatomical localization: stage 1, the tumor affects the optic nerve only; stage 2, the chiasm is affected (with or without optic nerve involvement); and stage 3, hypothalamic involvement and/or other nearby structures are involved. This classification has long been used to select patients for resection of optic nerve tumors and has been shown that tumors at the optic chiasm have a poorer outcome. A modified Dodge classification highlights tumors at locations where progressive enlargement could be associated with a further impairment in visual function in order to guide therapy management.

Treatment Monitoring
If isolated to one optic nerve without chiasm involvement, then resection is curative. If a tumor extends to the chiasm or more posteriorly, resection is reserved for symptom treatment. Size and visual symptoms are used in follow-up of OPGs. It is important to check for involvement of the optic nerves and associated NF1 brain findings. Contrast enhancement and perfusion changes are unfortunately not reliable markers of tumor response.

Differential Diagnosis

– Craniopharyngiomas (CPs): Cysts are common and larger and may have internal T1/FLAIR hyperintense signal (33%). CPs compress and displace optic chiasm, while OPGs are indistinguishable from it.

Tuber Cinereum Hamartoma (Hypothalamic Hamartoma)
Definition of Entity and Clinical Highlights

Tuber cinereum hamartoma or hypothalamic hamartoma (HH) is a benign non-neoplastic heterotopia typically occurring in the region tuber cinereum, a part of the hypothalamus located between the mammillary bodies and the optic chiasm. Pedunculated HHs are generally present with precocious puberty and seizures. Sessile HHs are characterized by typical gelastic seizures.

Basic Epidemiology/Demographics/Pathophysiology

Their true incidence is unknown but has been estimated to be from as high as 1 in 50–100,000 to 1 in 1 million. HHs hallmark are disorganized networks of neurons and astrocytes, not dissimilar in some respects to other structural lesions associated with epilepsy, such as cortical dysplasia, and cortical tubers found in tuberous sclerosis complex. Symptoms often begin in early infancy and are progressive resulting in general cognitive and functional disability. Secondary generalized epilepsy can be developed typically between 4 and 10 years of age and involves the appearance of multiple seizure types – complex partial seizures with or without secondary generalization, tonic-clonic seizures, and "falling" seizures.

Pathological Features

HHs are composed of abnormally distributed but cytologically normal, mature, various sized neurons and glia, including fibrillary astrocytes and oligodendrocytes. Immunohistochemistry demonstrates extensive production of synapse-associated proteins. In contrast to cortical dysplasia, atypical large ganglion-like balloon cells are almost never seen.

Clinical Scenario and Indications for Imaging

HHs are typified by epilepsy, developmental delay, central precocious puberty, visual problems, and behavioral disorders. Gelastic seizures are not pathognomonic to HHs, being seen in cryptogenic cases or in association with temporal lobe epilepsy. Adult-onset patients tend to present with non-gelastic seizures and have a milder epilepsy syndrome with less severe learning difficulties and behavioral problems. A more benign disease course is also seen in children with Pallister-Hall syndrome (PHS) – an autosomal dominant inheritable disorder characterized by HHs, central polydactyly, imperforate anus, bifid epiglottis, and panhypopituitarism.

Imaging Technique and Recommended Protocol

High-resolution T1 and T2 sequences in coronal and sagittal planes centered on the midline. Post-contrast T1 sequences help in differentiating HH from gliomas. Full brain protocol should be performed for associated abnormalities such as holoprosencephaly.

Interpretation Checklist and Structured Reporting

Sessile or pedunculate mass in the hypothalamic area, tuber cinereum, or mammillary bodies. HHs can have variable size and are isointense to gray matter in T1 WI and slightly hyperintense or isointense in T2 WI. No enhancement. In large HH some cystic areas may be seen (Fig. 56 and 57).

CT Findings

Small suprasellar mass with homogeneous density.

MR Findings

T1w: isointense/slightly hypointense to gray matter.

T2w: isointense/slightly hyperintense to gray matter.

T1w with contrast: absence of contrast enhancement.

MRS: reduced NAA/Cr ratio has been described and probably is related to reduced number of functioning neurons and increase of gliotic tissue in comparison to normal gray matter. Increased myoinositol and increased Cho/Cr compared to the amygdala have also been reported.

Pearls

The imaging characteristics of HHs significantly reduce the differential as most of the other lesions encountered in the region have either markedly different signal intensity or demonstrate enhancement.

Treatment Monitoring

Size monitoring during medical therapy, probably more than 95% remain refractory to medication alone. Surgical resection/disconnection is also a possible option in case of large lesions and/or inefficient medical treatment. Approximately 25% of the cases have a more benign course, without development of an epileptic encephalopathy and with preserved cognition.
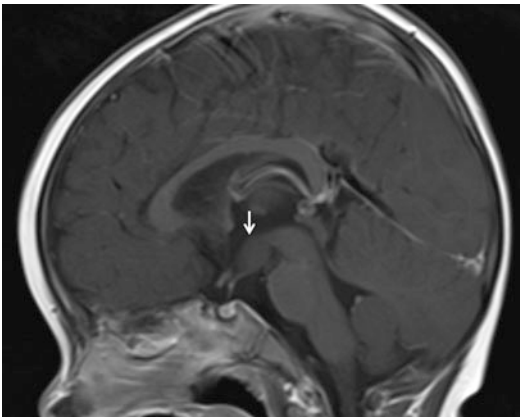
Fig. 56 Sagittal T1 WI C+ demonstrates a broad-based, sessile hypothalamic hamartoma without contrast enhancement (arrow)

Differential Diagnosis

– **Chiasmatic/hypothalamic astrocytoma**: sporadic or in NF1 patients. Frankly hyperintense in T2 and with variable contrast enhancement. Fusiform enlargement of the chiasm/optic nerves/hypothalamus is seen.
– **Craniopharyngioma**: presence of cysts, calcification, and enhancement of the solid portion/cyst walls allows differentiation with HHs.
– **Langerhans cell histiocytosis**: different clinical setting (diabetes insipidus), thickening of stalk. Look for associated LCH lesions in the skull.
– **Lipoma**: fatty signal in all the sequences.
– **Ectopic neurohypophysis**: small area of T1 hyperintense signal along the stalk or floor of the third ventricle. Absent normal pituitary "bright spot."

Non-diffuse Astrocytic Tumors

Pilocytic Astrocytoma (PA)

Definition of Entity and Clinical Highlights

PAs are slow-growing, generally well-demarcated tumors (WHO grade I) that are frequently cystic with a brightly enhancing mural nodule.
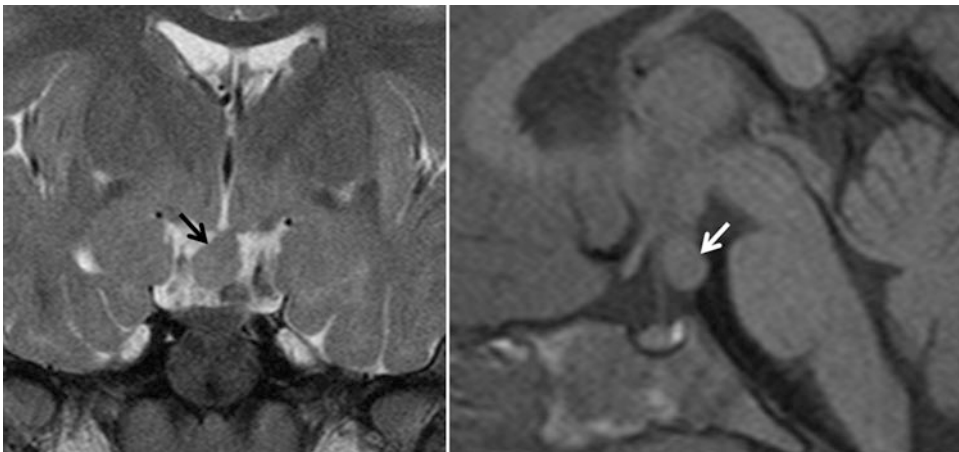
Fig. 57 Typical appearance of pedunculated hypothalamic hamartoma in T2 WI (black arrow) and T1 WI (white arrow)

**Basic Epidemiology/Demographics/
Pathophysiology**
75% of the PAs occur in the first two decades of life without gender predisposition. There is marked association between NF1 and PAs with approx. 20% of NF1 patients having PAs in early childhood.

Pathological Features
PAs feature elongated cells with long processes that form a densely fibrillary background, alternating with regions of loose and microcystic appearances. Rosenthal fibers are frequently encountered differentiating these tumors from other astrocytomas. Some areas may mimic diffuse astrocytomas and even oligodendrogliomas. PAs (GFAP and S100 positive in immunohistochemistry) often have a tandem duplication of chromosome 7q34, which is associated with a BRAF-KIAA fusion gene (lacking in NF1 patient), and the supratentorial PAs may have BRAF V600E mutations.

Clinical Scenario and Indications for Imaging
The supratentorial PAs are less common in the pediatric population, and their clinical manifestations are variable depending on the site (i.e., seizures if located in the temporal lobe).

Imaging Technique and Recommended Protocol
Please refer to CPAs in section "Posterior Fossa Tumors."

Interpretation Checklist and Structured Reporting
Most of the cases of supratentorial PAs are located along the optic pathways and are more frequent in NF1 patients (Figs. 58 and 59). Imaging features reflect the low grade of the tumor and are similar to the ones located in the posterior fossa: absent diffusion restriction, presence of enhancement, cystic components, and low perfusion in most of the cases (Fig. 60). As for the posterior fossa location, possible pitfalls are presence of lipid/lactate peaks on MRS and areas of high perfusion on PWI.

Treatment and Monitoring
Overall good prognosis following complete surgical resection (5-year and 10-year survival >95%) with fibrillary variants tending to have slightly worse prognosis compared to the cystic tumors.

Pilomyxoid Astrocytoma

Definition of Entity and Clinical Highlights
Pilomyxoid astrocytoma (PMA) is a recently described entity with similar features as PA. WHO considers PMA to be a grade 2 variant of PA (though formal grading does not exist in the 2016 classification update) with distinct histological characteristics and a poorer prognosis.

**Basic Epidemiology/Demographics/
Pathophysiology**
PMAs are usually seen in the young pediatric population and infants (mean age of 10–18 months); however, recent reports have indicated that PMAs can occur in adults. As it is a relatively newly classified entity, its epidemiology is not clear.
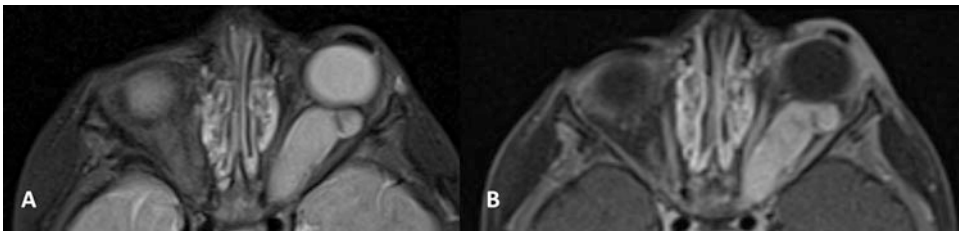
Fig. 58 Axial T2 (**a**) and T1 C+ (**b**) of the orbits. There is fusiform enlargement of the left optic nerve with prominent enhancement and associated proptosis, in keeping with optic pathway glioma
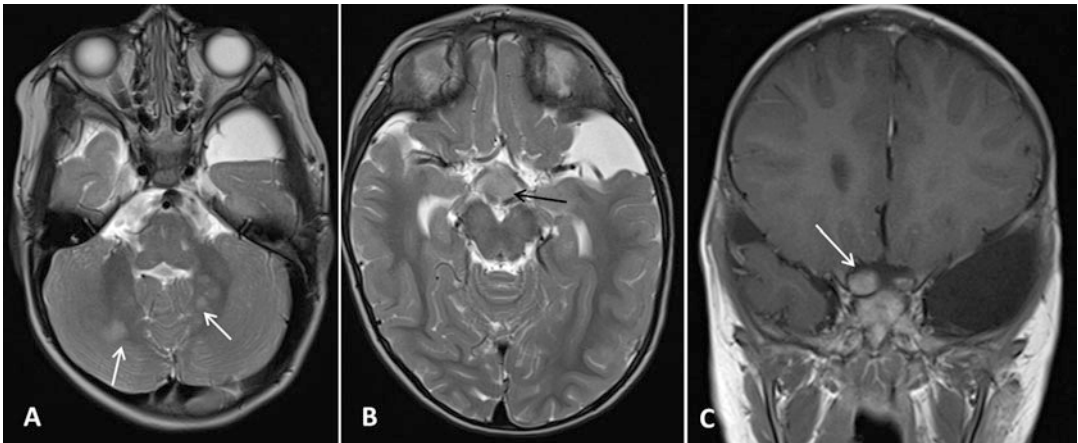
Fig. 59 Axial T2 (**a** and **b**) and coronal T1 C+ (**c**) in a patient with NF1. Multiple NF1-related foci of abnormal signal (FASI) are noted in the cerebellar white matter (arrows in **a**). There is also a hypothalamic glioma (arrow in **b**) and right OPG (arrow in **c**)

Pathological Features

PMAs are well-circumscribed and differentiated histologically from PAs because of the lack of Rosenthal fibers, calcification, and eosinophilic granular bodies. PMAs also lack the biphasic appearance (dense cellular areas alternating with loose cystic areas) usually present in PAs.

Clinical Scenario and Indications for Imaging

See PAs.

Imaging Technique and Recommended Protocol

See PAs.

Interpretation Checklist and Structured Reporting

PMAs are more frequent in the optic chiasm and hypothalamus but can occur everywhere in the neuraxis. PMAs are isointense on T1 and hyperintense on T2, which is enhanced homogeneously or heterogeneously after the injection of gadolinium. The ADC values and T2 signal intensity are generally higher than in PAs, which indicates the proportion of myxoid matrix. PMAs often present with hemorrhages and foci of necrosis (being thus more heterogeneous appearance in comparison to PAs) (Fig. 61). There are no reliable radiological findings allowing differential diagnosis between these two entities.

Treatment and Monitoring

PMA management is controversial with a tendency to recommend adjuvant therapy (i.e., chemotherapy or radiotherapy) in cases of tumor recurrence or partial resection. The gross total resection is the most favorable outcome predictor. In view of the significant trend of regrowth and cerebrospinal fluid (CSF) spread, a strict follow-up is recommended.

Pleomorphic Xanthoastrocytoma

Definition of Entity and Clinical Highlights

Pleomorphic xanthoastrocytomas (PXAs) are rare, low-grade (WHO grade II) astrocytomas found in young patients often associated with temporal lobe epilepsy. The prognosis is generally good, but the tumors may recur after subtotal resection and some PXAs progress to higher-grade malignant gliomas (WHO grade III).
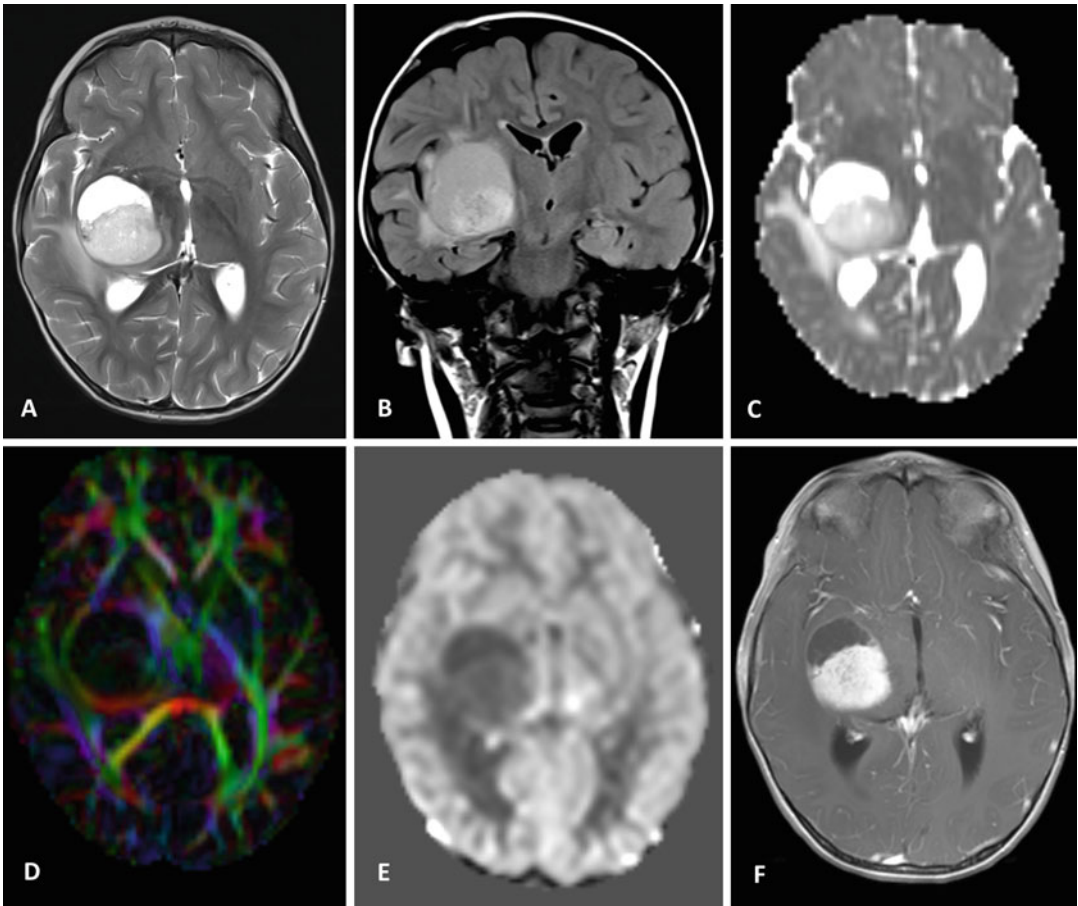
Basic Epidemiology/Demographics/ Pathophysiology

PXAs account for 1% of primary brain tumors. The peak incidence age is in the second to third decades of life.

Pathological Features

PXAs are characterized by markedly pleomorphic cells, eosinophilic granular bodies, prominent

Fig. 60 Axial T2 (**a**), coronal FLAIR (**b**), axial ADC maps (**c**), axial DTI color FA maps (**d**), axial ASL rCBF map (**e**), and axial T1 C+ (**f**). Typical MRI appearances of pilocytic astrocytoma: the mass is partially cystic with relatively poor surrounding vasogenic edema, no diffusion restriction, and homogeneous contrast enhancement of the solid portion. Note that the white matter bundles surrounding the mass are displaced but not infiltrated (**d**) and that the mass shows low perfusion (low signal in **e**). Radiological features are consistent with low-grade tumor in the right basal ganglia/thalamus

reticulin deposition, and a superficial meningocerebral location. BRAF V600E mutations are common, and CDKN2A/B deletions may also be present.

Clinical Scenario and Indications for Imaging

Typically (~75% of cases), the patients with PXAs present with long-standing partial complex seizures. Other symptoms include dizziness and headache.

Imaging Technique and Recommended Protocol

See PAs.

Interpretation Checklist and Structured Reporting

PXAs are typically supratentorial, superficial (cortically located) masses with cystic components, enhancing nodules and dural tail.

CT Findings

Skull remodeling due to a long-standing growing lesion.

MR Findings

T1w: Solid portion isointense to gray matter; cystic portion with similar signal to CSF in all sequences. 3D-T1w may show rare cases with associated cortical dysplasia.
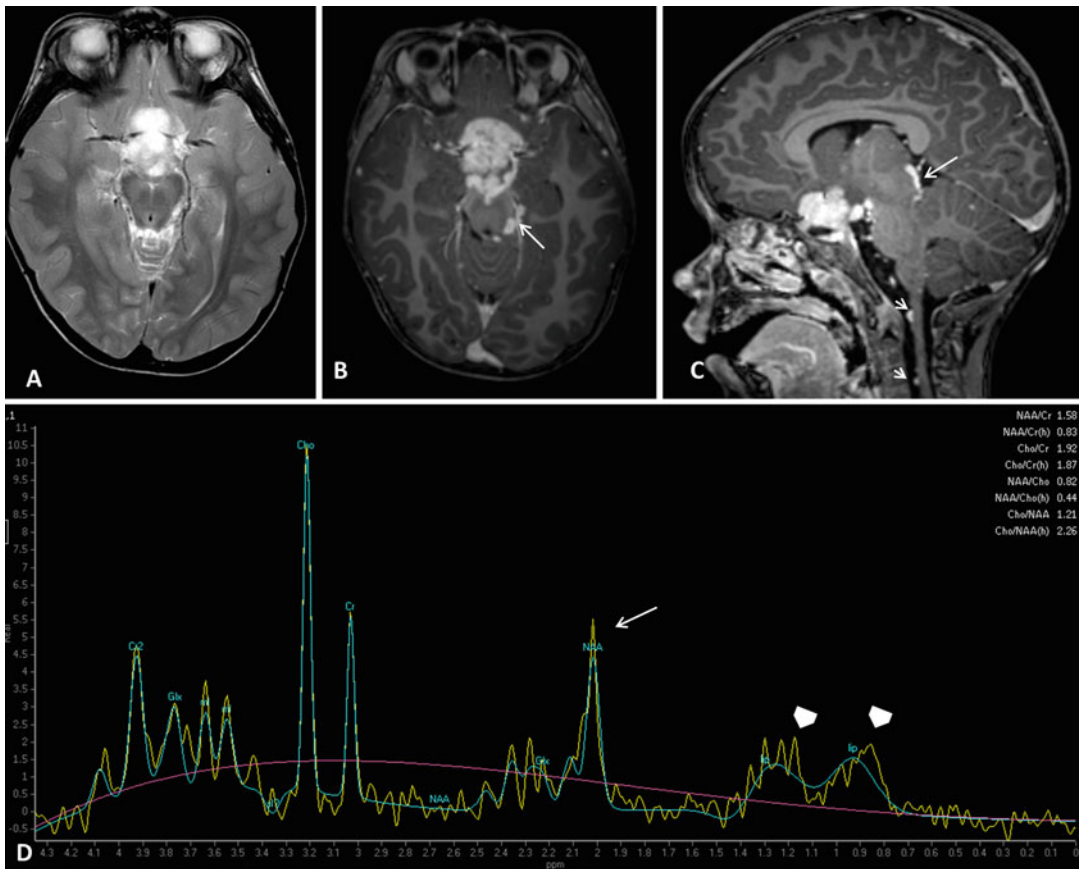
Fig. 61 Axial T2 (**a**), axial and sagittal T1 C+ (**b** and **c**), and MRS (**d**) in a patient with biopsy-proven pilomyxoid astrocytoma BRAF V600 mutation negative. A large enhancing mass is visible in the suprasellar region with extensive CSF dissemination in the brain (long arrows in **b** and **c**) and spine (short arrows in **c**). MRS shows reduction of NAA (arrow in **d**) and lactate doublet (arrowheads in **d**)

T2w: Hyperintense solid nodules with CSF-like cysts. Edema is rare (Fig. 62a).

T1w with contrast: Strong enhancement is often demonstrated together with dural tail. In rare cases, PXA may metastasize with multiple enhancing nodules along the surface of brain and spine (Fig. 62c).

DWI: No restriction (low cellularity) (Fig. 62b).

Pearls

A superficial mass with dural tail diagnosed in a young adult with this kind of epilepsy is strongly suggestive of PXA.

Treatment Monitoring

Resection is the treatment of choice. Follow-up needs to include the brain and spine with contrast.

Differential Diagnosis

– Pilocytic astrocytoma: not cortically based but often located in the optic pathways. No dural tail is present.
– Ganglioglioma: cortically based lesion without dural tail and with typical nodule and cystic structure (though not in all cases).
– Dysembryoplastic neuroepithelial tumor (DNET): DNET may have multicystic appearance; contrast enhancement is not as frequent and as strong as in PXA. No dural tail.
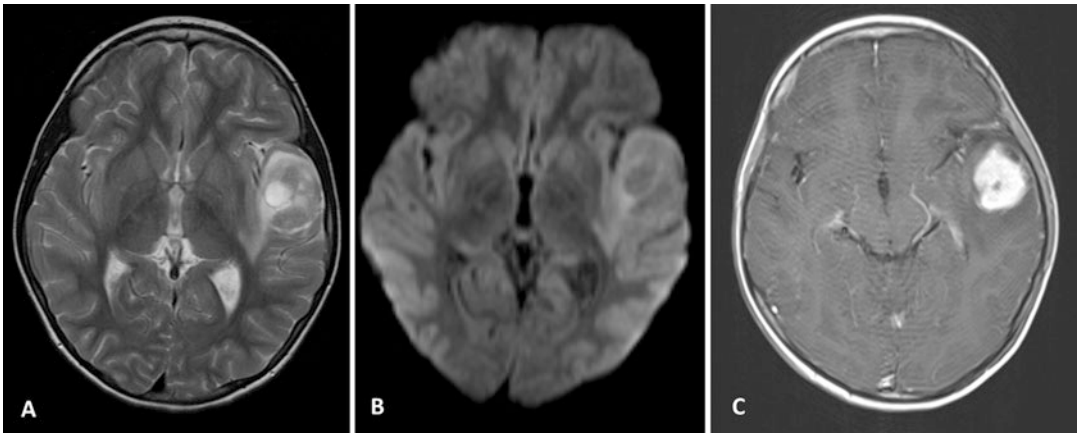
Fig. 62 Axial T2 (**a**), axial DWI (**b**), and axial T1 C+ (**c**) in a patient with pleomorphic xanthoastrocytoma. The tumor appears as mixed solido-cystic temporal mass (most frequent location) with avid enhancement of the solid portion and no diffusion restriction

– Meningioma: extra-axial lesion, with dural tail but more homogeneous enhancement and typical obtuse angle with the surface of the brain. Older patients without epilepsy.

Subependymal Giant Cell Astrocytoma

Definition of Entity and Clinical Highlights
Subependymal giant cell astrocytomas (SEGAs) are benign, slow-growing tumors usually arising in the walls of the lateral ventricles. They are the most common brain tumor in patients with tuberous sclerosis and may occur exclusively in this patient group. They can be either asymptomatic or symptomatic (due to obstructive hydrocephalus and intractable seizures).

Basic Epidemiology/Demographics/Pathophysiology
SEGAs are rare, low-grade brain tumors that generally develop during the first two decades of life in 10–20% of patients with tuberous sclerosis complex (TSC). TSC is characterized by the development of SEGAs, subependymal nodules (SEN), cortical tubers, and cortical migration tracts. SEGAs represent 1–2% of all pediatric brain tumors and usually arise near the foramen of Monro. SEGAs likely develop from SEN, but the molecular mechanisms underlying their progressive growth, in contrast to SEN, are unknown so far.

Pathological Features
SEGAs consist of spindle cells, gemistocytic-like cells, and giant cells. According to the present WHO classification, SEGAs belong to the group of astrocytic neoplasms, even though they have both glial and neuronal expression patterns.

Clinical Scenario and Indications for Imaging
SEGAs are often asymptomatic. When symptoms occur, they are usually a result of obstructive hydrocephalus.
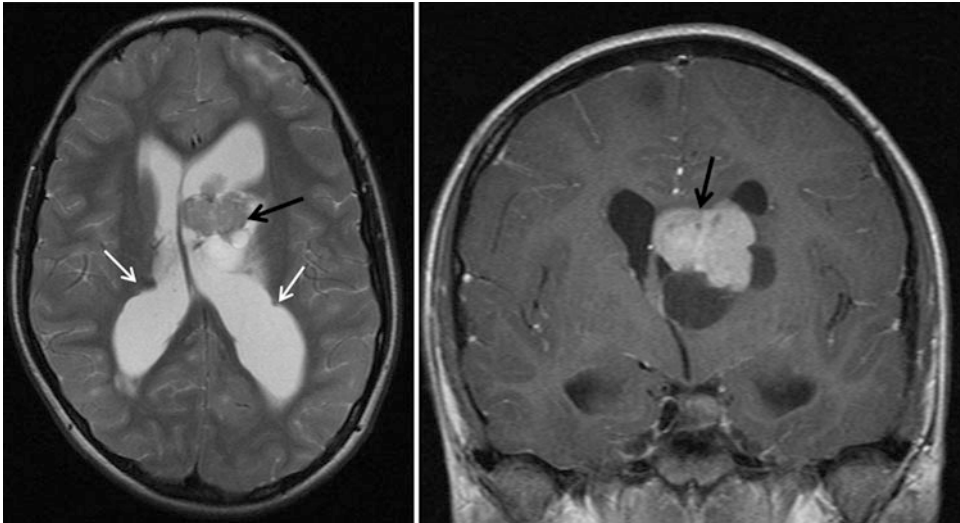
Imaging Technique and Recommended Protocol
See PAs.

Interpretation Checklist and Structured Reporting
Intraventricular mass (>1 cm and/or growing overtime) in the region of the foramen of Monro in patients with tuberous sclerosis (Fig. 63).

CT Findings
SEGAs may show internal calcifications and associated partial hydrocephalus.

Fig. 63 Axial T2 (left) and coronal T1C+ (right) in a patient with TSC. There is a mixed solido-cystic, enhancing mass in the region of the left foramen of Monro (black arrows) with associated hydrocephalus. Multiple subependymal nodules are noted along the ventricular walls, and there are some areas of cortical/subcortical dysplasia (tubers) in the left frontal lobe

MR Findings

T1w: iso−/hypointense unless calcium is prominent (increased T1w signal).

T2w: heterogeneously hyperintense with foci of low signal related to calcium. Hydrocephalus and associated periventricular edema.

T2∗w/SWI: foci of signal blooming related to the presence of calcium.

T1w with contrast: strong enhancement (similar to other SENs).

Pearls

It is not possible to distinguish SEN from SEGA on the basis of signal and contrast characteristics. Enlargement overtime, size, and location at the level of the foramen of Monro allow diagnosis of SEGA over SEN.

Treatment Monitoring

Follow-up after resection is indicated though surgery treatment is often curative. Note that a possible postsurgical complication is an intraventricular hemorrhage. These tumors may be responsive to treatment with the mechanistic target of rapamycin (mTOR) inhibitors sirolimus and everolimus.

Differential Diagnosis

SEGA theoretically goes in differential with all other intraventricular tumor of the childhood (i.e., choroid plexus papillomas, central neurocytoma, and intraventricular astrocytoma). The fact that this tumor is practically present only in TSC patients makes diagnosis straightforward.

Diffuse Astrocytic Tumors

In light of the new 2016 WHO classification, diffuse astrocytic tumors are classified on the basis of molecular abnormalities and histological grade/pattern of growth. For pediatric patients, tumors diagnosed as grade I or II are often referred to as low-grade glioma (LGG), while those diagnosed as grade III or IV are known as high-grade glioma (HGG). Unlike in adults, pediatric LGG is unlikely to transform to HGG. Main molecular groups of diffuse astrocytic tumors are IDH-mutant vs IDH-wild-type (within each level, IDH-mutant astrocytomas have a significantly better prognosis compared with their IDH-wild-type counterparts), H3-K27 M (i.e., diffuse midline gliomas), and 1q/19q-codeletion,

which is typical of oligodendrogliomas (ODGs) and extremely rare in children.

Imaging Technique and Recommended Protocol

Brain and spine MRI with contrast, MR perfusion, MRS, and diffusion techniques are useful in distinguishing low- from high-grade lesions and IDH phenotyping (DWI and MRS).

Diffuse Astrocytomas (Low and High Grade)

Definition of Entity and Clinical Highlights

Diffuse ACs show diffusely infiltrative growth within the CNS. The tumor cells often invade individually or as groups of cells to form a network throughout the neuropil. This results in aggregation of neoplastic cells around the neurons and blood vessels and under the pial membrane. Grade II diffuse gliomas are most prevalent in the cerebral hemispheres.

Basic Epidemiology/Demographics/ Pathophysiology

Diffuse low-grade astrocytomas account for ~5% of all tumors in children aged 0–14 years. High-grade astrocytomas (WHO grades III–IV) are less common, with incidence rates of 0.08 for anaplastic astrocytoma and 0.14 for glioblastoma (GBM). Diffuse LGG are most prevalent in the cerebral hemispheres, followed by the diencephalon, the brain stem, and the cerebellum and spinal cord being the least frequent. Survival for pediatric patients with low-grade diffuse glioma (hemispheric and cerebellar regions) is very good due to the high near total resection rates. Deep-seated midline tumors cannot often be completely resected, and the survival rate relies on the secondary adjuvant treatment.

Pathological Features

ACs show elongated or irregular, hyperchromatic nuclei and eosinophilic, glial fibrillary acidic protein (GFAP)-positive cytoplasm.

Noteworthy is that ODGs have rounded nuclei, often with perinuclear halos, calcification, and rich delicate vasculature. ACs are graded histologically according to their most anaplastic-appearing areas (nuclear atypia and increased mitotic activity in grade III lesions; microvascular proliferation and necrosis in grade IV tumors). Diffuse astrocytic tumors display more elongated nuclei with a densely fibrillar background, while in oligodendroglioma the nuclei appear round and uniform, classically with cytoplasmic clearing giving a fried egg appearance.

IDH mutation status is a stronger prognostic factor than histological grade. TP53 mutations occur in 40–80% of adult diffuse glioma cases (commonly with IDH1/2 mutations). TP53 mutations in pediatric diffuse ATs are much less common (<5%) but are more frequent in pediatric HGGs. Alterations in BRAF (which represents a therapeutically targetable molecular event) have been identified across the spectrum of pediatric LGGs, including diffuse ACs. BRAF V600E mutations in diffuse ACs are common, with most reports suggesting an incidence of ~40%. BRAF V600E-mutant tumors show frequent CDKN2A deletion (possibly more aggressive clinical behavior). CDKN2A is a tumor suppressor gene found on chromosome 9p21 that functions as a negative G1 cell cycle regulatory gene.

Histone variant H3.3 mutations are identified in DIPGs and midline HGGs. Mutations at position 27 are observed only in midline gliomas, involving the brain stem and spinal cord. Alternate histone mutations at position 34 (G34R) are observed in hemispheric (not in midline) HGGs, but not in pediatric LGGs. Other studies have identified the presence of K27M histone H3 mutations in diffuse midline LGGs. Testing for K27M in all midline tumors might be warranted as it suggests a more aggressive clinical course than that seen with BRAF-mutated tumors (Fig. 64).

Clinical Scenario and Indications for Imaging

Children with ACs may be asymptomatic or commonly experience headaches, tiredness, listlessness, or seizures.
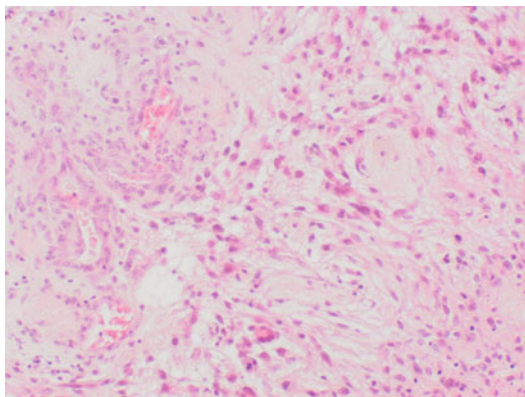
Fig. 64 H&E-stained high-power image of a glioblastoma with pleomorphic glial tumor cells and endothelial proliferation

Interpretation Checklist and Structured Reporting

Non-enhancing mass in the cerebral white matter with relatively benign image characteristics. Infiltration along the white matter tracts is frequently observed.

CT Findings

Hypodense, poorly defined mass. Internal calcification or necrotic areas are very rare.

MR Findings

T1w: homogeneous hypointense mass with infiltrative pattern along white matter bundles.

T2w/FLAIR: homogeneous increase signal with possible areas of low T2w intensity. Mass effect on the midline and extension are better demonstrated on T2/FLAIR sequences (Fig. 65a).

T1w with contrast: enhancement is usually absent; tumors progressing to high grade may show intrinsic enhancement (Fig. 65b).

PWI: low perfusion in low-grade astrocytomas. Increase of perfusion values is indicative of possible anaplastic transformation (Fig. 65c).

DWI: restricted diffusion is absent in low-grade diffuse astrocytoma. Areas of anaplastic transformation are often characterized by diffusion attenuation (Fig. 65d). Areas suggestive of high-grade transformation should be the target for biopsy (Fig. 65e, f).

MRS: increase in lipids and myoinositol. Reduction of NAA and increased choline have been described in association with higher tumor grade. MRS results need to be considered in conjunction with other MRI findings (in particular PWI) in the evaluation of the tumor grade. MR spectrum editing for 2-hydroxyglutarate is useful to further look for IDH-mutant tumors.

Imaging features of GBM are similar in adult and children and include enhancing irregular rim with central necrosis. In children there is tendency to develop internal hemorrhages in comparison to adult counterparts (Fig. 66); furthermore, the molecular profile is different (despite similar histological appearance). A case of hemorrhagic GBM with molecular diagnosis of H3-K27M mutation (diffuse midline glioma) is shown in Fig. 68.

Pearls

– Gliomatosis cerebri (GC) is a term that has been removed from the recent WHO classification because it does not represent a specific entity; however, this term can still be used to describe a specific pattern of growth with involvement of three or more cerebral lobes. Despite GC is a low-grade appearing mass on images, it shows aggressive clinical behavior (Fig. 67).
– Biopsy is suggested also in non-resectable cases in order to characterize the molecular profile of the tumor and the histological grade.

Treatment and Monitoring

In pediatric ACs, complete tumor resection is the most significant predictor of favorable outcome. Diffuse ACs are rarely amenable for complete resection, and radiation treatment (with adverse long-term effects) has been applied. Currently, a more conservative low-dose chemotherapy and debulking approach is the primary strategy for unresectable diffuse AC management. Multiparametric MR imaging with conventional sequences and advanced MR techniques (PWI, MRS) increase the sensitivity in diagnosis of high-grade transformation or distinguishing between treatment-related changes and tumor relapse.

Differential Diagnosis

– Ischemia: acute symptoms predominate, and the radiological abnormalities are localized in
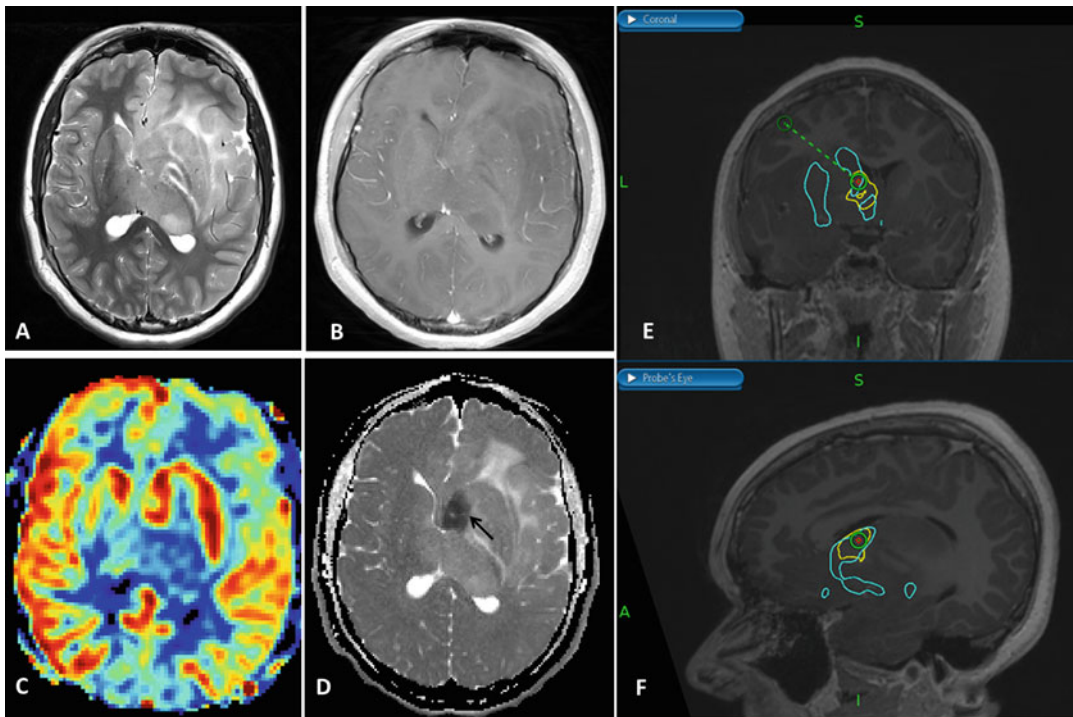
Fig. 65 Diffuse astrocytoma. Axial T2 (**a**) and T1 C+ (**b**) show an infiltrative, non-enhancing mass in the left frontal lobe, temporal lobe, and basal ganglia. The tumor has an area of high rCBF on ASL (**c**) with some restricting component on ADC (arrow in **d**). Combination of rCBF and ADC maps are used to target the biopsy (the blue line in E and F represents the high rCBF area and yellow line the low ADC area; green: biopsy tract in the intersection of the two areas)

a vascular territory (unless of metabolic origin, but in this case multiple ischemic areas are generally noted). In acute phase, striking DWI restriction. No/minimal mass effect and absent infiltration along the white matter tracts.

– Oligodendroglioma: extremely rare in children, with common calcifications.

– Cerebritis: sometimes difficult to distinguish on the basis of images. Clinical context is different (i.e., signs of infection). Herpes encephalitis involves gray matter of the temporal lobes and limbic system usually on both sides but with asymmetrical distribution.

– Glioblastoma multiforme: strong enhancement and central necrosis.

Interpretation checklist and structured reporting: Imaging features of GBM are similar in adult and children and include enhancing irregular rim with central necrosis. In children there is a tendency to develop internal hemorrhages in comparison to adult counterparts (Fig. 66); furthermore the molecular profile is different (despite similar histological appearance). A case of hemorrhagic GBM with molecular diagnosis of H3-K27M mutation (diffuse midline glioma) is shown in Fig. 68.

Neuronal and Mixed Neuronal-Glial Tumors

Dysembryoplastic Neuroepithelial Tumor

Definition of Entity and Clinical Highlights

Dysembryoplastic neuroepithelial tumors (DNETs) are benign, supratentorial tumors encountered in children and young adults with a long-standing history of intractable focal epilepsy and typically no other neurological signs.
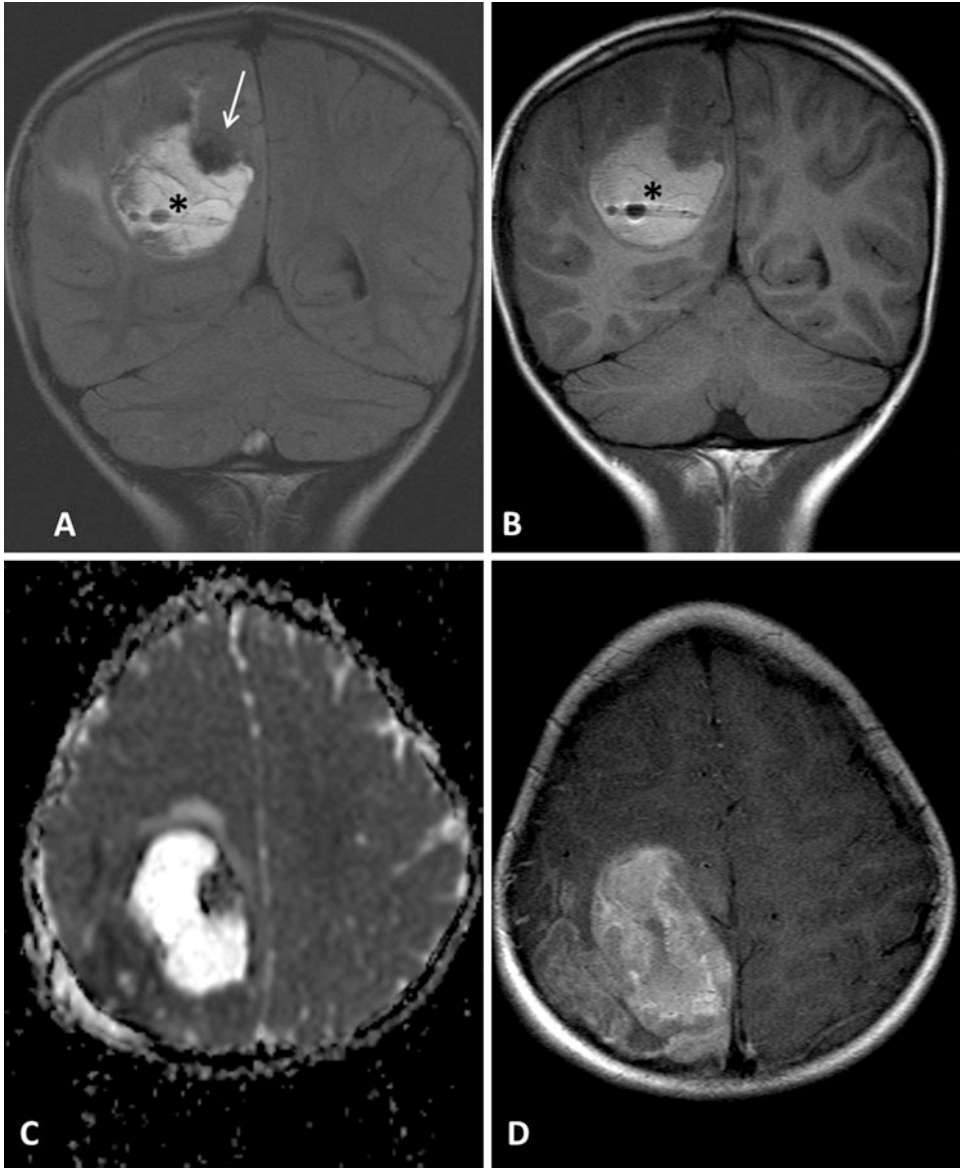
Fig. 66 Right hemispheric glioblastoma multiforme (GBM). Coronal FLAIR (**a**), coronal T1 (**b**), axial ADC (**c**), and axial T1 C+ (**d**). The tumor has a cystic component with high-density fluid (asterisk in **a** and **b**), an area of hemorrhage in its supero-mesial aspect (arrow in **a**), restriction, and enhancement of the solid component

Basic Epidemiology/Demographics/ Pathophysiology

Slight male predilection with possible association with Noonan syndrome. The potential locations of DNETs include the temporal lobe (predominantly), frontal lobe, caudate nucleus, cerebellum (presenting with ataxia), and pons.

Pathological Features

Hallmarks include entrapped cortical neurons, foci of dysplastic cortical organization, multinodular architecture, and a columnar structure (specific glioneuronal element – SGNE) oriented perpendicular to the cortical surface. If only SGNE is present, DNET is called "simple." If
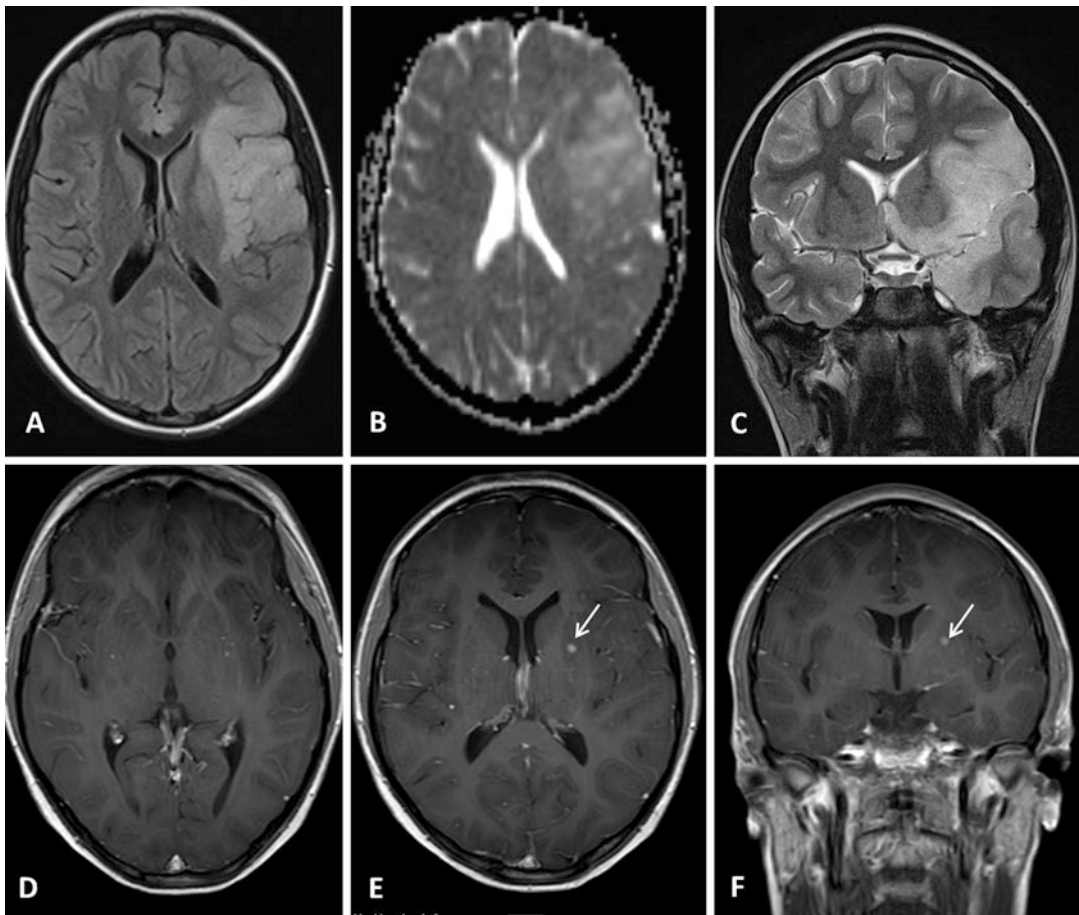
Fig. 67 Diffuse infiltrative glioma with radiological characteristics of gliomatosis cerebri. Axial FLAIR (**a**), axial ADC maps (**b**), coronal T2 (**c**) axial, and coronal T1 C+ (**d**–**f**). Note that the majority of the tumor is not enhancing apart from a small focus (arrows in **e** and **f**)

SGNE with multinodular architecture coexist, DNET is characterized as "complex." The majority of tumors express S100 and OLIG2 with variable CD34, NOGO-A, and myelin-oligodendrocyte glycoprotein expression and often BRAF V600E mutation. DNETs' architecture resembles astrocytoma or oligodendroglioma, but IDH1/2, TP53 mutations, or codeletion of 1p and 19q are not present (Fig. 69).

Clinical Scenario and Indications for Imaging
Children or young adults with seizures of childhood onset.
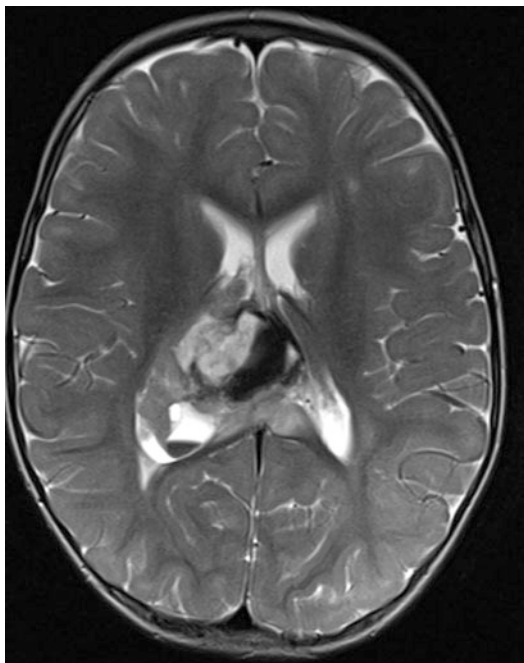
Imaging Technique and Recommended Protocol
Brain MRI with contrast.

Interpretation Checklist and Structured Reporting
Well-defined, exophytic cortical mass with "bubbly" appearance and hyperintense FLAIR rim.

CT Findings
Low-density peripheral brain lesion with associated scalloping of the skull (slow growth) and calcifications in about 1/3 of the cases.

Fig. 68 Right thalamic GBM with intraventricular extension, multiple internal areas of hemorrhages, and infiltration of the splenium of the corpus callosum
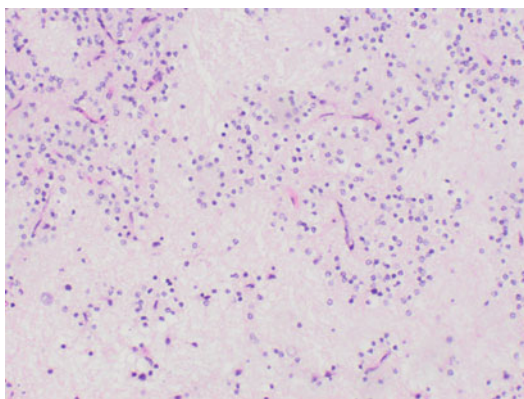
Fig. 69 H&E-stained high-power image of a dysembryoplastic neuroepithelial tumor with a relatively loose network of glial tumor cells and so-called floating neurons in the matrix

MR Findings

T1w: hypointense mass with possible microcystic appearance.

T2w: hyperintense mass with "bubbly" appearances and absent/minimal surrounding edema (Figs. 70a and 71a).

FLAIR: slightly hyperintense signal with typical external rim of high signal (Figs. 70b and 71b).

DWI: no restriction unless rare internal bleeding occurs.

T1w with contrast: no enhancement in most of the cases (80%), differentiating DNETs from gangliogliomas.

Pearls

Association with cortical dysplasia is frequent on pathology. Rarely, tumor recurrence or even malignant transformation may occur. If lesion looking like a DNET enhances avidly, consider more aggressive tumors, and look for metastases (additional spine imaging suggested).

Differential Diagnosis

- Ganglioglioma: it shows more often nodular enhancement, calcifications, and cystic appearance.
- Focal cortical dysplasia (FCD): blurring of the gray/white matter junction without mass effect or scalloping of the overlying bone. Type IIIb (Blumcke classification) may have subcortical T2/FLAIR hyperintense signal but no hyperintense rim.
- Pleomorphic xanthoastrocytoma: typical enhancing mass with dural tail.

Treatment and Monitoring

Surgery is indicated for refractory seizures but lesions in eloquent cortex are best managed conservatively. Postsurgically, most patients are seizure-free, but seizure incidence seems to increase in the long term with the main risk factors being age >10 years and longer duration of epilepsy (>2 years) prior to surgery.

Ganglioglioma and Gangliocytoma

Definition of Entity and Clinical Highlights

Gangliogliomas and gangliocytomas comprise a spectrum of low-grade tumors (WHO grade I) characterized by a dysplastic neuronal population with neoplastic glial cells in gangliogliomas and large, well-differentiated neurons in gangliocytomas.
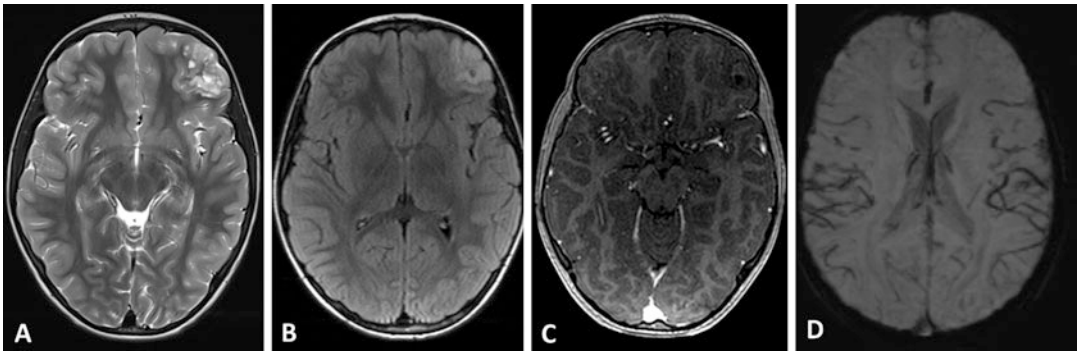
Fig. 70 Left frontal DNET with typical cortical/subcortical location, multicystic "bubbly" appearance, lack of enhancement and of internal calcifications. Axial T2 (**a**), axial FLAIR (**b**), axial T1 C+ (**c**), and axial SWI (**d**)
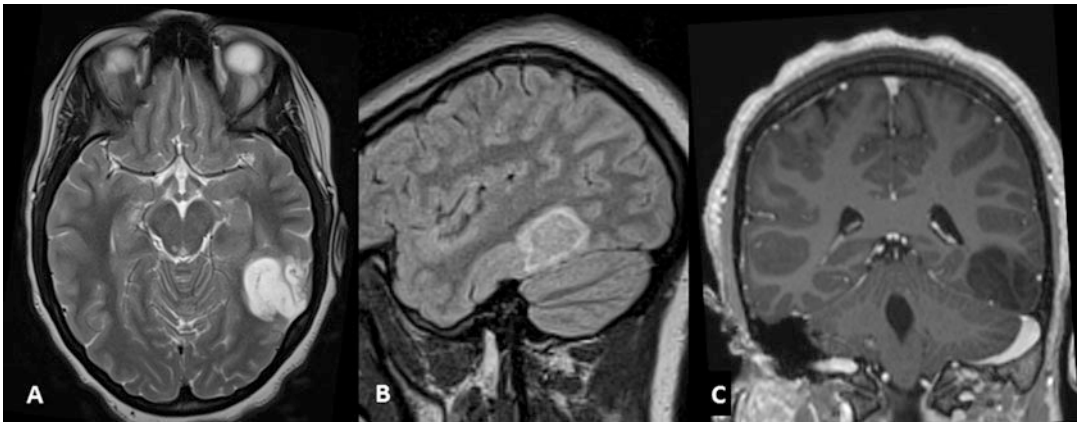
Fig. 71 Axial T2 (**a**), sagittal FLAIR, and coronal T1 C+ in a patient with temporal DNET. Typical peripheric FLAIR bright rim sign is seen in **b**

Seizures and long-standing epilepsy are the clinical hallmarks.

Basic Epidemiology/Demographics/ Pathophysiology

Children and young patients without gender predominance are affected. These tumors may arise anywhere in the neuraxis; however most are supratentorial and located in the temporal lobes. Gangliogliomas are rare (~10% of primary cerebral tumors in children). Gangliocytomas account for 0.1–0.5% of all brain tumors.

Pathological Features

Gangliogliomas are positive for the following neuronal markers: synaptophysin, neurofilament protein, MAP 2, chromogranin-A, GFAP, and CD34 (70–80%). BRAF V600E mutations are encountered in 20–60% of gangliogliomas (they carry higher risk for recurrence after standard therapy), which are IDH negative. Midline, low-grade gangliogliomas may harbor both the H3F3A mutation and BRAF V600E in both the glial and neuronal components. The ganglioneurocytomas are pathologically closely related and also appear with small mature neoplastic neurons. The key feature in distinguishing gangliocytomas from gangliogliomas is identifying a lack of neoplastic glial cells (GFAP negative tumors).

Clinical Scenario and Indications for Imaging

Children and young adults with usually a long-standing history of epilepsy. Indistinguishable

clinical differences between gangliogliomas and gangliocytomas.

Interpretation Checklist and Structured Reporting

Solid-cystic enhancing mass centered in the cortex in the temporal or parietal lobes.

CT Findings

Mixed solid and cystic (50% of the cases) components with scalloping of the adjacent skull and enhancement. Calcifications are seen in one-third of the cases.

MR Findings

T1w: hypo−/isointense solid mass with cystic component. Internal calcifications can be hyperintense.

T2w/FLAIR: heterogeneous signal of the solid portion with associated CSF-like signal of the cystic component. Typically, there is no edema (Fig. 72a, b).

T2∗w (GE/SWI): calcified areas show blooming signal loss.

T1w with contrast: contrast enhancement varies from none to marked and may be solid or rim-enhancing (Fig. 72c).

Pearls

The minority of gangliogliomas (5%) may show aggressive behavior and histopathologic features and are then called anaplastic gangliogliomas (WHO grade III). The transformation into high-grade tumors refers usually to the glial component (into a GBM) and rarely to the neuronal component (into a neuroblastoma). Do not confuse gangliocytoma with dysplastic cerebellar gangliocytoma (Lhermitte-Duclos disease).

Treatment and Monitoring

Surgical resection with good prognosis (even after subtotal resection) is initially attempted though late recurrences can occur (up 20 years later). Incomplete resection is often achieved in the spinal cord, and local recurrence is very common. Radiation therapy is not recommended for patients after complete resection. Aggressive management with radiation and chemotherapy is indicated in anaplastic gangliogliomas. Resection is curative in gangliocytomas, which do not undergo anaplastic dedifferentiation.

Differential Diagnosis

– Pilocytic astrocytoma: very similar nodulo-cystic appearance but different location (cerebellum and optic pathways) and often not associated with seizures.
– Dysembryoplastic neuroepithelial tumors (DNETs): less common enhancement and calcifications. "Bubbly" appearance is characteristic but not always present.
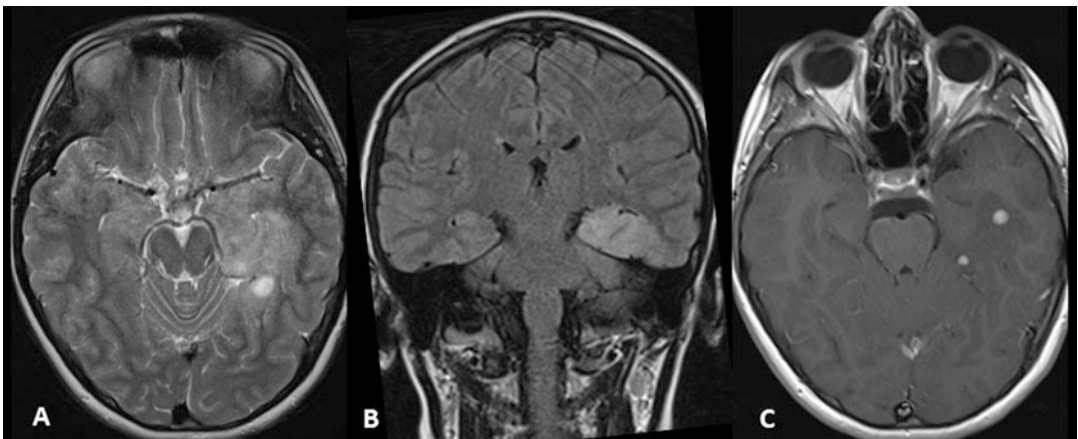
Fig. 72 Left temporal ganglioglioma. Axial T2 (**a**), coronal FLAIR (**b**), and axial T1 C+ (**c**). Two small nodules of enhancement are demonstrated in post-contrast sequence

– GBM: central necrosis, irregular peripheral enhancement, and extensive surrounding edema. The solid portion may show restriction due to high cellularity.

Desmoplastic Infantile Astrocytoma/Ganglioglioma

Definition of Entity and Clinical Highlights
Desmoplastic infantile astrocytoma and desmoplastic infantile ganglioglioma, previously considered separate entities, are now grouped together in the 2016 WHO classification of CNS tumors due to the similar clinical, radiological, and pathological findings.

Basic Epidemiology/Demographics/Pathophysiology
These tumors, initially believed to occur only in up to 2-year-old children, have been observed in patients as old as 25 years of age (M:F ratio approx. 1.5–2:1).

Pathological Features
Histologically they are heterogeneous with a divergent astrocytic and ganglionic differentiation and a prominent desmoplastic stroma; more primitive cells may be observed. The solid peripheral desmoplastic component is composed of meningeal tumor cells. High number of mitoses can mimic the features of malignant astrocytomas. Rarely, BRAF V600E mutations have been observed. The leptomeningeal desmoplastic component is positive for vimentin, GFAP, and variably SMA. The neuroepithelial component is positive for GFAP and synaptophysin if ganglionic cells are present.

Clinical Scenario and Indications for Imaging
Typically, rapidly increasing head circumference with symptoms usually presenting in a short time after birth. Seizure activity is rarely present.

Interpretation Checklist and Structured Reporting
Large cyst with cortically based solid nodule in a young child. The solid aspect of the tumor has aggressive radiological features such as low T2 WI signal and increase restriction.

CT Findings
Large solid-cystic mass with prominent feeding arteries on CTA. No calcifications. There is mass effect and possible surrounding edema.

MR Findings
T1w: isointense to brain parenchyma.

T2w/FLAIR: the cyst has CSF-like signal. Solid portion is typically hypointense in T2w.

DWI: reduced diffusivity in the solid portion due to high cellularity.

T1w with contrast: strong enhancement of the solid nodules and meninges. Dural tail may be seen (Fig. 73).

Pearls
Large cystic tumors with a peripheral solid component abutting and attached to the meninges. The incidence peak is 4–6 months, and the main clinical sign is enlarging head size. It is critical to evaluate the exact extent of the tumor as better prognosis if complete resection is achieved.

Treatment and Monitoring
Treatment consists of surgery, with chemotherapy in cases of incomplete resection. Most studies indicate that gross total resection results in long-term survival. Radiation therapy is usually considered only when other options have been exhausted.

Differential Diagnosis
– Pleomorphic xanthoastrocytoma (PXA): PXA may look identical to desmoplastic infantile astrocytoma/ganglioglioma, but the patient's age is different and PXAs are usually smaller at diagnosis.
– Supratentorial embryonal tumors (ETMRs): the presence of prominent cystic component is rare in these tumors, which often have internal areas of necrosis. ADC values are lower in ETMRs, which often do not enhance.
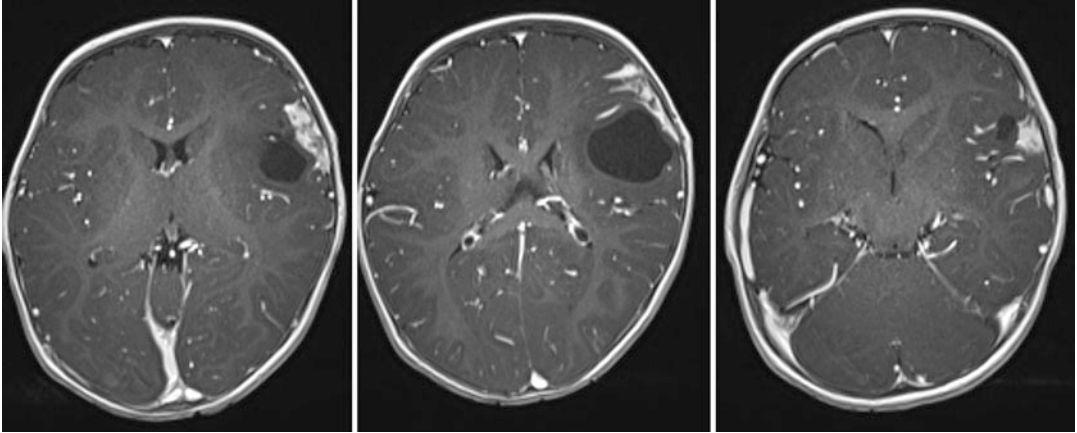
Fig. 73 Axial T1 C+ in a child with desmoplastic infantile ganglioglioma. Note the large internal cyst and characteristic leptomeningeal involvement

Diffuse Leptomeningeal Glioneuronal Tumor (DLGN)

Definition of Entity and Clinical Highlights
Diffuse leptomeningeal glioneuronal tumor (also previously known as primary leptomeningeal oligodendrogliomatosis or disseminated oligodendroglial-like leptomeningeal tumor of childhood) is a rare entity, recently designated in the 2016 WHO classification of CNS tumors, characterized by diffuse leptomeningeal enhancement, associated hydrocephalus, and cystic changes. Histologically DLGNs are low grade, but the prognosis is poor due to difficulties in treating the hydrocephalus.

Basic Epidemiology/Demographics/ Pathophysiology
The median age at diagnosis is 5 years (range 5 months to 45 years) with moderate male predilection.

Pathological Features
Defining features are predominant and widespread leptomeningeal growth, an oligodendroglial-like cytology (desmoplastic fibrous response admixed with cells with perinuclear haloes and cytoplasmic swelling), and evidence of neuronal differentiation in a subset of cases. Round to oval nuclei with finely granular dispersed chromatin are typical. Most tumors have

concurrent BRAF-KIAA1549 gene fusion and either 1p deletion or 1p/19q-codeletion in the absence of mutations in IDH. DGLNs are negative for neurofilament and EMA and show diffuse immunoreactivity for MAP 2, synaptophysin, and S-100. DLGNs have not yet been assigned a grade in the 2016 WHO classification of CNS tumors.

Clinical Scenario and Indications for Imaging
Most patients present acutely with signs and symptoms of increased intracranial pressure due to hydrocephalus, cranial neuropathies, and other leptomeningeal signs.

Interpretation Checklist and Structured Reporting
Diffuse enhancement of the meninges, particularly evident in the posterior fossa structures, with possible extension along the surface of spine and cerebrum.

CT Findings
CT demonstrates similar to MRI features, within its limitations.

MR Findings
Widespread leptomeningeal enhancement and thickening, often most prominent along the spinal cord, posterior fossa, and brain stem. Intraparenchymal and intramedullary enhancing nodules can also be seen.

Pearls

A fairly specific characteristic on images is the presence of countless subpial cysts (high T2, low T1, FLAIR attenuating) which may represent dilated perivascular spaces (Fig. 74). Cerebrospinal fluid (CSF) cytology is often negative despite high protein levels, and diagnosis usually requires meningeal biopsy.

Differential Diagnosis

– Tuberculous leptomeningitis: infectious constellation with fever, headache, vomiting, and neck stiffness. Cranial nerve palsies are common.
– Leptomeningeal carcinomatosis: known or suspected underlying primary CNS tumors or distant tumors (hematogenous spread pathway). Common symptoms include spine or radicular/sensory abnormalities, nausea, and vomiting, and focal neurological deficit without meningism is a cardinal symptom.
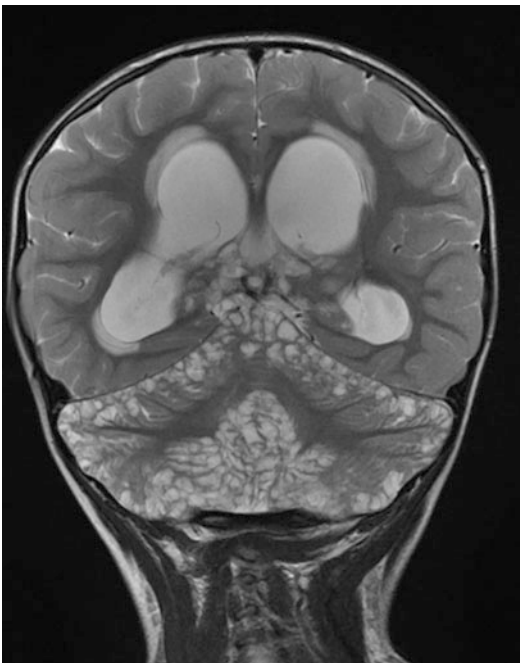
Fig. 74 Diffuse leptomeningeal glioneuronal tumor mainly involving the posterior fossa with associated hydrocephalus

Treatment and Monitoring

Optimal treatment is unknown, and these tumors can have a relatively indolent course. Chemotherapy is often attempted before radiation. Mitotic activity, Ki67 >4%, and microvascular proliferation were associated with worse survival.

Supratentorial Ependymoma

Definition of Entity and Clinical Highlights

Ependymomas are generally considered grade II tumors, but histological features as high cellularity and the presence of mitoses warrant the designation "anaplastic ependymoma" (grade III). In ependymomas, location is a powerful prognostic, and the supratentorial ependymomas (STEs) in children contain a characteristic RELA fusion chromosome that confers a poor prognosis compared with the intermediate prognosis in the pediatric posterior fossa ependymomas.

Basic Epidemiology/Demographics/ Pathophysiology

STEs account for 30% of ependymomas, being within or abutting the ventricles. Intraventricular, intraparenchymal/pure cortical forms (making approx. 40% of the cases) have been described. It has no gender predilection, and the peak manifestation is in the adult age group (mean age, 18–24 years).

Pathological Features

STE is a primary glial tumor arising from ependymal cells. Histopathologically, they resemble ependymoma elsewhere demonstrating ependymal rosettes and perivascular pseudorosettes. A strong neurofilament light polypeptide 70 expression in supratentorial ependymoma has been correlated with better progression-free survival.

Clinical Scenario and Indications for Imaging

The most common clinical presentation in the intraparenchymal form is headache, seizures, focal neurological deficits, or gait disturbances. Intraventricular tumor presents with features of raised intracranial tension.

Imaging Technique and Recommended Protocol

Brain and spine MRI with contrast, perfusion, MRS, and diffusion techniques add information about the presence of anaplasia. DTI/tractography may help in the preoperative planning.

Interpretation Checklist and Structured Reporting

Supratentorial mass in young children with calcified, cystic, and hemorrhagic components.

CT Findings

Calcium and hemorrhagic changes.

MR Findings

T1w: imaging in T1WI reflect the heterogeneously of this neoplasm with areas of cystic-necrotic degeneration that are hypointense or calcium and blood which may appear hyperintense.

T2w/FLAIR: generally, hyperintense with surrounding edema. Well-defined margin between the mass and the surrounding parenchyma (Fig. 75b).

DWI: variable, depending on the histological grade, may have striking restriction if anaplastic component is prevalent (Fig. 75c).

PWI: generally, demonstrates high perfusion with poor return to baseline due to fenestrated blood vessels and incomplete blood-brain barrier (Fig. 75d). The rCBV may be increased approximately five times more in grade III tumors.

MRS: elevated choline and reduced NAA (non-specific features). MRS with short TE has described as showing increased glutamine and glutamate. MRS is a useful tool to distinguish tumor recurrence from treatment-related changes.

T1w with contrast: heterogeneous enhancement mild to strong (Fig. 75a).

Pearls

Ependymomas in different locations, despite looking alike on histology, show completely different molecular profile, histological grade, age predilection, and prognosis. It has been hypothesized that STEs originate from the embryonic ependymal remnants in the brain parenchyma with predilection for frontal, temporal, or parietal lobes. Supratentorial ependymomas more often contain a separate solid and cystic component as compared to infratentorial ependymomas.

Treatment Monitoring

Patients with STEs may have a better survival rate than patients with posterior fossa ependymomas, because gross total resection is more commonly achieved. The 5-year survival rate after complete resection is approx. 60–80% whereas for subtotal resection is 10–75%. Early postsurgical assessment is important to confirm complete resection or presence of residuum. Radiotherapy is usually reserved for incomplete excised or anaplastic tumors similar to our case. Notably, the prognostic significance of ependymoma grade is dubious.

Differential Diagnosis

– Pilocytic astrocytoma: location within optic pathways. Low-grade imaging features of the solid portion.
– Embryonal hemispheric tumors (ETMR): always have aggressive radiological appearances (e.g., very low diffusion). ETMR usually do not enhance.
– Glioneuronal tumors: centered in the cortex, associated with epilepsy, cystic and nodular appearances rather than internal areas of necrosis-cystic degeneration.
– Choroid plexus tumors: located within the ventricles, centered on the plexus. Rare supratentorial, intraventricular ependymomas may have similar appearances.

Choroid Plexus Tumors

Choroid Plexus Papilloma: Choroid Plexus Carcinoma

Definition of Entity and Clinical Highlights

Choroid plexus papillomas (CPPs) are benign (WHO grade I) neuroepithelial intraventricular tumors. Histologically, they resemble normal choroid plexus and has been postulated they represent local hamartomatous overgrowths.

Choroid plexus carcinomas (CPCs) are aggressive tumors with invasion of neural tissue and frequently extraventricular extension into brain parenchyma.
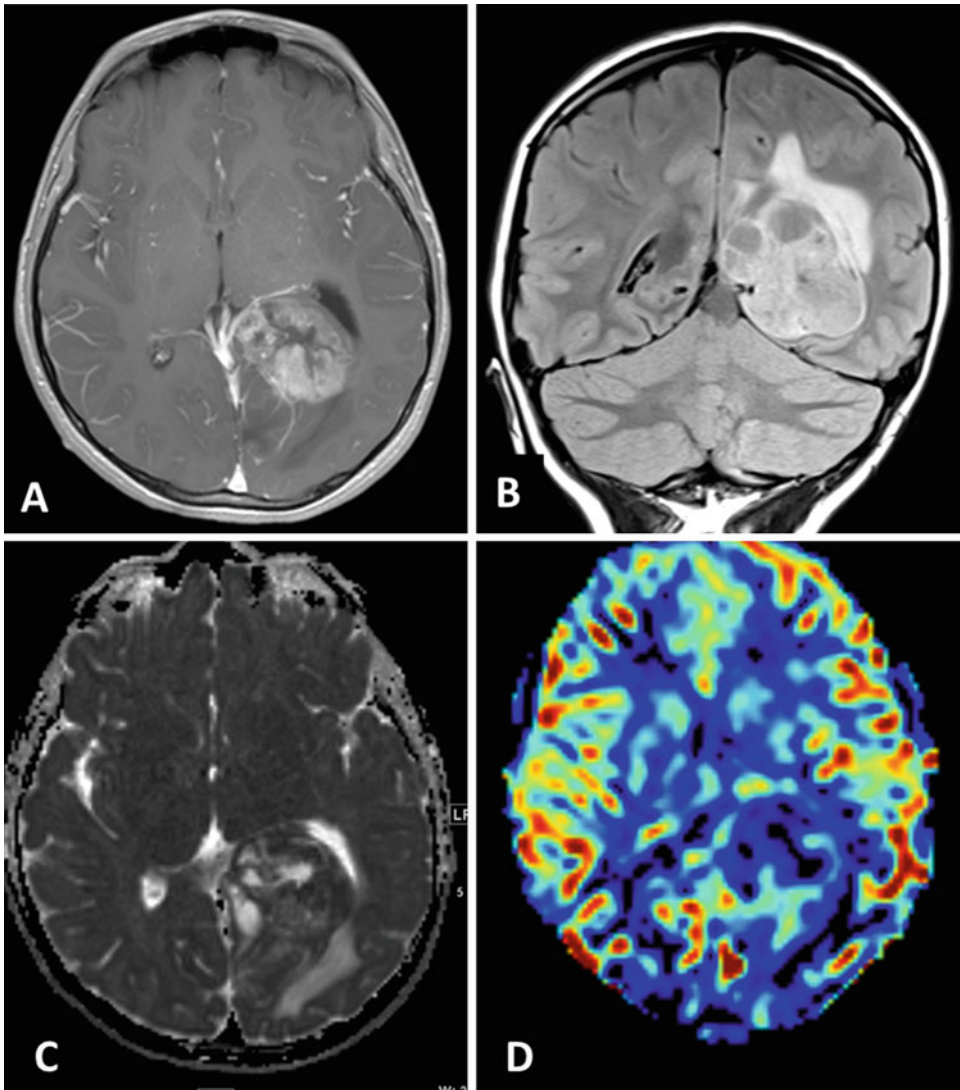
Fig. 75 Supratentorial anaplastic ependymoma. The mass is characterized by heterogeneous contrast enhancement (**a**), mixed internal structure and surrounding edema best seen in FLAIR (**b**), diffusion restriction of the solid part (low ADC values in **c**), and moderate peripheral perfusion (ASL rCBF maps in **d**)

Basic Epidemiology/Demographics/ Pathophysiology

CPPs are uncommon tumors occurring more commonly in pediatric (2–6% of all pediatric tumors) rather than in adult populations (0.5% of all brain tumors). Their vast majority is observed supratentorially in children under the age of 1–5 years. An association with Aicardi syndrome and Von Hippel-Lindau disease has been found.

CPCs occur also predominantly in children within the first 5 years of life. CPCs are rarer than CPPs. CPC can be manifested in the context of Li-Fraumeni syndrome (mutation in the TP53 tumor suppressor gene).

Pathological Features

CPPs are classified as WHO grade I neoplasms, and CPPs with increased mitotic activity (≥2 mitoses per high-power field) are primarily
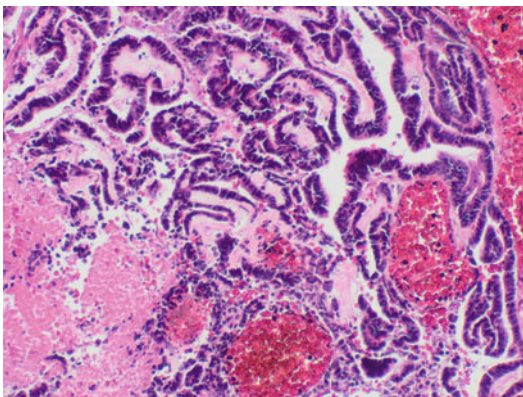
Fig. 76 H&E-stained high-power image of a choroid plexus carcinoma with necrosis, bleedings, and typical papillary tumor architectures

classified as atypical CPPs (WHO grade II). CPPs are macroscopically characterized as cauliflower-like masses. They contain uniformly apical microvilli and scatted cilia, akin to neuroepithelial cells. The growth fraction (MIB-1) is less than 2% for grade I tumors. CPPs are positive for cytokeratins, vimentin, and variably S100 and KIR7.1.

CPCs are characterized by dense cellularity, mitoses (>5 per 10 high-power fields), nuclear pleomorphism, focal necrosis, loss of papillary architecture, and invasion of neural tissue. Micro-calcifications and hemorrhage may be present. S100 is often negative; p53 protein is positive in individuals with TP53 mutation; and KIR7.1 is positive in ~50% of cases (Fig. 76).

Clinical Scenario and Indications for Imaging

Hydrocephalus is seen in over 80% of cases with CPPs/CPCs due to the combination of CSF over-production and decreased arachnoid granulation resorption. Symptoms include increasing head circumference and papilloedema. Neural invasion in CPCs may result in focal neurological dysfunction.

Imaging Technique and Recommended Protocol

MRI brain and spine with contrast.

Interpretation Checklist and Structured Reporting

CPP is centered in the choroid plexus (usually in the trigone) with strong enhancement and lobulated appearance.

CT Findings

CPPs/CPCs generally look hypodense or isodense to the brain parenchyma; however 1/5 of the cases have fine speckled internal calcifications (Fig. 77a). Hydrocephalus represents a possible imaging feature.

MR Findings

T1w: lobulated mass most often located in the atrium of the lateral ventricle.

T2w/FLAIR: variable signal from hypointense to hyperintense. On T2w multiple internal vessels ("flow voids") are demonstrated. Presence of edema within the parenchyma is more suggestive of carcinoma (Fig. 77b).

DWI: variable; diffusion signal may be influenced by the presence of blood or calcium (Fig. 77c).

T2∗ GRE/SWI: blooming from calcifications/hemorrhage.

T1w with contrast: strong and relatively homogeneous enhancement (Fig. 77d) resulting in a cauliflower-like appearance. It is important to acquire contrast-enhanced T1w images of the spine as both CPP and CPC can spread through the CSF. Cystic component may be present.

Pearls

Differentiating choroid plexus carcinoma from papilloma is not possible on the basis of radiological appearances. Presence of necrosis, heterogeneous enhancement, cystic components, and massive edema in the brain parenchyma are more suggestive of CPC. CSF seeding is also more common in carcinomas.

Differential Diagnosis

– Medulloblastoma: in the posterior fossa with DWI restriction and low T2w signal.
– Ependymoma: supratentorial ependymomas are generally located outside the ventricles and have much more prominent heterogeneity.
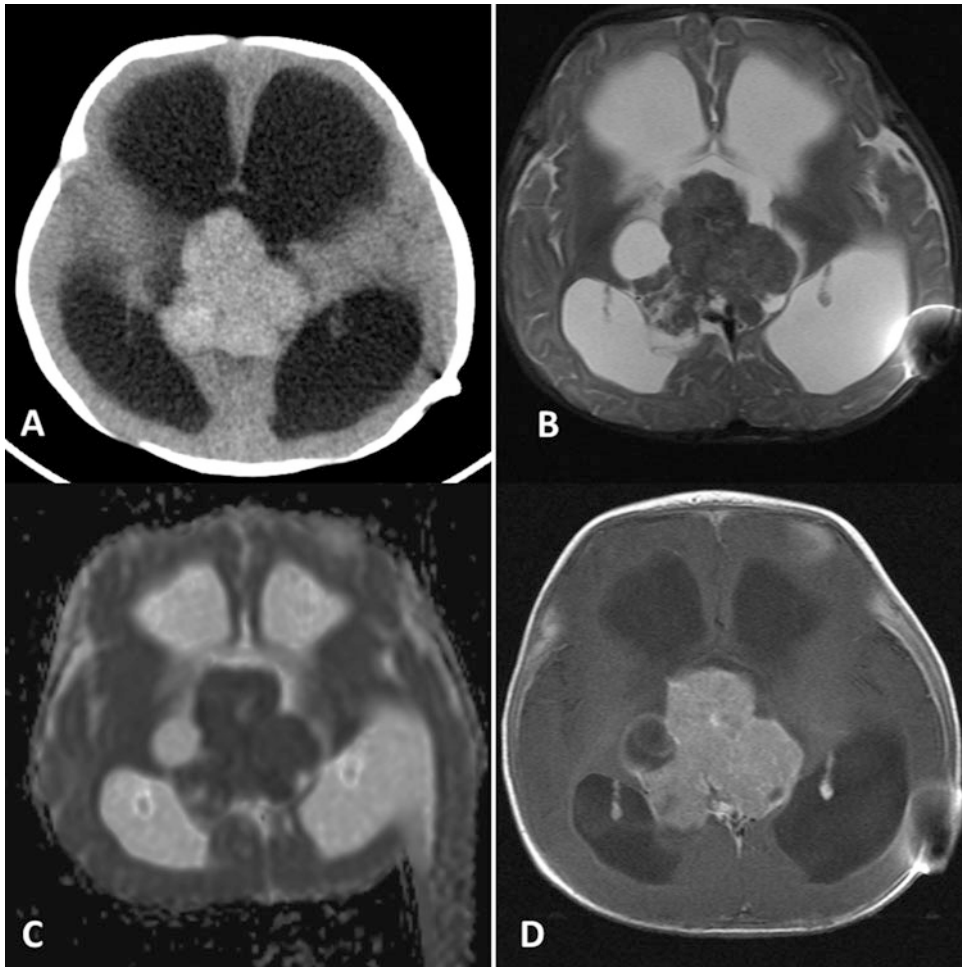
Fig. 77 Third ventricular choroid plexus papilloma presenting as typical lobulated (cauliflower-like) mass with relatively high density in CT (**a**), low T2 signal (**b**) and ADC values (**c**), and strong enhancement (**d**)

– Intraventricular ependymomas are more often located in the fourth ventricle.
– Subependymal giant cell astrocytoma: always found in a clinic-radiological context of TSC. Typical location is the foramen of Monro.
– Choroid plexus metastases: multifocal areas of tumor with normal-appearing choroid plexus. Primary underlying neoplasm is usually known.

Treatment and Monitoring

Resection is reserved for large or symptomatic CPPs; small, asymptomatic suspected CPPs can be monitored conservatively without any treatment unless they enlarge. After total resection, only atypical CPPs practically recur. Subtotally resected CPPs have also a benign course. Adjuvant radiation therapy is not indicated but may be useful for recurrent tumors that are inoperable. Leptomeningeal seeding may occur with histologically benign tumors.

The invasive nature of CPCs precludes gross total surgical excision (achieved in approx. 50% of the cases). Prognosis is poor, with a median survival of approximately 2.5 to 3 years. If resection is incomplete, a 5-year survival can be approx. 25%. The presence of a *TP53* mutation,

brain invasion, and CSF seeding are worse prognostic factors. Adjuvant radiation appears to be beneficial but many patients are too young. Multi-agent chemotherapy has been also utilized.

Embryonal Tumors (Supratentorial)

Embryonal Tumor with Multilayered Rosettes

Definition of Entity and Clinical Highlights
Embryonal tumors with multilayered rosettes (ETMR) (2016 WHO classification) are highly malignant tumors with varied embryonal histology (previously labeled embryonal tumor with abundant neuropil and true rosettes (ETANTR), ependymo-blastoma, CNS primitive neuroectodermal tumor, and medulloepithelioma) sharing C19MC gene amplification, thus suggesting that these are the one entity with variable growth pattern.

Basic Epidemiology/Demographics/Pathophysiology
ETMR are rare tumors affecting young children (median age 2 years) being more common in girls, unlike the other CNS embryonal tumors, in which boys are equally or more commonly affected.

Pathological Features
ETMSs are rare small round blue cell tumor with mixed acellular and highly cellular areas consisting of undifferentiated neuroepithelial cells, well-differentiated neuropil, and ependymoblastic rosettes showing no epithelial-like formation (a medulloblastoma feature). The characteristic C19MC gene alteration can be detected by fluorescence in situ hybridization (FISH).

Clinical Scenario and Indications for Imaging
Patients may present with signs and symptoms of increased intracranial pressure, seizures, hemi-paresis, cerebellar signs, or focal neurologic signs.

Interpretation Checklist and Structured Reporting
ETMR most commonly arises in the supra-tentorial compartment, often in the frontal or parietotemporal lobes, with 30% in the cerebellum or brain stem, with surrounding edema, often with significant mass effect.

MR Findings
T1w: hypointense mass.

T2w/FLAIR: hyperintense mass.

DWI: highly attenuated diffusion.

T2∗ GRE/SWI: blooming from calcifications/hemorrhage has been reported.

T1w with contrast: patchy or no contrast enhancement.

MR spectroscopy: prominent choline peak, high ratio of choline/aspartate in line with the tumor hypercellularity.

Pearls
On MRI, the extremely high cellularity accounts for low ADC values and variable T2w signal. Differently from other embryonal tumors, such as medulloblastomas, ETMR is characterized by minimal or absent enhancement (Fig. 78).

Differential Diagnosis
Depending on the tumor location of the tumor, the differential diagnosis includes:

– Medulloblastoma
– AT/RT

Treatment and Monitoring
ETMRs have a poor prognosis and median survival of <1 year. Maximal surgical resection plus chemotherapy and/or radiation therapy may result in prolonged survival in some cases.
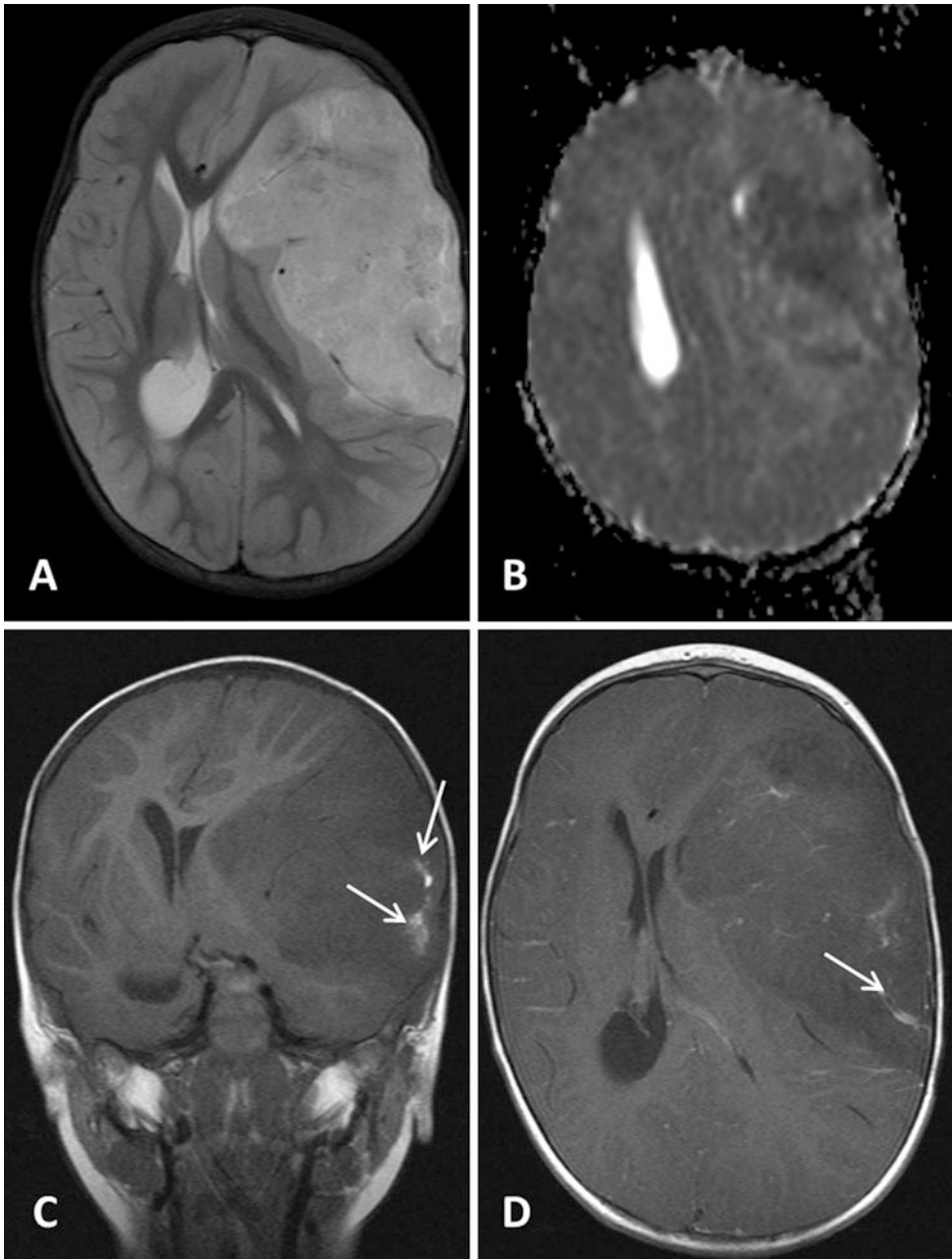
AT/RT (See Section "Posterior Fossa Tumors")

Report Checklist
1. Location of the tumor (intra−/extra-axial, posterior fossa/supratentorial, precise location – particularly important in case of posterior fossa mass for the differential diagnosis).

Fig. 78 Supratentorial embryonal tumor in an 18-month-old female. Axial T2 (**a**) demonstrates a large left hemispheric mass with midline shift and compression of the lateral ventricle. There are some areas of diffusion restriction noted on ADC maps (**b**) and no enhancement (**c** and **d**). Internal calcifications are seen as spontaneous hyperintense T1 signal (arrows)

2. DWI characteristics – low ADC denotes high cellularity.
3. Other signal characteristics.
4. Effect on the surrounding tissue (mass effect, infiltration, vascular compression).
5. Presence of distant metastases (remember for non-enhancing embryonal tumors use DWI as well).
6. Follow-up: presence of image findings in keeping with metastases vs postsurgical changes versus therapy-related changes (it is important to look at the original signal characteristics of the mass and the use of perfusion to diagnose pseudo-progression).
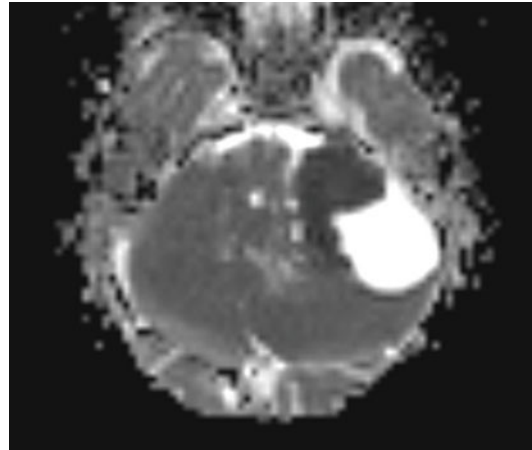
Sample Case with Report

Clinical Indication

An 8-month female with seizures and vomiting. CT done urgently in a district general hospital showing acute hydrocephalus. Please perform neuroaxis MRI with contrast to assess for obstruction cause and possible lesion CSF seeding.
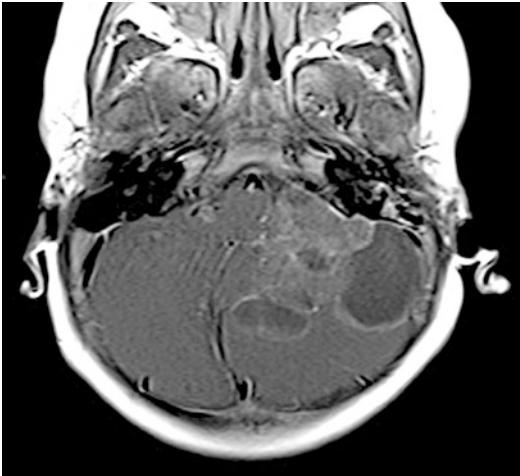
Axial T2-W Images

Apparent diffusion coefficient map

Axial T1-weighted image after gadolinium

Findings

MRI brain: There is a large mixed solid/multi-cystic tumor with peripheral cystic components centered in the left CPA. The solid component demonstrates patchy, mild enhancement and restricted diffusion.

Extensive mass effect is evidenced by near effacement of the fourth ventricle, with resultant supratentorial obstructive hydrocephalous.

The mass ascends to the level of the midbrain, compressing the pons anteriorly and effacing the left ambient cistern.

Inferiorly, a cystic component encroaches upon the perimedullary cisterns and the foramen magnum.
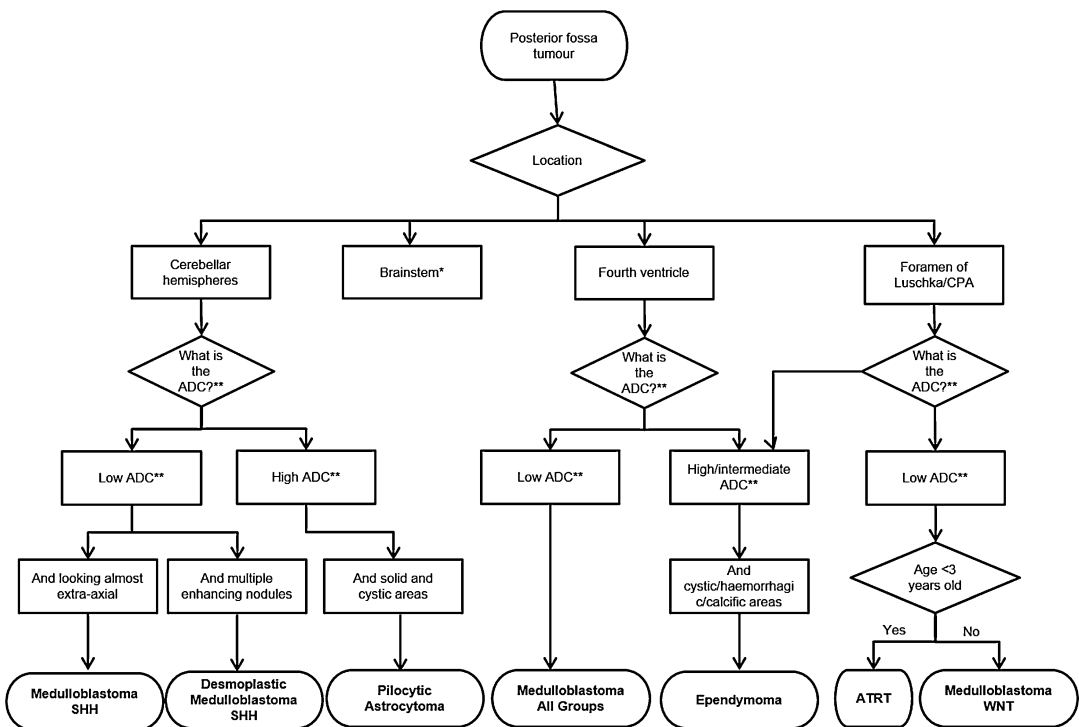
MRI spine: No current evidence of pathological enhancement to suggest metastatic disease.

Impression

Findings in keeping with embryonic tumor. Given the location and peripheral cystic components at this age, AT/RT is the most likely diagnosis.
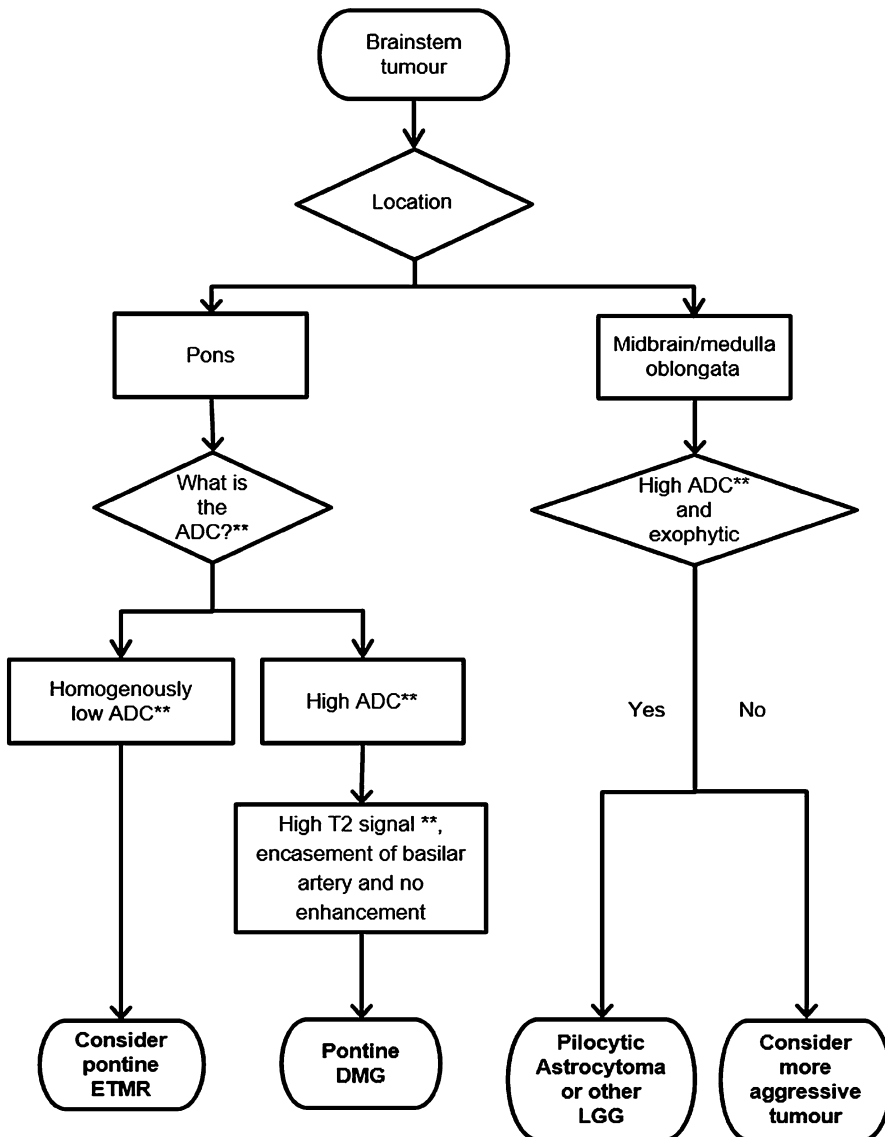

Fig. 79 Relative to gray matter. (Reprinted with permission from D'Arco F, Khan F, Mankad K, et al. Pediatric Radiology 2018 Dec;48 (13):1955–1963)

Flow Charts for Systematic Diagnostic Approach of Posterior Fossa Tumors in Children

∗∗Relative to gray matter. (Reprinted with permission from D'Arco F, Khan F, Mankad K et al. Pediatric Radiology 2018 Dec;48

(13):1955–1963). The radiological classification of posterior fossa tumors largely depends on location and ADC values (Fig. 79). For brainstem tumors specifically, differential diagnosis is driven by location, growth pattern and ADC (Fig. 80).

Fig. 80 Relative to gray matter. (Reprinted with permission from D'Arco F, Khan F, Mankad K, et al. Pediatric Radiology 2018 Dec;48 (13):1955–1963)

References

Awa R, et al. Neuroimaging diagnosis of pineal region tumors-quest for pathognomonic finding of germinoma. Neuroradiology. 2014;56:525–34.

Barboriak DP, et al. Serial MR imaging of pineal cysts: implications for natural history and follow-up. AJR Am J Roentgenol. 2001;176(3):737–43.

Brandao LA, Young Poussaint T. Posterior fossa tumors. Neuroimaging Clin N Am. 2017;27(1):1–37.

Calao AM. Pituitary adenomas in childhood. [Updated 2017 Dec 26]. In: De Groot LJ, Chrousos G, Dungan K, et al., editors. Endotext [Internet]. South Dartmouth: MDText.com, Inc.;2000.

Cauter V, et al. Integrating diffusion kurtosis imaging, dynamic susceptibility-weighted contrast-enhanced MRI, and short echo time chemical shift imaging for grading gliomas. Neuro Oncol. 2014;16:1010–21.

Claire Faulkner C, et al. KIAA1549-BRAF 15-9 fusions are more frequent in the midline than within the cerebellum. J Neuropathol Exp Neurol. 2015;74(9): 867–72.

D'Arco F, et al. Cerebrovascular stenosis in neurofibromatosis type 1 and utility of magnetic resonance angiography: our experience and literature review. Radiol Med. 2014;119(6):415–21.

Dumrongpisutikul N, et al. Distinguishing between germinomas and pineal cell tumors on MRI imaging. AJNR Am J Neuroradiol. 2012;33:550–5.

Fang A, Mayer P. Magnetic resonance imaging of pineal region tumors. Insights Imaging. 2013;4:369–82.

Ferry NB, et al. Embryonal tumor with abundant neuropil and true rosettes (ETANTR): a new distinctive variety of pediatric PNET: a case-based update. Childs Nerv Syst. 2010;26:1003–8.

Fèvre-Montange M, et al. Prognosis and histopathologic features in papillary tumors of the pineal region: a retrospective multicenter study of 31 cases. J Neuropathol Exp Neurol. 2006;65(10):1004–11.

Frühwald MC, et al. Atypical teratoid/rhabdoid tumors – current concepts, advances in biology, and potential future therapies. Neuro Oncol. 2016;18(6):764–78.

Gibson P, et al. Subtypes of medulloblastoma have distinct developmental origins. Nature. 2010;468(7327): 1095–9.

Good CD, et al. Surveillance neuroimaging in childhood intracranial ependymoma: how effective, how often, and for how long? J Neurosurg. 2001;94(1):27–32.

Hwang JH, et al. Proton MR spectroscopic characteristics of pediatric pilocytic astrocytomas. AJNR Am J Neuroradiol. 1998;19(3):535–40.

Jaremko JL, et al. Value and limitations of diffusion-weighted imaging in grading and diagnosis of pediatric posterior fossa tumors. AJNR Am J Neuroradiol. 2010;31:1613–6.

Jin B, Feng XY. MRI features of atypical teratoid/rhabdoid tumors in children. Pediatr Radiol. 2013;43(8):1001–8.

Koeller KK, Rushing EJ. From the archives of the AFIP: pilocytic astrocytoma: radiologic-pathologic correlation. Radiographics. 2004;24:1693–708.

Koral K, et al. Imaging characteristics of atypical teratoid–rhabdoid tumor in children compared with medulloblastoma. AJR Am J Roentgenol. 2008;190: 809–14.

Larkin S, Ansorge O. Pathology and pathogenesis of pituitary adenomas and other sellar lesions. [Updated 2017 Feb 15]. In: De Groot LJ, Chrousos G, Dungan K, et al., editors. Endotext [Internet]. South Dartmouth: MDText.com, Inc.;2000.

Linscott LL, et al. Pilomyxoid astrocytoma: expanding the imaging spectrum. AJNR Am J Neuroradiol. 2008;29: 1861–6.

Löbel U, et al. Quantitative diffusion-weighted and dynamic susceptibility-weighted contrast-enhanced perfusion MR imaging analysis of T2 hypointense lesion components in pediatric diffuse intrinsic pontine glioma. AJNR Am J Neuroradiol. 2011;32(2):315–22.

Löbel U, et al. Discrepant longitudinal volumetric and metabolic evolution of diffuse intrinsic pontine gliomas during treatment: implications for current response assessment strategies. Neuroradiology. 2016;58(10): 1027–34.

Lyle MR, et al. Newly identified characteristics and suggestions for diagnosis and treatment of diffuse leptomeningeal glioneuronal/neuroepithelial tumors. Child Neurol Open. 2015;2:1–7.

Mittal S, et al. Hypothalamic hamartomas. Part 1. Clinical, neuroimaging, and neurophysiological characteristics. Neurosurg Focus. 2013;34(6):E6.

Moore W, et al. Pleomorphic xanthoastrocytoma of childhood: MR imaging and diffusion MR imaging features. AJNR Am J Neuroradiol. 2014;35:2192–6.

Nicholas D'Ambrosio N, et al. Craniofacial and intracranial manifestations of Langerhans cell histiocytosis: report of findings in 100 patients. Am J Roentgenol. 2008;191(2):589–97.

Parmar HA, et al. Fluid-attenuated inversion recovery ring sign as a marker of dysembryoplastic neuroepithelial tumors. J Comput Assist Tomogr. 2007;31:348–53.

Patay Z, et al. MR imaging characteristics of wingless-type subgroup pediatric medulloblastoma. AJNR Am J Neuroradiol. 2015;36(12):2386–93.

Patjer KW, et al. Molecular classification of ependymal tumors across all CNS compartments, histopathological grades, and age groups. Cancer Cell. 2015;27: 728–43.

Perreault S, et al. MRI surrogates for molecular subgroups of medulloblastoma. AJNR Am J Neuroradiol. 2014a;35(7):1263–9.

Perreault S, Lober RM, Carret AS, et al. Surveillance imaging in children with malignant CNS tumors: low yield of spine MRI. J Neurooncol. 2014b;116(3): 617–23.

Poussaint TY. Pediatric brain tumors. In: Newton HB, Jolesz FA, editors. Handbook of neuro-oncology neuroimaging. New York: Elsevier; 2008. p. 469–84.

Prayer D, et al. MR imaging of intracranial disease associated with Langerhans cell histiocytosis. AJNR Am J Neuroradiol. 2004;25(5):880–91.

Pu Y, et al. High prevalence of pineal cysts in healthy adults demonstrated by high-resolution, noncontrast brain MR imaging. AJNR Am J Neuroradiol. 2007;28(9):1706–9.

Rodriguez FJ, et al. Disseminated oligodendroglial-like leptomeningeal tumor of childhood: a distinctive clinico-pathologic entity. Acta Neuropathol. 2012;124:627–41.

Rossi A, et al. Neuroimaging of pediatric craniopharyngiomas: a pictorial essay. J Pediatr Endocrinol Metab. 2006;19(Suppl 1):299–391.

Rumboldt Z, et al. Apparent diffusion coefficients for differentiation of cerebellar tumors in children. AJNR Am J Neuroradiol. 2006;27:1362–9.

Ryall S, et al. A comprehensive review of paediatric low-grade diffuse glioma: pathology, molecular genetics and treatment. Brain Tumor Pathol. 2017;34:51–61.

Sadeghi N, et al. Effect of hydrophilic components of the extracellular matrix on quantifiable diffusion-weighted imaging of human gliomas: preliminary results of correlating apparent diffusion coefficient values and hyaluronan expression level. AJR Am J Roentgenol. 2003;181:235–41.

Saleem SN, et al. Lesions of the hypothalamus: MR imaging diagnostic features. Radiographics. 2007;27(4):1087–108.

Schroeder JW, et al. Pediatric sellar and parasellar lesions. Pediatr Radiol. 2001;41(3):287–98.

Seeburg DP, et al. Imaging of the sella and parasellar region in the pediatric population. Neuroimaging Clin N Am. 2017;27:99–121.

Smith AB, et al. From the archives of the AFIP. Lesions of the pineal region: radiologic-pathologic correlation. Radiographics. 2010;30:2001–20.

Tamburrini G, et al. Desmoplastic infantile ganglioglioma. Childs Nerv Syst. 2003;19:292–7.

Tamrazi B, et al. Pineal region masses in pediatric patients. Neuroimaging Clin N Am. 2017;27:85–97.

Taylor MD, et al. Molecular subgroups of medulloblastoma: the current consensus. Acta Neuropathol. 2012;123(4):465–72.

Trehan G, et al. MR imaging in the diagnosis of desmoplastic infantile tumor: retrospective study of six cases. AJNR Am J Neuroradiol. 2004;25:1028–33.

Vaghela V, et al. Advanced magnetic resonance imaging with histopathological correlation in papillary tumors of pineal region: report of a case and review of the literature. Neurol India. 2010;58:928–32.

Watanabe T, et al. Pineal parenchymal tumor of intermediate differentiation: treatment outcomes of five cases. Mol Clin Oncol. 2014;2(2):197–202.

Witt H, et al. Delineation of two clinically and molecularly distinct subgroups of posterior fossa ependymoma. Cancer Cell. 2011;20(2):143–57.

Yuh EL, et al. Imaging of ependymomas: MRI and CT. Childs Nerv Syst. 2009;25:1203–13.

Zamora C, et al. Supratentorial tumors in pediatric patients. Neuroimaging Clin N Am. 2017;27:39–67.

Zimmer A, et al. Tumors of the sellar and pineal regions. Radiologe. 2014;54(8):764–71.